8-2006

Characterization of Membrane Potentials in Vascular Smooth Muscle of Hagfish, Lamprey and Trout

Prentiss Jones Jr.
Western Michigan University

CHARACTERIZATION OF MEMBRANE POTENTIALS IN VASCULAR SMOOTH MUSCLE OF HAGFISH, LAMPREY AND TROUT

by

Prentiss Jones Jr.

A Dissertation
Submitted to the
Faculty of The Graduate College
in partial fulfillment of the
requirements for the
Degree of Doctor of Philosophy
Department of Biological Sciences

Western Michigan University
Kalamazoo, Michigan
August 2006

CHARACTERIZATION OF MEMBRANE POTENTIALS IN VASCULAR SMOOTH MUSCLE OF HAGFISH, LAMPREY AND TROUT

Prentiss Jones Jr., Ph.D.

Western Michigan University, 2006

The objective of this study was to characterize membrane potentials in systemic arteries of Pacific hagfish, *Eptatretus stouti,* Rainbow trout, *Onchorhyncus mykiss*, and Sea lamprey *Petromyzon marinus*. Previous studies have characterized membrane potentials in piscine tissue. However, these studies utilized non-vascular tissues such as cardiac muscle and skeletal muscle (69, 161). Characterization of membrane potentials in fish vasculature is without precedent in the literature. The hypothesis of this study was that membrane potentials in fish vascular smooth muscle differ little between species when comparable vasculature is evaluated.

Histological evaluations were conducted to assess the suitability of fish arteries for electrophysiology studies. Arteries were histologically prepared and examined using microscopy (n=35 slides). These examinations revealed vascular components (e.g., endothelial cells, connective tissue, and smooth muscle cells) similar to that reported in other animals (21, 27, 32, 62, 71, 92, 110, 131, 134, 159, 160). Osmometry and spectrophotometric techniques were used to prepare species specific physiological saline solutions for use in histology and electrophysiology experiments.

Resting membrane potential and the response to changes in extracellular potassium was evaluated in hagfish and lamprey dorsal aortas and trout efferent branchial arteries. Membrane potentials were measured using sharp microelectrodes

to impale continuously perfused arteries. Membrane potential in unstimulated systemic arteries were similar: -52.7 ±2.9 mV, n=15 (hagfish), -54.3 ±5.2 mV, n=32 (lamprey) and -48.3 ±1.6 mV, n=27 (trout) ($p > 0.05$, ANOVA). Increasing the perfusate KCl concentration to 100 mM depolarized hagfish vascular smooth muscle cells 42.6 ±6.6 mV, n=5 and 80 mM KCl depolarized lamprey vascular smooth muscle cells 40 ±2 mV, n=7. Switching the KCl concentration back to normal re-polarized potassium depolarized cells.

Unexpectedly, the anesthetic used in this study (benzocaine) altered vascular tone. The effects of benzocaine on vascular tone were subsequently evaluated using a gas chromatography/mass spectrometry method developed for this study and via myography. Benzocaine induced contraction in lamprey aortas and relaxation in trout arteries.

The present study suggests that membrane potentials are similar in comparable fish vasculature despite differences in vascular morphology and differences in the composition of intracellular and extracellular constituents. Additionally, this study suggests benzocaine possesses vasoactive properties in fish systemic arteries at anesthetic concentrations.

INFORMATION TO USERS

The quality of this reproduction is dependent upon the quality of the copy submitted. Broken or indistinct print, colored or poor quality illustrations and photographs, print bleed-through, substandard margins, and improper alignment can adversely affect reproduction.

In the unlikely event that the author did not send a complete manuscript and there are missing pages, these will be noted. Also, if unauthorized copyright material had to be removed, a note will indicate the deletion.

ProQuest Information and Learning Company
300 North Zeeb Road
P.O. Box 1346
Ann Arbor, MI 48106-1346

ACKNOWLEDGMENTS

First and foremost may GOD be praised and may honor be bestowed upon my parents Prentiss and Elizabeth Jones who have encouraged me through the years. To my brother and sisters, your thoughts and prayers were food for the soul.

To my dissertation committee: Dr. Leonard Ginsberg thanks for honoring without hesitation your commitment to serve in spite of the demands required of your position at Western Michigan University. Dr William Jackson your scholarly critique and review were invaluable. You challenged me to go beyond the surface of the subject. Dr. Olson thanks for freely opening and welcoming me into your laboratory and giving of your time and resources. Your dedication to the pursuit of knowledge is admirable. Dr Spitsbergen, when all seemed lost, you stepped in with timely support and encouragement. Thanks for running the gauntlet; your help will not be forgotten.

Special thanks to Dr. Rick Hoover, Dr. David Jentz, Rebecca Hearington, Linda Hinkle, Kay Hoffmeister, Kathleen Murphy and numerous other South Bend Medical Foundation friends and peers.

This endeavor would have been unbearable without the sacrifice and devotion of my loving wife Ellen. Ellen thanks for the countless precious hours you patiently listened and waited. To my daughters Nadia and Jennifer, thanks for being my personal pep squad and for not begrudging the many days I spent away from you.

This work is dedicated to the loving memory of Ellen Haron and Master Sergeant Percy L. Meriwether whose legacy of determination and perseverance I shall forever cherish.

Prentiss Jones Jr.

Table of Contents

Table of Contents-Continued

LIST OF TABLES

LIST OF FIGURES

CHAPTER 1

INTRODUCTION

Review of Literature and Purpose of the Study

Vascular smooth muscle cells like the cells found in other types of smooth muscle (e.g., gastrointestinal, pulmonary, uterine) manifest a potential difference across the innermost layer and the immediate opposite outer layer of the plasma membrane. The potential difference exists due to differences in the concentration of cations and anions on opposing sides of the plasma membrane, differential permeability of the plasma membrane to these ions, impermeable intracellular anions, and the activity of pumps and transporters (1, 51, 54, 57, 87, 108, 109, 126). This potential difference is referred to as membrane potential.

Membrane potential plays a significant role in several vital smooth muscle functions such as; the regulation of intracellular calcium levels, controlling the activity of plasma membrane components (e.g., ion channels), modulating the contractile apparatus, and maintenance of vascular tone (19, 31, 78, 86, 105, 108).

It has been reported in numerous studies that despite differences in the structural arrangement, anatomical location, and functional requirements of the various smooth muscle types, the quantitative value for smooth muscle membrane potential is similar and is typically in the range of –60 to –40 millivolts (1, 27, 55, 108, 109, 126, 131). Surprisingly studies involving the characterization of membrane potential in vascular smooth muscle of fish are lacking. To my knowledge, this vital

fundamental aspect of vascular smooth muscle function has not previously been reported in fish.

The purpose of the present study was to gain insight into the electrochemical activity of vascular smooth muscle in fish by characterizing membrane potential in post-gill systemic arteries. In this study, the following questions were addressed: (1) How does the quantitative value of vascular smooth muscle membrane potential compare between fish and other animals; (2) Are there similarities in vascular smooth muscle membrane potential between fish species that share identical habitats (i.e., lamprey and trout); and (3) Are there similarities in vascular smooth muscle membrane potential between closely and distantly related (i.e., hagfish and lamprey versus trout) fish species? To answer these questions, blood and tissue specimens collected from 196 fish were studied: 26 Pacific hagfish, 26 Rainbow trout, 132 Sea lamprey and 12 Steelhead trout.

Osmoregulation: A Distinguishing Characteristic in Hagfish, Lamprey and Trout

Differences in the osmoregulatory capacity of hagfish, lamprey and trout are a prominent characteristic that distinguishes these fish. In the present study, observed differences in the plasma osmolality and major ionic constituents further supports their distinction. Comparatively, the differences between the saltwater hagfish (plasma osmolality = 1000 mOsm/kg, extracellular Na^+ and Cl^- each = 450 mM) and the freshwater lamprey and trout (plasma osmolality 250 -300 mOsm/kg, extracellular Na^+ and Cl^- each in the range of 100 - 150 mM) are striking and are of interest.

Hagfishes and lampreys belong to the order Cyclostomata (round mouths) and comprise a crucial phylogenetic position as the only surviving members of the most primitive class of jawless vertebrates (Agnatha). Hagfish (*Myxinae)* are strict marine fish that adjust their internal osmotic concentration to nearly match their external environment (osmoconformers) (60, 64, 122, 124, 157, 129, 133). Hagfish are unable to effectively regulate major ions (e.g., sodium and chloride). However, it has been suggested that hagfish and some other marine fish possess the capacity to regulate less abundant ions (e.g., magnesium and sulphate) (86, 129).

In stark contrast to the marine restricted hagfishes, lampreys (*Petromyzindae*) regulate their internal osmotic concentration in relation to their environment (osmoregulators). Some lampreys inhabit both freshwater and marine environments during periods of their lifecycle, while some have become landlocked and spend their entire lifecycle in a freshwater environment.

Differences in the osmoregulatory strategies of *Myxinae* and *Petromyzindae* have been proposed to indicate an ancient divergence of the two groups (124). Similar proposals and an increased use of cladistics in the 1970s led to debate of their united classification (59, 60, 79). In recent years, arguments have been presented that lampreys are the sister group to the jawed fish (gnathostomes), with the hagfish lineage having diverged as the basal lineage. However, subsequent studies suggest that hagfishes and lampreys uniquely share many structural characteristics that support the united classification argument (172). Later molecular evidence supports a

lamprey/hagfish grouping (148, 154) and confirms monophyly of *Myxinae* and *Petromyzindae* (96).

Rainbow trout and Steelhead trout, *Oncorhynchus mykiss*, are members of the teleostean class which includes bony fish that are predominately intolerant of variations in salt content of surrounding water (stenohaline) and bony fish that are tolerant of wide variations in salt content of surrounding water (euryhaline). Both rainbow and steelhead trout are euryhaline fish.

During the course of their life cycle, teleosts may be found in a broad range of habitats (e.g., freshwater to marine) (4). The diversity and abundance of teleosts account for their class having been the subject of the majority of the studies aimed at elucidating biochemical and physiological mechanisms utilized by fish to maintain adequate health, reproductive capacity and survival (81, 82, 111, 121, 143, 144, 168, 169, 173).

Hagfish

Although anatomically simple, the mesonephros (true functional kidney) of the hagfish is considered a limited source for the regulation of individual plasma ions, and likely shares regulatory functions with other organs such as the liver (127). Within the mesonephros, the epithelium of the archinephric duct (ureter) actively secretes ions and reabsorbs glucose in a manner similar to the proximal tubules of mammals. The functions performed by the mesonephros alone have been deemed minimally effective when compared to other vertebrates. Thus, the concentration of

their blood and urine ionic constituents is similar to that of seawater (60, 64, 122, 124, 127, 129, 133).

High concentrations of Na^+ and Cl^- present in hagfish body fluids results in a sera that is essentially in equilibrium (iso-osmotic) with the high concentrations of Na^+ and Cl^- in their seawater environment (64, 100, 133). As listed in Table 1, the major ions in hagfish plasma are not significantly different from that of seawater with the exception of magnesium. In the present study, the magnesium concentration in hagfish plasma was approximately 80% lower than the magnesium concentration reported for seawater. Other researchers have reported that the concentration of extracellular solutes in hagfish and several marine invertebrates to be in near equilibrium with seawater with the exception of magnesium and sulphate being substantially lower (approximately 50% for Mg^{2+} and 93% for SO_4^{2-}) (124, 127, 129).

Lamprey

Anatomically, the kidneys of lamprey are significantly different from that of hagfish (64). In fact, an intriguing similarity exists between the kidneys of lampreys and humans. Lampreys have the same number of glomeruli in relation to body weight as humans (129), suggesting that lamprey kidneys are more closely related to human kidneys than they are to hagfishes (40). Given the differences in renal function between hagfishes and lampreys, a difference in plasma ionic composition and plasma osmolality is not unexpected.

Non-migratory lamprey such as those currently inhabiting the Great Lakes of North America have become landlocked and spend their entire life cycle in a freshwater environment. However, given their ancestral origin, these landlocked species may possess residual marine osmoregulatory capacity despite their freshwater habitation (97).

Anadromous lampreys hatch in freshwater, migrate downstream to a marine environment as young adults then later return to freshwater as mature adults to spawn. Prior to migrating to a marine environment, anadromous lampreys develop marine osmoregulatory capacity (97) and during their return to freshwater (i.e., spawning migration), they undergo a marked reduction in their marine osmoregulatory capacity (122).

The ability of anadromous lampreys to survive in both environments has been the subject of numerous studies (4, 13, 129,130). Findings from these studies propose that anadromous lampreys in freshwater exhibit physiological mechanisms (e.g., uptake/excretion of ions by the gills and the excretion of hypoosmotic urine by the kidneys) similar to freshwater fish, suggesting that the gills and kidneys of lampreys are principle osmoregulatory organs.

Table 1. Major Ions in Hagfish Plasma

The composition of plasma constituents and osmolality of osmoconformers (e.g., hagfish) is dependent on their environment. The values listed below are not absolute given possible variability in the environment.

Animal/Fluid	Na^+ mmol l^{-1}	K^+ mmol l^{-1}	Ca^{2+} mmol l^{-1}	Mg^{2+} mmol l^{-1}	Cl^- mmol l^{-1}	Osmolality mOsm/Kg	Ref
Seawater	480	10	10	55	560	1033	1
Myxine glutinosa /plasma	487	8	4	9	510	1059	2
Myxine glutinosa /plasma	523	7.8	5.0	11.6	541	1095	3
Eptatretus burgeri plasma	531.8	12.4	6.5	10.1	397	1009.7	4

1. Barnes, H. *J. Exp. Biol.* 31:582-588, 1994
2. Robertson, J.D. *J. Zool.* 178:261-277, 1976
3. Robertson, J.D. *Comp. Biochem. Physiol.* 84A: 751-757, 1986
4. Inoue et al. *J. Exp. Biol.* 205:3535-3541, 2002

Trout

Freshwater teleosts (e.g., rainbow trout, steelhead trout) are hyperosmotic and tend to osmotically gain water from food, across the gill, and across the body surface. They are also hyperionic and tend to lose salts in urine and by diffusion across gills and skin. Salts are imported via diet and by active transport at the gill. Other anatomical structures such as highly developed glomerular nephrons in the kidney facilitate rapid filtration rates that results in blood that is hyperosmotic relative to the environment (64).

Specialized structures within the gill (e.g., chloride cells) and strictly defined functions (e.g., active transport of Na^+ and Cl^-) facilitate the maintenance of a plasma osmolality about one-third that of seawater (15, 89, 94, 99, 128).

As demonstrated in Table 2, despite differences in their external environment, marine teleosts maintain a plasma osmolality similar to freshwater teleosts (i.e., about one-third of seawater). Marine teleosts are hypoosmotic and tend to lose water through the gills, body surface, and in wastes. They offset the loss of water by drinking seawater and physiologically distilling it (i.e., desalination) in the esophagus. The esophagus is impermeable to water but is able to absorb Na^+ and Cl^- (85). Marine teleosts are also hypoionic and tend to gain salts across gills, body surface, and in food. Chloride cells in the gills similar to those found in freshwater teleosts are sites of ion transport (85). Cations (Na^+, K^+) are co-transported with Cl^- ions at the basal surface. Chloride passively exits anion channels at the apical surface, and Na^+ follows through leaky

tight junctions between cells (23). The kidney excretes other ions (K^+, Ca^{+2}, Mg^{+2}, SO_4^{-2}) in the hypertonic urine by tubular secretion.

By actively absorbing water and Na^+ and Cl^- in the intestines and secreting them without water across the gills, marine teleosts are able to maintain their blood concentration in a hypo-osmotic state relative to their environment.

Table 2. Marine and Freshwater Teleosts Osmolality

Plasma osmolality values are similar between marine teleosts and freshwater teleosts despite differences in their habitat (seawater versus freshwater). Both maintain a plasma osmolality approximately one-third that of seawater.

Animal/Fluid	Na^+ mmol l^{-1}	K^+ mmol l^{-1}	Ca^{2+} mmol l^{-1}	Mg^{2+} mmol l^{-1}	Cl^- mmol l^{-1}	Osmolality mOsm/Kg	Ref
Seawater	480	10	10	55	560	1033	1
Gadus morhua (Atlantic cod)	174	6	6.6	3	150	308	2
Salmo salar (Atlantic salmon)	165	2.4	-	-	150	365	3
Freshwater	1.5	0.2	3.0	0.6	1.4	-	4
Onchorhyncus mykiss (Rainbow trout)	152	-	-	-	127	289	4
Onchorhyncus mykiss (Rainbow trout)	151.8 ± 0.4 n = 5	1.2 ± 0.14 n = 5	2.27 ± 0.12 n = 5	1.02 ± 0.062 n = 5	127.4 ± 1.3 n = 5	294.4 ± 0.89 n = 5	This study

1. Barnes, H. *J. Exp. Biol.* 31:582-588, 1994
2. Sutton, A.H. *Comp. Biochem. Physiol.* 24:149-161, 1968
3. Waring, C.P. and Moore, A. *Aqua. Tox.* 66:93-104, 2004
4. Vedel, N.E, Korsgaard, B, Jensen, B.F. *Aqua. Tox.* 41:325-342, 1998

Smooth Muscle

Smooth muscle is present in linings of the digestive tract, respiratory passages, reproductive system, blood vessels and in several other tissues and organs. One of the fundamental components of smooth muscle is the spindle-shaped smooth muscle cell. Smooth muscle cells have elongated nuclei that are centered in the wider central portion of the cell (27, 37). The length of smooth muscle cells varies in accordance with their location and function (131, 142). Smooth muscle cells are not subject to voluntary control, but can respond to chemical, electrical and mechanical stimuli.

Smooth Muscle Physiology

The contraction of smooth muscle is slower than skeletal muscle but can be sustained for long periods. Smooth muscle can shorten to about one-quarter of its resting length and can generate a force, per cross-section area that is compatible to striated muscle, while consuming less energy (27, 131, 166).

The triggering mechanism for contraction is an influx of Ca^{+2} into the cell with depolarization of the plasma membrane or Ca^{+2} released from internal stores. Contraction ensues via cross-bridge cycling between phosphorylated myosin chains and actin filaments (166). (A detailed description of this process is provided in *Vascular Smooth Muscle Regulation* later in this work).

Vascular Smooth Muscle

Vascular smooth muscle normally maintains a state of partial contraction called muscle tonus, but this is subject to modulation by blood-borne hormones, nerves, local metabolites and endothelium derived vasoactive agents (37, 27, 131). The smooth muscle cells have receptors that can be acted upon by endogenous chemicals such as norepinephrine and vasopressin. These receptors are not limited to activation by endogenous chemicals but may be activated by exogenous chemicals (31, 37).

Vascular Smooth Muscle Anatomy

The anatomy of blood vessels (i.e., architecture and functional organization) is dictated by the vessel size, nuances of individual functions, the blood pressure carried, and the nature of the pulse wave experienced (159).

The typical architecture of blood vessels includes an intima with luminal endothelial cells and sub-endothelial fibroelastic connective tissue, a media formed of smooth muscle cells and connective tissue, and an adventitia formed of connective tissue, fibroblasts, nerve cells and ground substance that may blend with supporting soft tissues (153).

Vascular Smooth Muscle Classification

Vascular smooth muscle can be classified into two main patterns of mechanical activity, spontaneous rhythmic contractions (phasic) or no spontaneous

rhythmic contractions (tonic) (134, 140). Phasic mechanical activity is characterized by the development of spike action potentials during vascular smooth muscle depolarization phases and is demonstrated in certain vessels such as portal veins (134). Tonic mechanical activity is characterized by the production of "slow waves" in the membrane potential and graded depolarization rather than spiked action potentials (147). Tonic mechanical activity is demonstrated in middle and large arteries and limb veins (134, 146). Both phasic and tonic mechanical activities can be initiated in response to actions of surrounding nerves, humoral and local myogenic factors.

Vascular Smooth Muscle Biomechanics

The intrinsic properties of comparable vessels may differ between species. Robinson (134), made the following observations regarding vascular tissue: 1) Major differences in physiological and pharmacological responsiveness may be observed in vessels that differ in anatomical type within the same species and 2) Major differences in physiological and pharmacological responsiveness may be observed in morphologically similar vessels that serve different organs and tissues within the same species. Later studies conducted by others appear to support Robinson's observations (21, 92, 139, 147, 153).

In vitro inflation studies conducted on the aortas of three different invertebrate species, hagfish, and lamprey, demonstrated similar overall biomechanical properties for each case, despite differences in tissue structure (21). This study also revealed that

all tested vessels possessed the ability to expand and store elastic strain energy and the ability to recoil with minimal loss of energy. These functional abilities are displayed in the arteries of higher vertebrates and act to smooth the blood flow in the peripheral circulation, suggesting that aortas in the studied animals perform a similar function that is, smoothing pressure pulses from the heart (21, 134, 159).

Hagfish and lamprey have closed circulatory systems and aortic tissue architectures that closely parallel those of higher vertebrates (21, 159, present study). The wall structure of the arteries of hagfish and lamprey are very close to those of higher vertebrates, and given that their mechanical responses are similar to each other and those of higher vertebrates, it is likely that the corresponding tissue components behave in the same manner (21, 159).

Vascular Smooth Muscle Regulation

Regulation of tone and contractile response in vascular smooth muscle is dependent on an intricate array of alterable processes, such as, modulations in the activity of ion channels (e.g., voltage-gated L type Ca^{+2}, voltage-gated T type Ca^{+2}, ATP-sensitive K^+, large-conductance Ca^{+2} – activated K^+, voltage activated K^+, store-operated, stretch activated, Cl^-), shifts in the concentration of cytosolic Ca^{+2} and changes in membrane potential (19, 87, 105).

Calcium influx and membrane potential (discussed in detail in next section of this work) are closely coupled to the contractile response and tone of vascular smooth muscle. An increase in cytosolic Ca^{+2} concentration initiates vascular smooth muscle

contraction. Possible mechanisms for increasing cytosolic Ca^{+2} include: 1) transmembrane influx of extracellular Ca^{+2} through voltage gated Ca^{+2} channels; 2) release of Ca^{+2} from internal stores; 3) agonist induced activation of receptor operated channels; or 4) stretch induced opening of nonselective cation channels (20, 33, 57, 58, 78, 87, 105, 108, 119, 140).

Free Ca^{+2} in the cytosol binds with calmodulin forming a Ca^{+2}/calmodulin complex that activates myosin light chain kinase (MLCK). Activated MLCK in the presence of ATP, phosphorylates myosin light chains in the heads of the regulatory protein myosin. Phosphorylated myosin light chain thus allows cross-bridge cycling with the other regulatory protein (actin) present in vascular smooth muscle contractile apparatus; hence, vascular smooth muscle contraction is initiated (1).

The expression and activity of ion channels in the membrane of smooth muscle cells, concentration of free intracellular Ca^{+2}, and membrane potential changes are processes that decisively influence the regulation of vascular smooth muscle. Given these processes, it appears that the regulation of vascular smooth muscle is tightly controlled and is alterable via intrinsic and extrinsic factors.

Role of Membrane Potential in Vascular Smooth Muscle Regulation

As is the case for essentially all cells, anions and cations are distributed on both sides of the plasma membrane of vascular smooth muscle cells. The distribution of these ions establishes a potential difference across the plasma membrane (56). The potential for movement of ions across the membrane occur when there is an

imbalance in the electrical charge of ions (electrical gradient) or an imbalance in the concentration of ions (concentration gradient). As an example, the concentration of K^+ is high within vascular smooth muscle cells and low outside (86). Thus, a concentration gradient favors the movement of K^+ out of the cell exists. As K^+ moves out of the cell, the cell's interior becomes more negative resulting in an electrical gradient that opposes the concentration gradient. The potential difference that exists across a membrane is referred to as the membrane potential.

Membrane potential plays a prominent role in the regulation of vascular tone by regulating the influx of Ca^{+2} through voltage gated Ca^{+2} channels, influencing the release of Ca^{+2} from internal stores and the Ca^{+2} sensitivity of the contractile apparatus (51, 78).

Membrane potential is regulated within tight parameters and is determined by the functional activity and number of ion channels, transporters, receptors and exchangers (e.g., Ca^{+2} channels, Cl^- channels, K^+ channels, Na^+ channels, Na^+/K^+-ATPase, Na^+/H^+ exchanger, Cl^- exchangers) located in the plasma membrane (20, 75, 87, 108). Of the plasma membrane components listed above, K^+ channels such as ATP-sensitive K^+ channels, large-conductance BK_{Ca} channels, and voltage-activated K^+ channels have an important influence on membrane potential in vascular smooth muscle cells (51, 52, 75, 77, 78, 150).

To measure membrane potential the difference of the potential inside the cell is referenced to the potential outside the cell. Measurements taken of a cell at rest while no disturbances are occurring is referred to as the cell's resting membrane

potential. Membrane potential values vary from cell to cell and may range from about –90 mV to –20 mV with the typical membrane potential value for vascular smooth muscle cells being between –60 and –40 mV (56).

Membrane Potential Comparisons between Fish and Other Animals

Smooth muscle membrane potentials have been well studied in various tissue types (e.g., vascular, gastrointestinal, pulmonary) in numerous non-piscine animals (19, 57, 67, 87, 88, 93, 103, 140, 167). Membrane potential values obtained in these studies suggest that smooth muscle membrane potentials differ little between tissue types and species. No significant deviations from the quantitative values typically reported for smooth muscle membrane potential (i.e., -60 to –50 mV) were noted.

Electrophysiological studies involving fish vascular smooth muscle is lacking. However, studies involving non-vascular tissue have been conducted. The following represent a collection of results obtained from studies conducted in non-vascular tissue of fish.

The mean resting membrane potential reported for white skeletal muscle of Brown trout *Salmo trutta* was –86 mV ±2.9 mV, n=20 (7). Inoue (69), reported that the membrane potential in skeletal and caudal heart muscle of the hagfish *Eptatretus burgeri* Girard were –55 mV to –80 mV, mean –67 mV ±7.0 mV, n=16 (skeletal) and –30 mV to –60 mV, mean –43 mV ±, n=53 (caudal). The mean resting membrane potential of single isolated ventricular myocytes reported for Rainbow trout *Oncorhynchus mykiss* was –82.2mV ±1.9 mV, n=7. Vornanen (161), determined the

membrane potential of freshly isolated cardiac myocytes to be –75.2 mV ±0.82 mV, n=15.

The resting membrane potential for skeletal muscle is usually –90 to –65 mV or about 30 millivolts more negative than smooth muscle and slightly higher for cardiac muscle, -95 to –85 mV (41, 55). These studies suggest that membrane potential values of non-vascular tissue in fish are generally consistent with membrane potential values measured in comparable tissue in other animals.

Interactions between Drugs and Biological Systems

The interaction between a drug and a biological system can be divided into two branches; pharmacodynamics, the effect of a drug on the body; and pharmacokinetics, the way in which the body handles a drug (84). Acknowledgement of interactions between drugs and biological systems date back to the late 1800s and early 1900s and is credited to the discoveries of Paul Erhlich and John Langley (95). Erhlich noted that some synthetic organic agents possessed chemical specificities that imparted varied effects on biological systems; while Langley demonstrated that curare could inhibit nicotine induced contractions of skeletal muscles. Langley coined the term receptor to describe a biological component that interacts with a chemical agent (95). The research conducted by these two scientists forms the basis of the "receptor concept".

The receptor concept describes the quantitative aspects of pharmacodynamics and can be defined as: 1) Receptors largely determining the quantitative relations

between dose or concentration of the drug and pharmacologic effect, 2) Receptors being responsible for the selectivity of drug action and 3) Receptors mediating the actions of pharmacologic antagonists (132).

Pharmacokinetic processes that likewise occur and determine the concentration, rate and amount of time a drug will spend at a target site include: absorption, distribution, metabolism and excretion (132). Beginning from the time a drug is administered up to and beyond the observance of pharmacodynamic effects, these pharmacokinetic processes are occurring (8, 14).

Benzocaine

Benzocaine (4-aminobenzoic acid ethyl ester; Americane; Anaesthesin; Ethyl aminobenzoate; Ethyl p-aminobenzoate Subcutin; $C_9H_{11}NO_2$) was synthesized in the late 1800s and given the trade name Anaesthesin because of its favorable anesthetic properties and low toxicity (2, 118). Various formulations of Anaesthesin (e.g., lozenges, powders, pastes, ointments) were developed and marketed in the early 1900s (2).

Benzocaine can be synthesized by the esterification of p-aminobenzoic acid, or the reduction of ethyl p-nitrobenzoate. The physical properties of benzocaine of relevance to this study are: molecular weight 165.19; solubility in 20°C water (1 part to 2500), solubility in 20°C ethyl alcohol (1 part to 5); acid dissociation constant pk_a 2.8; mass spectral ions (70 eV) 92, 120 and 165.

Pharmacodynamics and Pharmacokinetics of Benzocaine

Benzocaine, whose structure is shown in Figure 1, is a long-established local anesthetic suitable for use in both human and veterinary medicine (2, 47, 101). Benzocaine has been reported to be an ideal general anesthetic for fish (45, 46, 102).

Benzocaine can be found in a variety of over-the-counter medicines, topical sprays and ointments. Unlike the amide local anesthetics, such as bupivacaine, lidocaine, and mepivacaine, benzocaine does not possess a tertiary amine that is ionized at physiological pH (118). Benzocaine consists of a lipophilic group (aromatic ring) connected to an ester group. Given its *in vivo* form (unionized and electrically neutral) and its lipophilic composition, benzocaine is ideally suited for crossing lipoprotein membranes (2, 6, 9, 45, 46, 47101, 102).

The relative *in vivo* proportion of ionized versus unionized benzocaine is governed by its pK_a and the pH of the body fluids according to the Henderson-Hasselbach equation: $pH = pK_a + \log [base/acid]$ (80). Because benzocaine is a weak base with a pK_a of 2.5, it is predominantly in the unionized form at physiological pH (~ 7.4).

Numerous studies have been conducted using benzocaine in experiments involving animals and countless reports describe the use of benzocaine in the medical treatment of both animals and man (25, 102, 149, 151). Unfortunately, even the most comprehensive of these studies and reports have not provided sufficient information regarding the absorption, distribution, metabolism, and finally the excretion of benzocaine.

Following its absorption, benzocaine is distributed in the general circulation. The distribution of benzocaine has not been well characterized for any animal model. However, absorption, non-target sites binding, blood supply, metabolism, and excretion, influence the distribution of benzocaine (80).

To be pharmacologically active following its absorption across the cell membrane, benzocaine must be distributed in active form and in sufficient quantity to its target receptor. It is widely accepted that voltage-gated Na^+ channels are a target receptors for benzocaine and other local anesthetics, and it is known that these local anesthetics inhibit the propagation of action potentials in excitable cells (65, 66, 162, 163, 164). It is believed that the actual binding site for these local anesthetics is inner pore moieties in the voltage-gated Na^+ channels (65, 77, 90, 163). It has been proposed that local anesthetics such as lidocaine and benzocaine block action potential generating Na^+ currents by shifting the steady-state inactivation of voltage-gated Na^+ channels to the hyperpolarizing direction (66, 162, 164).

Benzocaine undergoes rapid and extensive metabolism in the circulatory system of fish (98). In man, is believed that benzocaine is rapidly hydrolyzed by plasma or liver esterases to ethanol and p-aminobenzoic acid, although no quantitative excretion studies have been reported (6).

The plasma half-life of benzocaine is not well defined but is dependent on metabolism and excretion (2, 102). It is likely that the plasma half-life of benzocaine is short given that it possesses a hydrolyzable ester group and that esterases are ubiquitous enzymes in most animals. Biotransformation of benzocaine by the liver

and to a lesser extent by other organs (e.g., kidneys, lungs) and enzymes terminates its pharmacological activity and results in metabolites that can be excreted by the body.

Benzocaine possesses unique physical and chemical characteristics that allow it to be rapidly absorbed, distributed, metabolized and excreted by fish (46, 102, 151). As previously mentioned, the solubility of benzocaine in water is extremely poor, requiring large volumes of water to achieve a homogenous solution. In contrast, benzocaine readily dissolves in ethanol. The high miscibility of benzocaine in ethanol provides an ideal solvent to prepare stock solutions of benzocaine that can be rapidly added to water-based experiments involving aquatic animals (46, 72, 101).

Gills have extensive microvascular surface areas and receive the entire cardiac output and are optimal sites for absorptive interactions (50, 111, 115, 165). Absorption of lipophilic substances across highly vascular areas such as the gills in aquatic animals can result in elevated concentrations of that substance in the blood (50, 165). In experiments involving fish anesthetized in water containing ethanolic benzocaine, benzocaine was rapidly transported across the gills during respiration and into the circulatory system where it served as a fast acting general anesthetic (22, 38, 61, 70, 72).

In a study conducted by Hayton et al (61), tissue samples harvested from channel catfish ten days after exposure to benzocaine and its metabolites demonstrated the following rank-order profile: bile >> liver > trunk > kidney > head kidney > skin ~ red muscle > plasma > white muscle. This study suggests that benzocaine is likely to be found more readily in adipose tissue stores than in tissue

with higher water content and is supported by the finding that benzocaine concentrations tend to be higher in older and gravid animals (135).

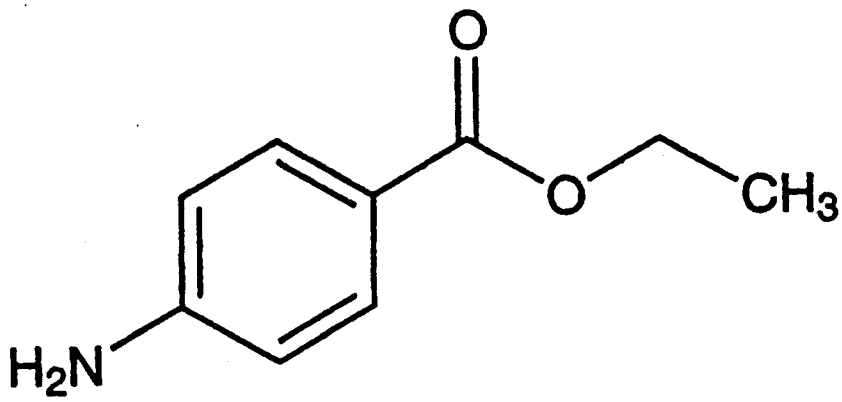

Figure 1. Chemical Structure of Benzocaine

Benzocaine ($C_9H_{11}NO_2$) is an ester type chemical commonly used as a short-acting local anesthetic.

Mol Wt 165.19, pKa 2.5, melts at 88-92°C, white or colorless crystals. Ethyl aminobenzoate, Americaine, Hurricaine (ingredient of Cepacol, Cetacine, Orajel).

Ethanol

Ethanol is a clear, colorless, hydroxylated, aliphatic hydrocarbon with a molecular weight of 46 (34). Ethanol is a simple chemical that is readily produced by a naturally occurring process referred to as fermentation (43). Ethanol is naturally produced when airborne yeasts metabolize simple sugars in honey, watery residues of overripe fruit, berries, vegetables, or grain (68). Yeasts then excrete ethanol and carbon dioxides as by-products of their metabolism. Ethanol is water and lipid soluble and is readily absorbed in body fluids and biological tissues (5). At equilibrium, the concentration of ethanol in body fluids and tissues is a function of the water content of that fluid or tissue (6).

Pharmacodynamics and Pharmacokinetics of Ethanol

The principle mechanism for the absorption of ethanol across cell membranes is passive diffusion. Ethanol is a small, uncharged, polar molecule that can easily cross cell membranes without active transport systems (34, 54). The rate of ethanol absorption is proportional to the concentration gradient of ethanol across the membrane and to a diffusion coefficient that is a constant for ethanol and the specific membrane (Fick's law). Fick's law of diffusion is defined by the following equation:

Rate of diffusion = kA(C1-C2)/D

Where: k = diffusion constant; A = surface area of membrane

C1-C2 =concentration gradient; D = thickness of membrane

The distribution of ethanol in man and other mammals has been well characterized (5, 34, 43, 68, 80). Limited information has been published regarding the distribution of ethanol in fish (49, 136, 137). Without suggesting that the distribution of ethanol in man and fish is identical, it is reasonable to assume that basic principles that govern the distribution of hydrophilic and lipophilic substances such as ethanol throughout the body in most vertebrates are similar (18, 104). Following the absorption of ethanol in the blood, the distribution of ethanol is influenced by several factors as previously mentioned above with the distribution of benzocaine. Namely, distribution is subject to the site of drug administration, binding of drug to non-target sites (e.g. serum albumin), blood supply, metabolism and excretion (80).

An inducible enzyme, alcohol dehydrogenase mediates the metabolism and excretion of ethanol. The biotransformation of ethanol by alcohol dehydrogenase to acetaldehyde, then ultimately to carbon dioxide and water, has been described in the metabolic profile of both man and fish (1, 104).

The rate of ethanol metabolism is said to follow zero-order kinetics (6). Zero order kinetics implies that a constant rate of metabolism occurs that is essentially independent of the amount of the target substance present. Metabolism consistent with zero order kinetics is well documented in mammals and has been demonstrated in fish exposed to varying concentration of ethanol (49).

Poly-Drug Pharmacokinetics

Poly-drug combinations may generate physiological responses that are much greater or lesser than the expected response (11, 68, 125, 152). As an example, the concomitant ingestion of the central nervous system depressant diazepam and ethanol exert an enhanced depression of the respiratory system (68, 80). The depressant effects of this combination are much greater than that of the depression caused by the each drug individually. In this example, the whole is greater than the sum of its parts, which, simply put, defines synergism.

In some cases, the combined effect of drugs is additive. An additive effect is a reasonable response that can be expected based on the sum of the individual drugs (80, 123). A counter example of the enhanced effect is demonstrated when theophylline and phenobarbital are co-administered. Phenobarbital promotes the metabolism of theophylline thus demonstrating a drug combination that produces a reductive effect (34). These poly-drug combinations highlight the importance of considering not only the potential impact of one chemical substance on physiological status but also the potential impact of concomitantly administered chemical substances.

Interestingly, benzocaine is commonly administered with ethanol. However, information regarding the physiological effects and the efficacy of this common combination are lacking. Experiments designed to evaluate the interactions between poly-drug combinations such as ethanol and benzocaine, provide useful information on the disposition of drugs and other chemicals when concomitantly administered.

CHAPTER 2

MATERIALS AND METHODS

Experimental Preparation

Animal studies were conducted in accordance with the National Research Council's *Guide for the Care and Use of Laboratory Animals* (U.S.A.) and the Indiana University School of Medicine, South Bend Center for Medical Education institutional guidelines for animal care and use. Animals used in this study were physically active and appeared to be in good health. Unless otherwise stated, animals were anesthetized by placing them in a holding tank containing five liters of aquarium water spiked with an anesthetic agent.

Animals

Sea lampreys (*Petromyzon marinus*; 80-381g) were caught during spawning migration (May through August) over six spawning seasons by the U.S. Geological Survey, Biological Resources Division (Millersburg, Michigan). Following transport to the University of Notre Dame, lampreys were kept in a 500 L rectangular tank in 12-14° C aerated circulating well water. Photoperiod exposure was 12h: 12h light: dark. A minimum acclimation period of at least two days was allowed prior to experimentation. The esophagus of spawning lamprey undergoes an anatomical change that prevents them from feeding, thus they were not fed.

Pacific hagfish (*Eptatretus stouti;* 70-120g) were collected from the Pacific Ocean near San Diego, California and maintained in seawater aquariums (Scripps Oceanographic Institute La Jolla, California). Following their transport from Scripps Oceanographic Institute to the University of Notre Dame, they were kept in aquariums containing artificial seawater (Instant Ocean Aquarium Systems, Eastlake, Ohio). The artificial seawater was re-circulated and maintained at 6-10°C on a 12h:12h light:dark photoperiod. Pacific hagfish were not fed.

Rainbow trout (*Onchorhyncus mykiss*; 500-1000g) were obtained from a commercial hatchery (Grand Haven, Michigan). Rainbow trout were maintained in 2000 L fiberglass aquariums with circulating well water (12-15°C) on a 12h:12h light:dark photoperiod and fed Purina® Trout Chow until examination.

Steelhead trout (n=12) were obtained from Bodine State Fish Hatchery (Mishawaka, Indiana) as part of the spawning program conducted January through February 2005 by the Indiana Department of Natural Resources.

Anesthetic Protocol

Benzocaine substocks were prepared by dissolving 1 gram of 4-aminobenzoic acid ethyl ester (benzocaine) in 10 ml of 95-99% ethyl alcohol. Holding tank anesthetic was prepared by adding 10 ml of benzocaine substock to 5000 ml of freshly

collected 10 -14°C circulating and aerated well water. Placing animals in a holding tank containing 5 L of holding tank anesthetic induced anesthesia.

Hagfish and lamprey remained in the holding tank until they were unresponsive to touch but exhibiting respiration. Rainbow trout remained in holding tanks until a loss of righting reflex was exhibited. A loss of righting reflex was defined as an inability to maintain correct swimming posture when manually turned.

Blood/Tissue Collection

Sea lamprey

Blood and/or tissue samples were collected from 132 anesthetized sea lamprey. Anaesthetized sea lamprey were weighed and placed dorsally on an ice chilled foam dissection table. A horizontal incision was made approximately 3 centimeters below the caudal most gill slit. Perpendicular lengthwise incisions were then made along both sides of the animal to expose the cardinal veins. Blood was drawn from the cardinal veins using 21-22 gauge venipuncture needles and transferred to Vacutainer® blood collection tubes. Blood collected for the analysis of ethanol and benzocaine was transferred to Vacutainer® blood collection tubes containing potassium oxalate and sodium fluoride. Blood collected for the analysis of ionic constituents was transferred to Vacutainer® blood collection tubes containing lithium heparin. Blood collected for osmolality measurements was transferred to Vacutainer® serum separator tubes containing lithium heparin. Immediately after transferring a sample the Vacutainer® tube was thoroughly but gently mixed,

centrifuged for fifteen minutes then refrigerated at 2 – 6° C until analysis. In some studies, a sample of the spiked aquarium water was collected from holding tanks prior to the addition of fish.

Pacific hagfish

Blood and/or tissue samples were collected from 26 anesthetized pacific hagfish. Anaesthetized pacific hagfish were weighed and placed dorsally on an ice layered dissection board. Cephalic and caudal ends were pinned to minimize spontaneous somatic contractions. Incisions as described for sea lamprey were made to expose the cardinal veins. Blood was drawn from the cardinal veins using 21-22 gauge venipuncture needles and transferred to Vacutainer® blood collection tubes. Collection tubes were thoroughly but gently mixed, centrifuged for fifteen minutes then refrigerated at 2 – 6° C until analysis.

Sea lamprey and *Pacific hagfish tissue collection*

The dorsal aorta (DA) was removed from anesthetized lamprey and hagfish (n = 68, lamprey; n = 26, hagfish). With the ventral surface of the animal exposed, three incisions were made through the skin with a sharp scalpel. A horizontal incision was made approximately 3 cm below the caudal most gill slit and two perpendicular lengthwise incisions were made along both sides of the animal. These incisions resulted in a caudally attached flap of skin, which allowed access to the inner body cavity. For some studies the liver was excised and placed in an appropriate 4°C

physiological saline solution. Internal organs (e.g., gonads, gut and kidneys) and surrounding connective tissue were removed to expose the DA. Using a pair of microsurgery scissors (Vannas) the entire length of both cardinal veins (orientated parallel to the DA on both sides) was incised. A trans-axial cut was made completely through the DA at the cephalic end just caudal to the cartilaginous structure that encases the heart. With a small tweezers (Dumont #4) the DA and its surrounding connective tissue were gently peeled towards the urogenital opening, and then cut. Care was taken to avoid excessive stretching of vessels. Excised DA was immediately placed in 4°C physiological saline solution. Isolated DA samples were further dissected from connective tissue in a water-jacketed dissection dish (Radnoti) or in an ice chilled glass dish mounted on a stereomicroscope.

Rainbow trout

One fish per experiment (n = 26) was transferred by a fish net from a 2,000 L aquarium to a holding tanking until a loss of righting reflex was confirmed (i.e., ability to maintain proper swimming position). Upon confirmation of loss of righting reflex, fish were removed and fully incapacitated with a sharp blow to the head. Fish were weighed then placed lengthwise on a tray layered with ice for collection of tissue samples and blood. Tissue samples (efferent branchial artery) were excised, rinsed and stored in 4° C HEPES buffered trout saline.

Using venipuncture technique, a 21-gauge needle was used to collect blood from the caudal vein. Each blood sample was transferred to Vacutainer® tubes, gently

mixed and centrifuged for fifteen minutes. Blood and tissue samples were refrigerated at 2 – 6° C until analysis.

Osmometry

Osmolality, not osmolarity is measured using a technique called Osmometry (44). Osmometry provides a direct quantitative measurement of the molal concentration of the total solutes in an aqueous solution (91). In the case of plasma samples, osmometry does not determine the fraction of plasma that is water. Rather, an evaluation of the solute content of the water contained in the plasma is determined by measuring its freezing point (44).

Calibrators, controls and sample unknowns were aliquotted then sequentially placed in a Fisk 2400® osmometer sample carousel (sample unknowns were analyzed in duplicate). The sample carousel was then re-centered to position 1 over the locating peg on the turntable spindle of the osmometer. During the analysis, the total number of particles present in the sample corresponded to the amount its freezing point was depressed below the freezing point of pure water. Using the Fisk 2400® osmometer, samples were super cooled several degrees below its freezing point. In this unstable state a mechanical agitation was automatically activated which induced crystallization. The heat liberated from the sample freezing caused the temperature to rise toward a plateau temperature, where a liquid-solid equilibrium (i.e., the freezing point) of the solution was measured.

Reagents

ACCUREF 290® Reference Solution; Probe Wiper Disc; Micro-Sample Tubes; 50 mOsm/Kg standard; 850 mOsm/Kg standard; 2000 mOsm/Kg standard

Instrumentation

Fiske 2400 Multi-Sample Osmometer

Osmolal Gap Measurements

Osmolal gap is the difference between the measured osmolality and the calculated osmolality. Discrepancies between the measured concentration and the calculated concentration are indicative of a deviation in the plasma water content from its normal content or the presence of an unrecognized solute. The osmolal gap can be used to determine the estimated concentration of a known substance suspected of causing osmolality abnormalities. A disturbance =10 mOsm/kg is considered abnormal (145). The osmolal gap may be elevated in the presence of low molecular weight compounds (e.g., ethanol) and as a result of the production of endogenous substances such as ketoacids and organic acids, occurring in some disease states (91).

Stock solutions of benzocaine (Sigma, F.W. 165.19) were prepared in distilled water at the following concentrations: 300, 500, 750, 1000 and 1250 mg/ml. Given the poor solubility of benzocaine in water, precise measurements were made to ensure that a 1g benzocaine to 2500ml water ratio was maintained. Ethanolic stock solutions were prepared in 95% ethyl alcohol (AAPER Alcohol and Chemical CO) at concentrations: 150, 300, 500, 750, 1000 and 1250 mg/ml.

Stock solutions were added to a holding tank containing 5 liters of aerated well water (lamprey) or aerated artificial seawater (Instant Ocean®) (hagfish). The holding tank was placed in a large container of chilled water to control the temperature (ice was added to the large container as needed). Fish were immediately removed from holding tanks when they were unresponsive to external stimuli.

Blood specimens were collected from lamprey and immediately centrifuged for fifteen minutes and refrigerated until analysis. Specimens were submitted for an analysis of ethanol by headspace gas chromatography, osmolality by freezing point depression osmometry and benzocaine via gas chromatography mass spectrometry.

Histological Examinations

Small segments of isolated lamprey (n=22) and hagfish dorsal aorta (n = 13) were histologically fixed by placing them in neutral buffered 10% formalin. Fixed tissue was embedded in paraffin then cut into 2–6 micrometer sections and placed on microscope slides. The Leica ST 4040® (an automated linear slide stainer) was used to make identically stained slides.

To prepare hematoxylin and eosin slides, each slide was deparaffinized in xylene. Deparaffinization is the process used to remove paraffin wax from the tissue and surrounding area on the slide. A deparaffinized slide should have a clear appearance with no white patches indicating residual wax (139). To prepare the tissue for staining with a dye the aqueous solution hematoxylin and eosin stain, deparaffinized slides were hydrated through a series of graded isopropanol solutions

until water was used (e.g., full strength, full strength, 65%, 65%, 50%, 40%, tap water). Sections should turn from clear to opaque. Clear patches on slides are an indication of residual paraffin wax that must be removed by repeating the deparaffinization process and the hydration step (139). Hydrated slides were stained in hematoxylin. Hematoxylin is a widely used natural dye that stains a variety of tissue components including nuclei, mitotic structures, elastic fibers, muscle and collagen (24, 139). Hematoxylin stained slides were then counterstained in eosin. Eosin combines with, and counter stains tissue bases. Finally slides were dehydrated in reagent alcohol then cleared in xylene. To preserve the stained tissue sections for subsequent handling and microscopic examination, slides were mounted with synthetic resin and appropriately sized coverslips. A control slide (human colon) was prepared along with the sample slides.

To prepare trichrome slides, each slide was deparaffinized in xylene as described above and hydrated with deionized water. Using a plastic Coplin jar, slides were placed in 40 ml Bouin's solution. The Coplin jar was loosely covered and placed in a microwave at 600 Watts for 25 sec. The heated solution was mixed with a plastic pipette for 45 sec. Slides were incubated in heated Bouin's for 5 minutes with frequent agitation of the Coplin jar. Bouin's solution is a fixative for preserving delicate structures (139). Slides were washed in running water until all yellow discoloration was removed from the tissue section (about 3 to 5 minutes). Slides were then rinsed in deionized water. Slides were stained in Weigert's iron hematoxylin for 10 minutes then rinsed in deionized water followed with a 3-minute wash under

running tap water. Weigert's iron hematoxylin is a strong oxidizer that serves as a link attaching the dye to the tissue (139). Slides were then rinsed in deionized water in preparation for staining. Slides were placed in 1% Biebrich Scarlet-acid fuchsin solution for 15 minutes, and then excess dye was rinsed off in deionized water. Biebrich Scarlet-acid is used to enter and stain acidophilic tissue (139). To differentiate colors between collagen and from acidophilic tissue, slides were placed in 5% phosphotungstic-phosphomolybdic acid for 10 minutes (139). Next, excess phosphotungstic-phosphomolybdic acid was drained from the slides and directly placed into 2.5% aniline blue solution for 8 minutes. Aniline blue solution was used to differentiate collagen (24, 139). After 8 minutes excess dye was rinsed off in deionized water. As a final step to further differentiate slides, slides were placed in 1% acetic acid for 1 minute. Dehydrated slides were mounted with synthetic resin and appropriately sized coverslips.

Reagents

Isopropanol; Gill Baker Hematoxylin (Surgipath®); Scott's Tap Water Concentrate®; Eosin-Y; Reagent Alcohol; Glacial Acetic Acid; Xylene; Bouin's Fluid, Sigma #HT10-1-33; Ferric chloride, Sigma #F-7134, 100g; Hematoxylin (C.I.75290), Fisher #H345; Reagent alcohol, Fisher; Hydrochloric acid, Concentrated, Fisher; Biebrich Scarlet (C.I.26905), Sigma B 6008; Acid fuchsin, Sigma A 3908; Phosphomolybdic Acid, ACS Reagent, Sigma P 0550; Phosphotungstic Acid, Sigma P4006; Aniline Blue (Methyl Blue C.I. 42780), Sigma M5528; Glacial acetic acid, Fisher

All reagents were analytical grade or of higher quality.

Instrumentation

Leica ST 4040 Linear Stainer

Sigma Accumate H2100, microwave

Smooth Muscle Myography

Vascular segments were cut from arteries and placed on a 100-130mm length of stainless steel wire fashioned with a hook at one end for vertical attachment to a force transducer (Grass FT-03®) and a hook on the opposing end to hold a vessel segment (3-6mm). A "coat hanger" type hook was feed through the vessel segment and attached to the bottom of a muscle chamber. This 2-wire and vessel configuration was lowered into a water-jacketed smooth muscle chamber (Radnoti) and filled with 4° C physiological saline. Air was supplied to the muscle chamber through a filtered inlet in the bottom of the chamber. The above protocol was adapted from a procedure described by Olson and Meisheri (112).

Myographic response (i.e., tension) of the vessel segment was measured using data collection software from Laboratory Technologies Corp. (Labtech Notebook) and hardcopies of data was recorded via polygraph (Grass 8TC®). Once resting tension was established for a given vessel, vessels were stimulated with 80 mM KCl. Resting tension values were reset following 80 mM KCl induced response.

Following the 80 mM KCl treatments, vessel segments were left undisturbed for approximately 45 minutes. Prior to experimentation, minor adjustments to resting tension were made as needed. To ensure that the magnitude of response (i.e.,

contraction or relaxation) for vessel segments was an accurate reflection of the pharmacological response, multiple treatments were conducted and the responses measured.

Isolation of Vascular Smooth Muscle Cells

Several protocols were developed (most unsuccessful) to isolate single lamprey dorsal aorta vascular smooth muscle cells. Initial attempts (n = 5) at isolation of lamprey dorsal aorta vascular smooth muscle cells exhibited signs of bacterial contamination rather than the presence of isolated vascular smooth muscle cells. Microorganism activity was observed via microscopy in the initial attempt aliquots.

To minimize the occurrence of bacterial contamination following the initial attempts, only lamprey with no overt signs of external contamination or infection were selected. Additionally, temperatures during isolation steps were closely monitored and reagents and buffers were filtered when possible. All dissection instruments were placed in boiling water for 15 minutes followed by a rinse in 95% ethanol. The incision area on the animal was disinfected with a 10% sodium hypochlorite solution (household bleach) prior to starting the dissection. These pre-dissection protocols appeared to address the concerns of bacterial contamination.

Initially, a physiological saline developed for rainbow trout (170), was used in dissociation and storage protocols. After additional failed cell isolation attempts (n=4), a chemical analysis was performed on samples of Wolf's rainbow trout saline and samples of lamprey blood. The analysis of these two samples revealed

discrepancies in the concentration of calcium, magnesium, and sodium. It was decided that a species-specific physiological saline would most likely provide the proper pH, required ions, and nutrient source for isolating vascular smooth muscle cells and conducting physiology studies. Using Wolf's rainbow trout saline protocol as a starting point, species-specific saline solutions were made.

Physiological saline solutions were prepared to closely match the composition of each animal's unique blood chemistry. Blood specimens were collected from lamprey, n=25; hagfish, n=15; rainbow trout, n=5 and immediately centrifuged for fifteen minutes and refrigerated until analysis. Diagnostic analyses were performed on a Hitachi 747 clinical chemistry analyzer (12) (Tables 3, 4, 5).

Adjustments were made to saline solution preparations until saline results were comparable to previously obtained plasma results. A series of adjustments and measurements (n = 6) resulted in the following preparation protocols for physiological saline solutions: Hagfish Physiological Saline Solution: NaCl 474 mM, KCl 8.05 mM, $CaCl_2.2H_2O$ 5.1 mM, $MgCl_2.6H_2O$ 9.0 mM, $MgSO_4.7H_2O$ 3.04 mM, Glucose 5.55 mM, HEPES (acid) 3.0 mM, HEPES (Na^+ salt) 6.99 mM; pH 7.8; Lamprey Physiological Saline Solution: NaCl 140 mM, KCl 5.4 mM, $CaCl_2.2H_2O$ 2.0 mM, $MgSO_4.7H_2O$ 0.8 mM, Glucose 5.0 mM, HEPES (acid) 3.0 mM, HEPES (Na^+ salt) 7.0 mM; pH 7.8; Trout Physiological Saline: NaCl 145 mM, KCl 3.0 mM, $CaCl_2.2H_2O$ 2.0 mM, $MgSO_4.7H_2O$ 0.57 mM, Glucose 5.0 mM, HEPES (acid) 3.0 mM, HEPES (Na^+ salt) 7.0 mM; pH 7.8.

Disaggregation of lamprey dorsal aorta vascular smooth muscle cells was attempted using enzymatic techniques, mechanical disruption techniques, and a combination of both. Enzymes used in this study included multiple types of collagenase, trypsin, elastase, dipase, hyaluronidase, and a ready to use enzyme solution that contained proteases and a proprietary buffer (VP 2000 Reagents).

Not all of these enzymes appeared to be effective. The first series of enzymatic experiments (n = 16) were conducted at various temperatures (4, 10, 25 and 37° C) for 4 hours. At 4 °C none of the enzymes used in this study were successful at isolating vascular smooth muscle cells from lamprey dorsal aorta. Using a 37° C incubation temperature for 4 hour was damaging to cells. Additional studies suggested that a temperature below 25° C was required to achieve the highest yield of viable isolated vascular smooth muscle cells. Digestion of non-cellular vascular components at lower temperatures was not as thorough as compared to digestions carried out at higher temperatures. To compensate for the loss of digestion at lower temperatures, the ratio of enzyme to tissue was increased. In addition to changes made in the incubation temperature, type of enzyme, and enzyme concentrations, changes were made to the enzyme incubation times. Times investigated ranged from 30 minutes to 16 hours.

Mechanical disaggregation of lamprey dorsal aorta was performed using two techniques: (1) Lamprey dorsal aorta was minced as fine as possible in 4-6° C lamprey physiological saline solution. The minced tissue was then placed in an ice chilled Petri dish containing a 2-inch square of 210-micron nylon mesh. The tissue

was gently rubbed across the mesh in an attempt to release free cells into the lamprey physiological saline solution. Large clumps of tissue and debris were removed by filtering the lamprey physiological saline solution through a 53-micron mesh filter, followed by filtering through a 37-micron mesh filter. The resultant eluate was centrifuged at 5-10° C. The pellet was then re-suspended in lamprey physiological saline solution for microscopic examination. Only a few intact cells were seen, many cell fragments were present.

In technique 2, lamprey dorsal aorta was finely minced in 4-6° C lamprey physiological saline solution and aspirated into a 10 ml syringe then forced through a 200 micron BD Bioscience Filcon® (Filcon® is a plastic single use self contained closed filter that can be attached to a syringe). The filtrate was collected in a clean syringe then filtered through a 50 micron Filcon® followed by filtration through a 30 micron Filcon®. The outcome for this technique was essentially the same as the first disruption technique described above (i.e., damaging to cells).

An enzymatic isolation technique was eventually developed that appeared to be far superior to the mechanical disruption method and is described in detail below.

Lamprey dorsal aortas were excised as previously described, opened lengthwise to expose the lumen then cut into small 3-4 mm sections and finely minced. The entire procedure was performed in a water-jacket dissection dish at 4 °C. The minced pieces were placed in 14°C Ca^{+2}-free lamprey physiological saline solution at pH 7.0 and used within 1 hour. Pieces were placed into an enzyme mixture modified from that previously described by Ma and Collodi, (92, personal

communication, June 1999). Enzymes were added to Ca^{+2}-free lamprey physiological saline solution as follows: (in mg ml^{-1}; 34.0 EDTA; 3.0 trypsin; 9.0 collagenase type XI [Sigma C-0130]; pH 7.0). Tissue pieces were placed in enzyme mixture and incubated at 14°C for 120-180 minutes. After incubation, undigested tissue pieces were removed from the enzyme mixture with an albumin moistened positive displacement pipette and the remaining cell suspension was centrifuged at 2000 g for 2 minutes. The supernatant was the drawn off and replaced with lamprey physiological saline solution containing 2 mM albumin. The centrifugation-washing step was repeated three times. After the third wash, cells were re-suspended in 200 μL of lamprey physiological saline solution containing 2 mM Ca^{+2}. Isolated vascular smooth muscle cells were examined using an Olympus CX-10 inverted microscope.

Table 3. Major Ionic Constituents in Sea Lamprey Plasma

Bichromatic photometry and ion selective electrode analysis was performed on sea lamprey plasma samples to quantify the major ionic constituents.

ID #	CALCIUM	CHLORID	SODIUM	POTASS	MAGNES	GLUCOSE	BICARB
1.	2.175	102	123	4.4	1.68	3.72	4
2.	2.375	114	128	3.2	1.72	3.22	9
3.	1.9	95	113	3.1	1.48	2.77	8
4.	2.2	98	114	3.3	1.52	3.11	13
5.	1.975	88	114	2.8	2.0	2.99	11
6.	1.925	101	119	4.4	2.0	3.99	13
7.	2.175	92	112	2.6	1.6	3.72	15
8.	1.95	117	130	2.4	1.39	2.72	3
9.	2.175	112	126	2.9	1.89	2.88	12
10.	2.125	108	130	3.2	1.48	1.72	8
11.	2.325	109	125	2.9	1.64	2.16	10
12.	2.375	106	130	1.9	1.35	1.78	12
13.	2.1	111	122	3.5	1.48	2.77	10
14.	2.15	101	132	2.3	1.39	N/A	12
15.	2.525	113	129	2.3	1.52	N/A	13
16.	2.125	105	124	2.2	1.35	N/A	9
17.	2.5	105	133	2.2	N/A	N/A	10
18.	1.975	116	135	3.3	N/A	N/A	9
19.	2.05	117	132	2.4	N/A	N/A	10
20.	1.9	112	124	2.6	N/A	N/A	15
21.	1.75	108	135	4.1	N/A	N/A	9
22.	2.325	96	113	2.9	N/A	N/A	7
23.	1.875	112	126	2.2	N/A	N/A	11
	2.275	103	125	2.6	N/A	N/A	8
	1.875	115	134	2.1	N/A	N/A	6
mean	2.124	106.24	125.12	2.9	1.60	2.89	9.88
SD	02	8.1	7.3	0.7	0.21	0.705	3.0
units	mmol/L	mEq/L	mEq/L	mEq/L	mmol/L	mmol/L	mEq/L

Table 4. Major Ionic Constituents in Pacific Hagfish Plasma

Bichromatic photometry and ion selective electrode analysis was performed on pacific hagfish plasma samples to quantify the major ionic constituents.

ID #	CALCIUM	CHLORID	SODIUM	POTASS	MAGNES	GLUCOSE
1.	3.875	555	565	8	10.5	0.279
2.	4.125	525	540	7	9.4	0.223
3.	3.875	520	535	7	9.2	0.390
4.	3.75	495	510	6.5	8.6	0.331
5.	4.0	490	510	6	8.8	0.223
6.	4.125	530	540	7	9.6	0.223
7.	4.625	548	549	9	12.1	0.167
8.	4.5	553	552	7.5	12.3	0.279
9.	4.5	557	553	9.1	11.7	0.501
10.	4.875	557	552	7.5	11.1	-
11.	4.625	480	490	7	12.5	-
12.	4.75	495	510	6.5	11.3	-
13.	3.75	400	410	5.5	9.2	-
14.	4.375	470	485	6.5	11.1	-
15.	4.25	455	470	5.5	10.7	-
mean	4.27	508.7	518.1	7.04	10.6	0.29
SD	0.37	45.4	41.4	1.07	1.31	0.11
units	mmol/L	mEq/L	mEq/L	mEq/L	mmol/L	mmol/L

Table 5. Major Ionic Constituents in Rainbow Trout Plasma

Bichromatic photometry and ion selective electrode analysis was performed on rainbow trout plasma samples to quantify the major ionic constituents.

ID #	CALCIUM	CHLORID	SODIUM	POTASS	MAGNES	GLUCOSE	BICARB
1	2.3	128	152	1.0	1.11	2.44	13
2.	2.325	128	152	1.4	1.02	2.94	15
3.	2.325	125	152	1.2	0.94	2.66	17
4.	2.05	128	151	1.2	1.02	3.11	16
5.	2.325	128	152	1.2	0.98	2.55	15
mean	2.27	127.4	151.8	1.2	1.02	2.74	15.2
SD	0.12	1.3	0.4	0.14	0.062	0.28	1.48
units	mmol/L	mEq/L	mEq/L	mEq/L	mmol/L	mmol/L	mEq/L

Intracellular Recording of Vascular Smooth Muscle Cells

Membrane potential was measured in the dorsal aortas of hagfish and lamprey and compared to membrane potential measured in the efferent brachial artery of the more advanced trout. Intracellular recordings of membrane potential were made using purchased, pre-pulled micropipettes (μTip, 0.1 μm ID 1.0mm OD, WPI) or micropipettes fabricated from borosilicate capillary glass (1.0mm OD 0.58mm ID, WPI) on a Flaming-Brown micropipette puller (Sutter Instruments Co. P-80/PC). Microelectrodes were created by filling micropipettes with 3M KCl. Typical resistances for the fabricated microelectrodes ranged from 30 to 80 MΩ. The resistance of purchased pipettes was not measured but were purported to have tip sizes = 0.1 microns.

Microelectrodes were held in microelectrode holders (WPI, model MEH3RF) attached to a head-stage, which was connected to the input of an intracellular preamplifier (Dagan Corporation Model 8700 Cell Explorer). The head-stage was held and controlled by a manual 3-way micromanipulator (Narishige). The output of the preamplifier was displayed on an oscilloscope (Leader Test Instrument Model LBO-514 Dual Trace/Dual Channel Oscilloscope) and also monitored and recorded with a digital multimeter (Radio Shack 46-Range Digital Multimeter with PC-MeterView® software) interfaced to a personal computer (Gateway E-2000 /Microsoft XP Professional).

The blood vessel perfusion system consisted of a water-jacketed horizontal blood vessel perfusion bath (Radnoti) mounted on a stereomicroscope (Nikon SMZ 10). A water-jacketed reservoir (Radnoti) was connected in-line with the perfusion bath and re-circulating chiller (Hadke). Chilled water (12-14°C for lamprey and rainbow trout; 8-10°C for hagfish) was circulated through all water-jacketed apparatus. The entire perfusion bath system was housed in a Faraday cage.

The inlet cannula of the perfusion bath was inserted into the lumen of the dissected artery segment then the end was tied with 7.0 silk sutures. The opposite segment end was similarly attached to the perfusion bath outlet cannula. The perfusion bath was then filled with cold (4°C) physiological saline solution and any segmental arterioles were tied off with silk sutures. Using Tygon® tubing, the outlet port of the reservoir was connected to the inlet cannula of the perfusion bath. Tygon® tubing was also attached to the outlet cannula to serve as a pressure regulator. The outlet tubing was raised or lowered to minimize fluctuations in pressure between the infusion end of the artery segment and the effluent end. A silver-silver chloride electrode, 0.015" diameter (A-M Systems) grounded to the preamplifier served as the reference electrode and was placed at the far end of the perfusion bath (74). A small-bore hollow stainless steel line connected to a peristaltic pump (Cole/Palmer) was placed in the perfusion bath to prevent overflow. The reservoir was filled with 4°C physiological saline solution, and then the outlet port was opened to allow the saline solution to flow through the cannulated artery. Intra-luminal flow was adjusted between 2 to 4 ml/min (personal communication, Jane Madden, PhD, Medical

College of Wisconsin, Milwaukee, WI.). The vessel was allowed to equilibrate prior to conducting membrane potential measurements.

Impalements were made by carefully advancing the micromanipulator held microelectrodes through the adventitial side of the cannulated artery. A successful impalement was defined as: 1) an immediate negative deflection with time allowed for a stable voltage; 2) an immediate return to baseline (within ± 5%) upon withdrawal of the microelectrode; and 3) a matching (within ± 10%) pre and post microelectrode resistance.

To investigate the effects of depolarizing stimuli, the K^+ concentration of the physiological saline solution perfusate was altered during membrane potential measurement. The following K^+ concentrations were used: 10; 20; 30; 40; 80 and 100mM. For hypoxia studies, physiological saline solution was added to 4°C water-jacketed reservoirs and saturated with compressed air (21% O_2) for normoxic solutions and N_2 for hypoxic solutions. Stainless steel tubing was used to connect the reservoir outlet to the perfusion bath inlet cannula to minimize the uptake of O_2 from room air.

Using an oxygen selective electrode (Microelectrode Inc.), the O_2 content was measured in the perfusate reservoir and in the effluent collected from the perfusion bath outlet cannula. An O_2 percent of zero was achieved in the perfusate reservoir and an O_2 content of ~ 7.6 mm Hg was measured in the outlet cannula effluent when solutions were equilibrated with N_2.

Vascular smooth muscle cells were impaled during normoxic exposure and transmembrane potential was allowed to stabilize. Following a stable transmembrane potential reading, hypoxic perfusate was allowed to flow through the vessel. Care was taken not to create pulsation in the cannulated vessel during perfusate switching.

Bichromatic Spectrophotometry of Plasma Constituents

Centrifuged samples were aliquotted into disposable instrument cups, then placed on the Hitachi 747® Chemistry analyzer. The Hitachi 747® automatically pipettes and proportions the appropriate sample from the instrument cup and reagent volumes into a cuvette (reaction cell). After sample was added to a reaction cell, reagent 1 was added without delay. After the reaction cell contents were mixed and allowed to incubate for an assay specific amount of time, reagent 2 was added. The absorbance at wavelength 570 nm was monitored between two measuring points. The change in absorbance was directly proportional to the concentration of analyte in the sample and was used by the Hitachi 747® to calculate and express the analyte concentration.

Reagents

CEDIA Chemistry Assays, Microgenics Corp.; 1N Sodium Hydroxide, A.R. grade; 2% Hitergent®; Cell Clean 90; CEDIA Calibrators for Chemistry Assays, Microgenics Corporation

Instrumentation

Boehringer Mannheim Hitachi 747® Analyzer

The Hitachi 747® is a fully automated high throughput chemistry analyzer that utilizes bichromatic spectrophotometry. Measurements of the reaction mixture were taken at a primary wavelength (570 nm) and a secondary wavelength (660 nm).

Ion Selective Electrode

Test tubes containing the sample and calibrators to be analyzed were loaded onto the sample sector of the fully automated Synchron LXi 725®. The chemistry tests to be analyzed were selected and the instrument calibrated. Upon completion of the calibration, the analytical analysis was automatically initiated.

Reagents

LX ISE® electrolyte buffer; LX ISE® electrolyte reference reagent

Calibrators

Sodium: 102, 150, 180 mmol/L; Potassium: 4.0, 10.0, 100 mmol/L

Chloride: 62, 109, 180 mmol/L; Urea Nitrogen: 10, 80 mg/dl; Urea mg/dl: 21, 171 mg/dl; Glucose: 50, 200 mg/dl; Creatinine: 1.0, 8.0 mg/dl; Calcium: 5.0, 15.0 mg/dl

Instrumentation

Beckman-Coulter Synchron LXi 725® Analyzer

Enzymatic Measurement of Ethyl Alcohol

The enzymatic method for ethanol is based on the principle that an enzymatic reaction involving alcohol dehydrogenase (ADH) catalyzes the oxidation of ethanol to acetaldehyde. During the reaction, the coenzyme nicotinamide adenine dinucleotide

(NAD) is reduced to NADH, which is measured at 340 nm. The following equation describes the reaction:

$$\text{Ethyl alcohol} + \text{NAD} \xrightarrow{\text{ADH}} \text{NADH} + \text{acetaldehyde}$$

The analytical protocol for the Diagnostic Reagents, Inc. (DRI) Ethyl Alcohol Assay® (i.e., enzymatic method) was consistent with that previously stated for the Hitachi 747® with the following exceptions; an ethanol negative and ethanol 100 mg/dl calibrator was used as references to quantitate samples by creating a standard curve. Measurements of the reaction mixture were taken at the primary wavelength (340 nm) and at the secondary wavelength (505 nm).

The change in absorbance at 340 nm is directly proportional to the concentration of ethanol in the sample and is used by the Hitachi 747® to calculate and express the ethanol concentration. The reaction rates on the Hitachi 747™ were calculated using the following formula:

$Cx = K(Ax - Ab) + Cb$

Where: Cx = Concentration of Sample

K = Concentration Factor (determined during calibration)

Ax = Mean of absorbances of Sample + Reagent 1

Ab = Mean of absorbances of Blank + Reagent 1

Cb = Concentration of Blank (STD. 1)

A quantitative concentration =10 mg/dl was interpreted as positive, lesser concentrations were interpreted as negative. A fresh aliquot of each sample identified

as positive for ethanol by the enzymatic method was subsequently submitted for a more definitive analysis of ethanol via headspace gas chromatography.

Reagents

Ethyl Alcohol Assay®, DRI; Ethyl Alcohol 100 mg/dl Calibrator, DRI;

Normal saline, (Sodium Chloride solution, 0.85%), LABSCO

Instrumentation

Boehringer Mannheim Hitachi 747® Analyzer

Ethanol by Headspace Gas Chromatography

Headspace gas chromatography is based on Henry's law of physics, which states that the ratio of a dissolved substance in an aqueous solution is dependent on temperature, pressure and concentration in the aqueous medium. Thus, a volatile compound (e.g., ethanol) may be measured by analyzing the vapor in equilibrium with the liquid. Samples containing volatile compounds liberate a gas when heated to its boiling point. In this study, a sample of the liberated gas i.e., "headspace gas" was injected in the gas chromatograph.

To identify volatile compounds, the retention times of the calibrating standard was compared to the retention times of the unknown. The criterion for positive volatile identification was: compared retention times must agree within ±5% percent. In batches of samples analyzed in this study, the retention times of the internal standard seldom varied by more than ±2% (approximately 200 samples, inclusive of

standards and controls were analyzed using the headspace gas chromatography technique).

Ethanol was quantitatively measured by headspace gas chromatography via a Varian 3300® Gas Chromatograph connected to a Tekmar 7000/7050® Headspace Analyzer. 100 mcL of working internal standard (80.0 mg/dl n-Propanol) and 100 mcL of sample were added to a 20-ml sample vial. The sample vial was covered with an aluminum cap ring fitted with a Teflon® lined septum. The cap ring was tightly crimped and placed in the Tekmar® Headspace Autosampler for sample preconditioning. The Tekmar® Headspace Autosampler was used to inject a sample of headspace gas into a heated transfer line connected to the Varian 3300® Gas Chromatograph.

A flame ionization detector was installed in the gas chromatograph for the detection of hydrocarbons. Hydrocarbon analytes were detected as CHO^+ fragments as they burned in a hydrogen/air flame. These fragments created a measurable current between two electrodes.

The Hewlett Packard 3396A® data integrator was used to generate chromatograms and to measure the area of target volatile compounds and the internal standard in each chromatogram. Samples with a quantitative ethanol concentration equal to or greater than the instrument limit of detection (i.e., 5.0 mg/dl) were considered positive for ethanol.

Prior to analysis, the following protocols were used to prepare standards and program the instruments:

Standards

1-Propanol, Fisher, Certified Grade; 2-Propanol (Isopropanol), Fisher, HPLC Grade; Methanol, Fisher, HPLC Grade; Ethanol, 100%, Aaper Alcohol and Chemical Co., USP and Acetone, Fisher, HPLC Grade.

Standard Preparation

Working Internal Standard (80.0 mg/dl n-Propanol in deionized water)

1-Propanol and deionized water (1:1000).

Working Standard (Based on densities at 25°C)

Standards were equilibrated to 25°C in a water bath. Quantities listed below were transferred to a 1-liter volumetric flask and diluted to volume with deionized water.

Volatile	Required ml	Final Conc. mg/dl
Methanol	1.0	80.0
Acetone	0.5	40.0
Isopropanol	1.0	80.0
Ethanol	1.0	80.0

Instrumentation:

Tekmar 7000/7050® Headspace Analyzer: Platen = 80°C; Valve = 100°C; Line = 100°C.

Varian 3300® Gas Chromatograph: Column temperature = 80°C; Injector temperature = 190°C; Detector temperature = 200°C.

Analytical column: Carbopack B, 60/80 mesh, coated with 5% Carbowax 20 m - 4 meter.

Benzocaine by Gas Chromatography/Mass Spectrometry

Benzocaine and Aprobarbital in plasma were first acidified pH (1-2) then extracted at neutral pH with methylene chloride. The organic phase was separated from the plasma and dried under nitrogen. The sample was reconstituted in isopropyl alcohol then analyzed by Gas Chromatography/Mass Spectrometry.

500 µL of plasma, 100 µL of working internal standard, 500 µL of 1.5 M ammonium sulfate and 100 µL of 3N HCl were added to a glass test tube then immediately vortex mixed at high speed for 5 seconds. 5 ml of methylene chloride was added to each tube then capped tightly with a Teflon®-lined cap. Tubes were placed on a rotator for 4 minutes at 35 RPM. Tubes were then placed in a centrifuge for three minutes at 3000 RPM. The upper aqueous layer was removed by aspiration, taking care to aspirate as little of the organic layer as possible. The organic layer was decanted into 15 ml conical bottom tubes, taking care to avoid transfer of any residual aqueous phase. The organic phase was concentrated by complete evaporation under nitrogen at 45°C - 55°C. The concentrated extract was then reconstituted with 200 µL isopropanol and vortex mixed for 30 seconds then transferred to a gas chromatography/mass spectrometry injection vial and tightly sealed with an aluminum ring cap fitted with a Teflon®-lined septum.

A capillary column heated via temperature programming of the gas chromatograph produced adequate separation between benzocaine and the internal standard, aprobarbital. Helium carrier gas was supplied to the capillary column via

constant pressure at the head of the column. An ionization voltage of 70 eV was used for electron impact fragmentation.

Three major ions for benzocaine and two major ions for aprobarbital were monitored. For each analytical run, the ion ratios of the calibrating standard were used to set criteria for positive identification of a benzocaine in unknowns or control samples. The ions selected for monitoring were masses 92, 120 and 165 for benzocaine and masses 124 and 167 for aprobarbital.

When a sample extract was injected into the gas chromatograph injection port, the sample was immediately volatilized. Analyte(s) in the sample were swept towards the capillary column and partitioned between the stationary phase and the gas phase. Aprobarbital had the greatest affinity for the stationary phase, spending a longer time in that phase and consequently taking longer to reach the mass selective detector. Vaporized substances (i.e., molecules) were introduced into the mass spectrometer directly from the capillary column. As the molecules were introduced into the mass spectrometer, they were bombarded with a stream of high-energy electrons. The absorbed energy caused fragmentation of the molecules to produce both positive and negative ions. In the bombardment process, the loss of a single electron produced the positively charged "molecular ion." This ion represented the intact molecule and is the ultimate precursor to all fragment ions. Prior to analysis, the following protocols were used to prepare reagent and standards and to program the instrument:

Standards/Reagents

Methanol, HPLC grade, Fisher; Methylene Chloride, HPLC grade, Fisher; Hydrochloric Acid, AR grade, Fisher; Ammonium Sulfate, AR grade; Isopropanol, HPLC grade, Fisher; Hydrochloric Acid, 3N: 25 ml concentrated HCl added to a 100-ml graduated cylinder containing approximately 50 ml deionized water then diluted to volume with deionized water. Ammonium Sulfate, 1.5M: in a 1000-ml Erlenmeyer flask approximately 500 ml of deionized water was added to 198 g of ammonium sulphate mixed then diluted to 1000 ml with deionized water.

Instrumentation

Hewlett-Packard HP G1800A GCD Chemstation

Instrument Conditions: Inlet: 270°C; Detector: 280°C; Splitless injection; Initial temperature = 100°C; Oven Ramp: 17°C/minute, 275°C-1.0 minute, 20°C/minute 290°C 6.0 minute.

Analytical column: Phenylmethylsilicone

Ion source pressure: = 1.2×10^{-5} torr. Carrier gas: Ultra-pure helium at 35 ml/minute.

Statistics

Method comparisons were made by student's *t-test* and multiple comparisons of means by analysis of variance followed with student-Newman Keul's tests. Differences between pairs of results (e.g., headspace gas chromatography and enzymatic method) were evaluated by paired *t-test*. Changes in membrane potential between cells of the same vessel were compared using paired *t*-test. Comparison of membrane potential between vessels was made using the unpaired *t*-test.

CHAPTER 3

RESULTS

Histology of Systemic Arteries

Segments of systemic arteries were prepared for examination by light microscopy. Microscopic examination of these arteries was conducted to assess tissue composition and the extent of smooth muscle present. Examination of hagfish (n=13) and lamprey (n=22) dorsal aortas revealed that each vessel type was composed of a thin endothelial layer, basal elastic lamina, connective tissue, smooth muscle, and an adventitial layer. Both vessel types gradually tapered in caliber from cephalic to caudal regions. The endothelial layer for both vessel types was composed of a single layer of endothelial cells aligned with the long axis of the vessel. The chief component of the media was spirally arranged smooth muscle intertwined with connective tissue. The dorsal aorta of hagfish was from two to four cell layers thick, whereas the dorsal aorta of lamprey was much thicker, from twenty to thirty cell layers. The thickness and structural complexity of the adventitial layer was greatest for lamprey dorsal aorta.

Hematoxylin/eosin and Masson (Trichrome) stains were used to perform histological evaluations of hagfish and lamprey systemic arteries. The pH basic hematoxylin solution stained the acidic properties of the vascular smooth muscle, such as the nucleus, mucin cartilage and calcium deposits dark blue. The pH acidic eosin solution stained the basic tissue constituents (i.e., cytoplasm, erythrocytes and collagen) varying shades of red. Three dyes in the Trichrome stain provided a

distinction between muscle and collagen tissue: black (Nuclei); red (cytoplasm, keratin, muscle fibers); blue (collagen, mucin). The acid dye, Biebrich scarlet-acid fuchsin, stained the acidophilic cytoplasm, muscle fibers and collagen. The phosphotungstic-phosphomolybdic acid diffused the Biebrich scarlet-acid fuchsin out of the collagen fibers. Aniline blue replaced the acid thus rendering the collagen blue.

Stained tissue sections revealed cellular structures, patterns of cell arrangement and morphological similarities (e.g., fibroblasts and myocytes) consistent with such features present in higher vertebrate systemic arteries.

Hematoxylin/eosin stained vascular smooth muscle cell nuclei in the dorsal aorta of both hagfish (Fig. 2) and lamprey (Fig. 3) blue and cytoplasm and other tissue constituents varying shades of red.

Muscle was distinguished from collagen by using trichrome stain, which dyed vascular muscle (red), collagen (blue) and nuclei (black) in hagfish dorsal aorta (Fig. 4) and in lamprey dorsal aorta (Fig. 5). A Trichrome stained transverse slice through a lamprey mid-body revealed distinctly stained muscle layers, collagen bundles and cell nuclei. An example of the specificity of the trichrome dye was demonstrated in slides taken from the mid-body sections where nuclei of erythrocytes in the lumens of the dorsal aorta and cardinal veins were distinctly stained black (Figures 6 and 7).

When compared to the lamprey dorsal aorta, hagfish dorsal aorta appeared to be more "primitive". The predominant vascular architecture in the hagfish dorsal aorta was a relatively thin support matrix associated with a sparse smooth muscle cell population. Hagfish dorsal aorta vascular architecture was consistent with the type of

vascular architecture expected where there is a low intra-vascular blood pressure. Lamprey dorsal aorta exhibited not only a thicker wall structure than hagfish dorsal aorta, but exhibited a moderately dense population of smooth muscle cells embedded in a lattice-like structure of supportive connective tissue. The paucity of smooth muscle in hagfish dorsal aorta may explain the comparatively low rate of successful microelectrode impalements (hagfish 15%, lamprey 35%; n = 80 attempts) obtained for transmembrane potential measurements in this study.

No formal measures were taken to establish the age of fish, however, observation of external characteristics such as healed wounds, coloration and thickness of skin were noted. Histological examination of the dorsal aorta from "older appearing" lamprey (i.e., fish with multiple external scars and thick skin) routinely showed a more prominent arrangement of elastic fiber fragments (e.g., collagen) and less smooth muscle with an accumulation of background substance.

These histological examinations suggest that variations in the number of smooth muscle cells, amount of elastic tissue and the network of connective tissue may contribute to differences in the physiological behavior and functional response of the different vessel types.

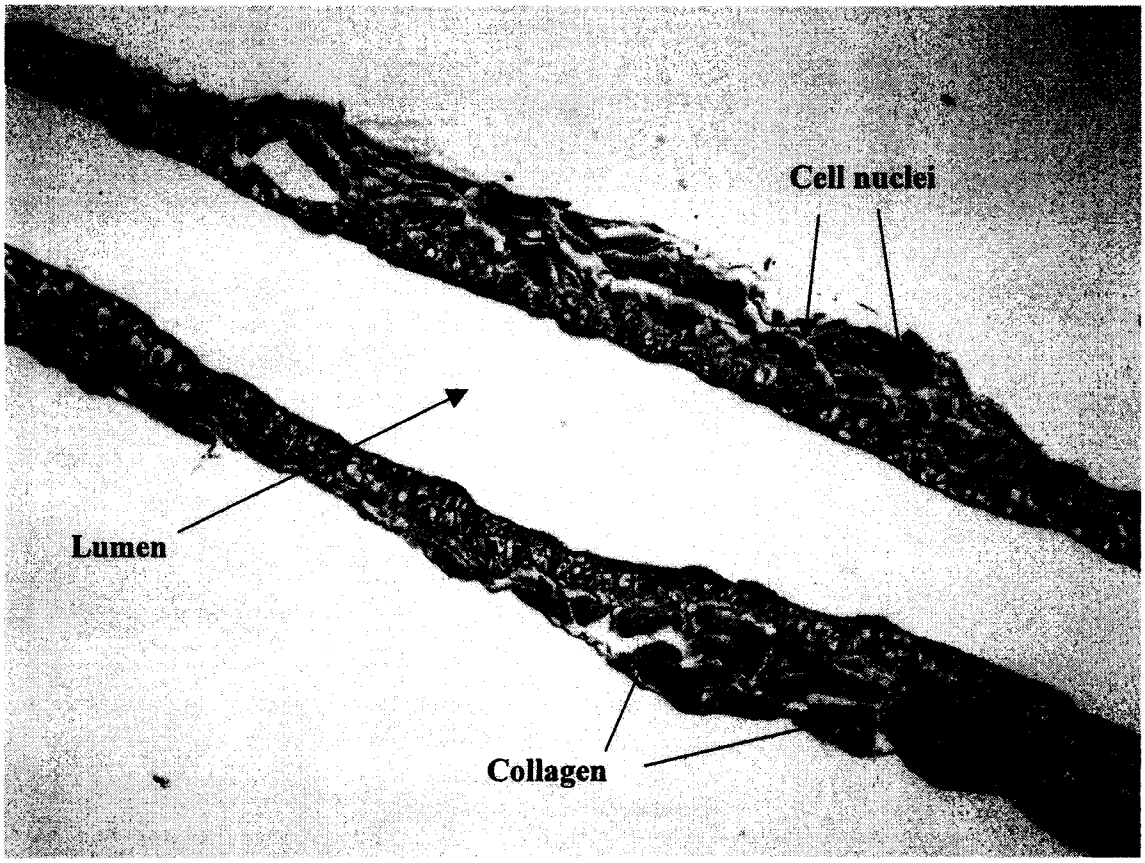

Figure 2. Hematoxylin/Eosin Stain of Hagfish Dorsal Aorta

Vascular smooth muscle cell nuclei are darkly stained. Only 2-3 layers of vascular smooth muscle cells are present with a thin band of collagen.

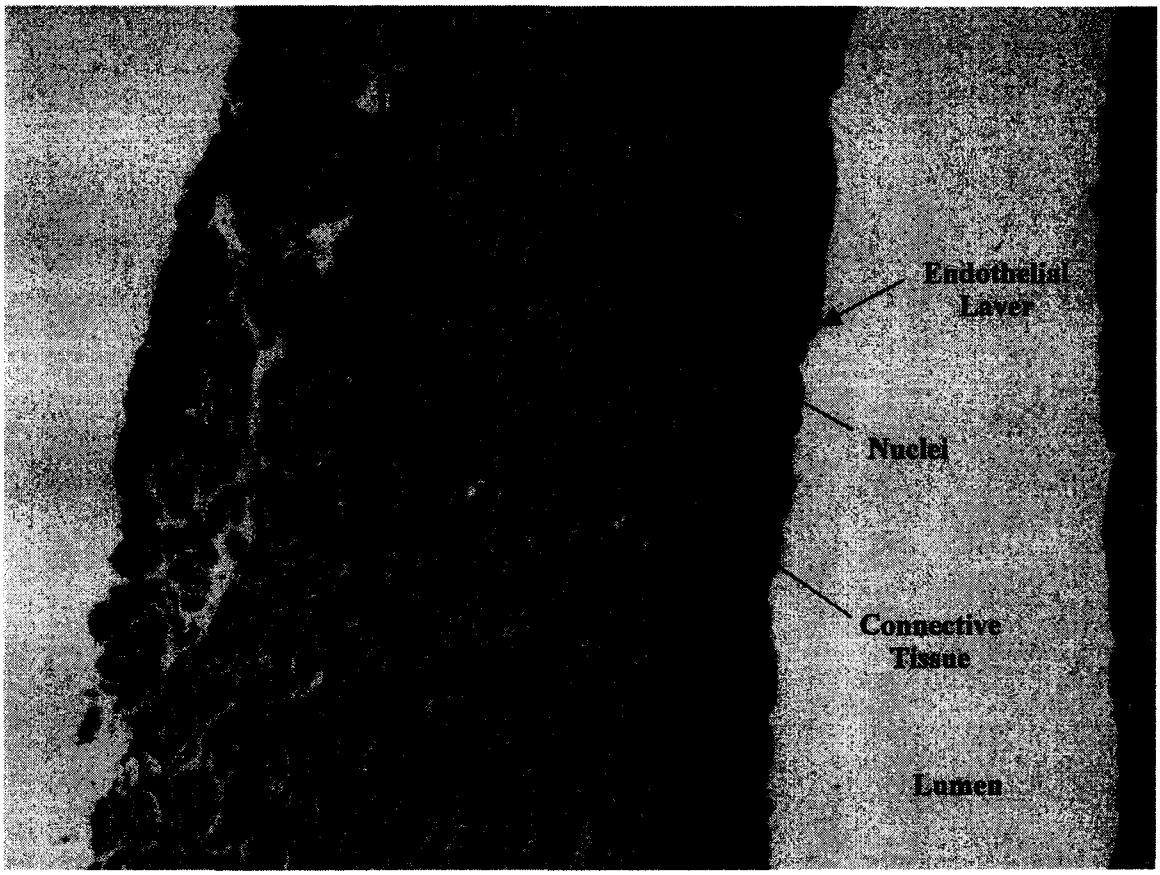

Figure 3. Hematoxylin/Eosin Stain of Lamprey Dorsal Aorta

Vascular smooth muscle cell nuclei are darkly stained. Multiple layers of vascular smooth muscle cells are present with an extensive network of connective tissue.

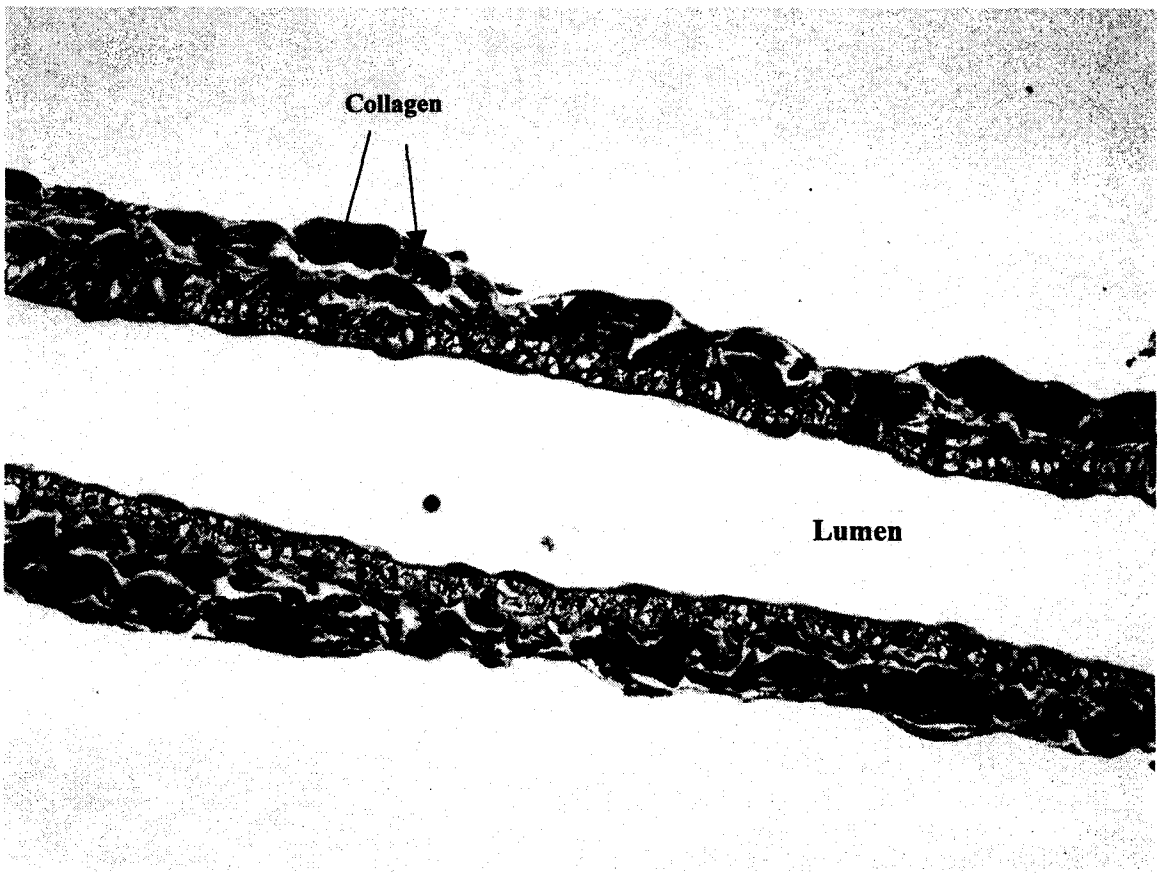

Figure 4. Masson Trichrome Stain of Hagfish Dorsal Aorta

Connective material (e.g., collagen) is stained with a distinctive blue color.

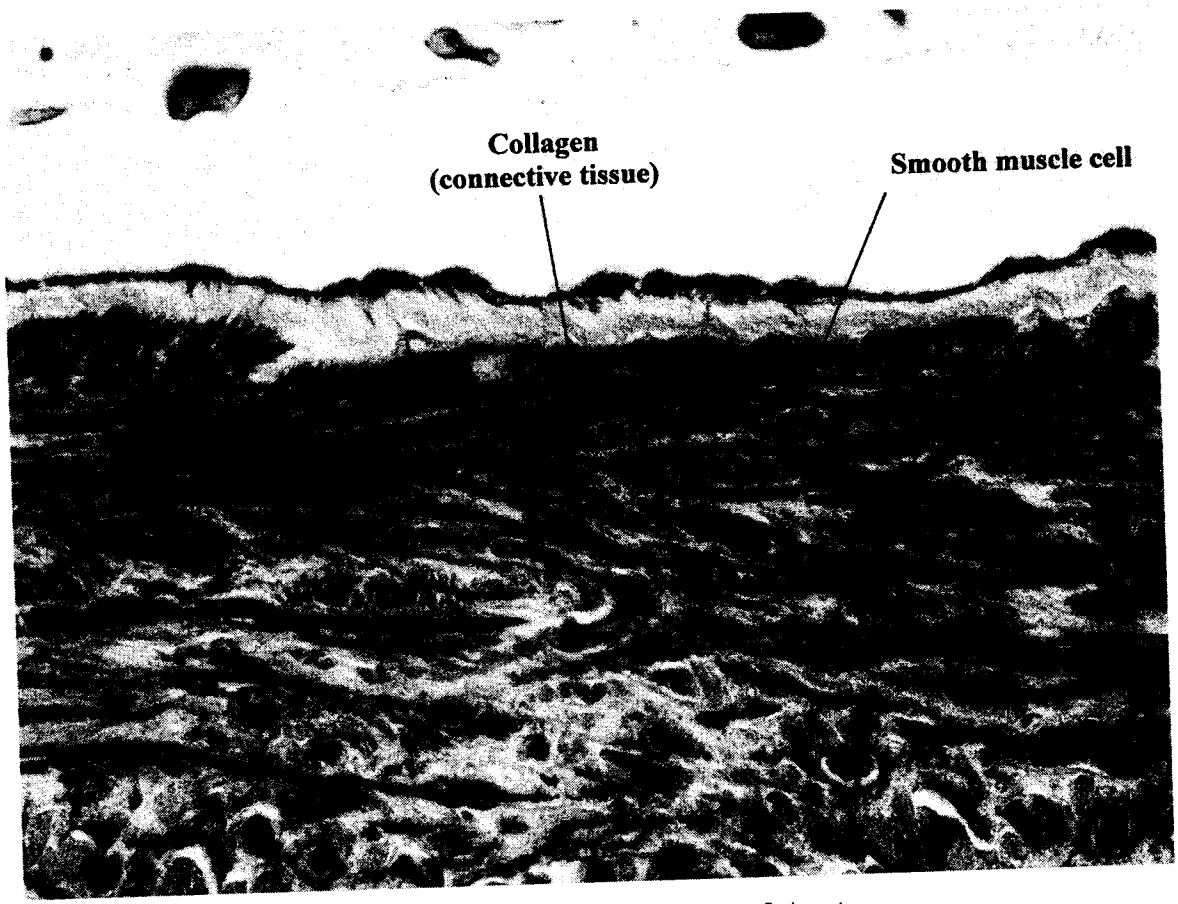

Figure 5. Masson Trichrome Stain of Lamprey Dorsal Aorta

Collagen is readily distinguished from smooth muscle.

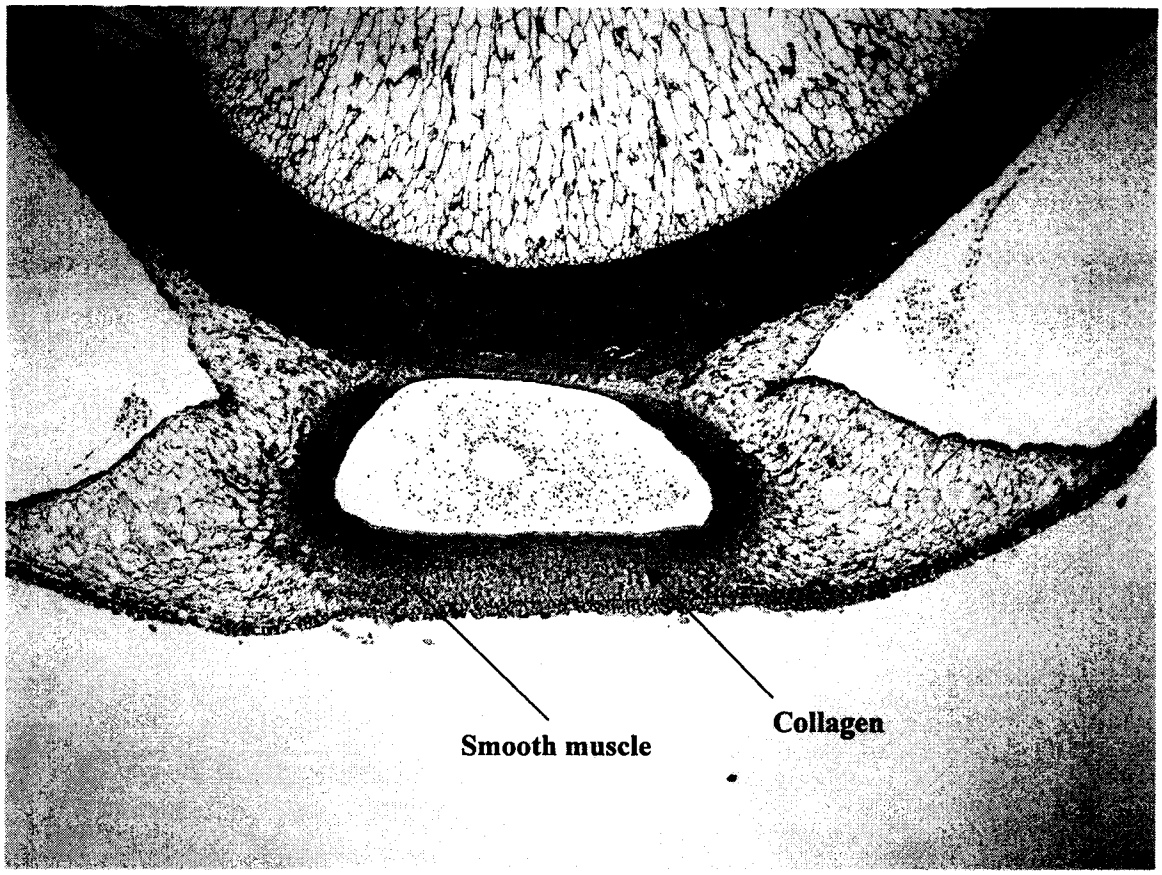

Figure 6. Masson Trichrome Stain of Lamprey Mid-Body -I

Masson Trichrome stain stained smooth muscle in the dorsal aorta red and collagen layers blue.

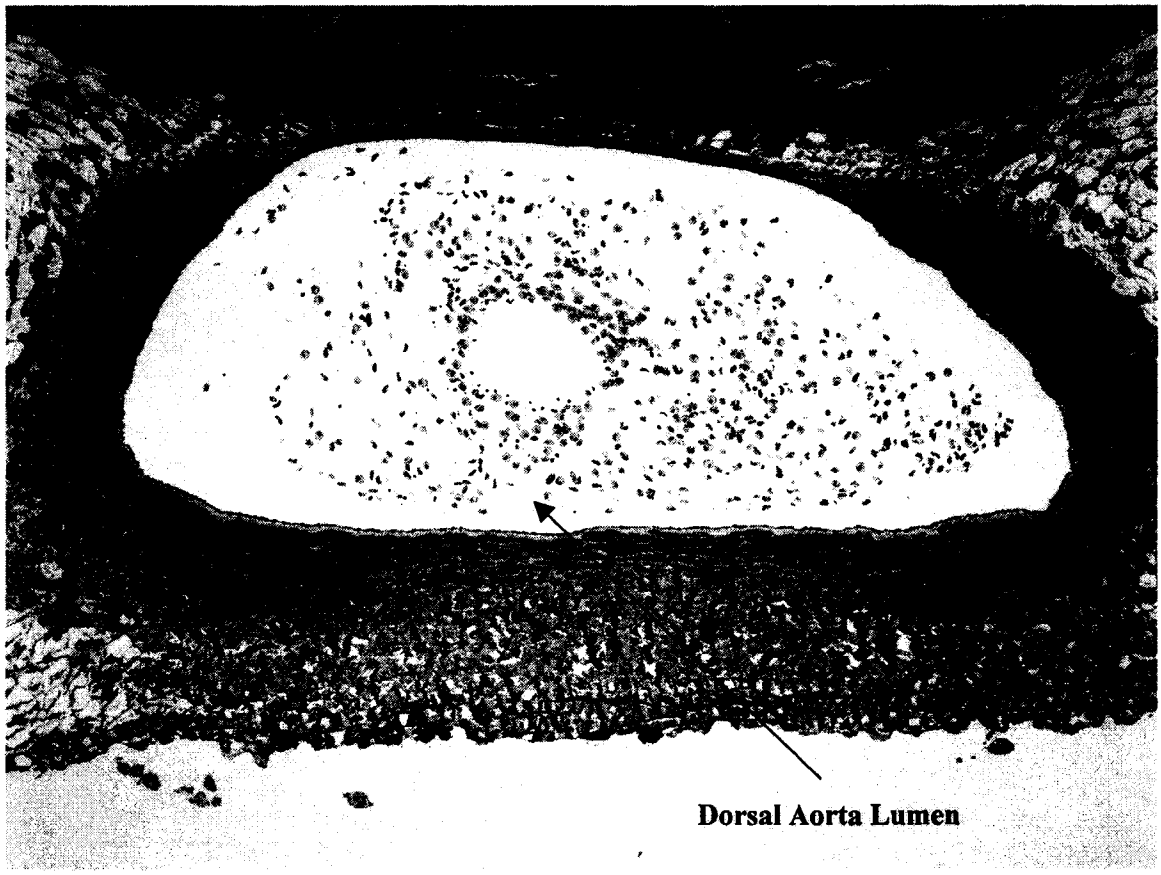

Figure 7. Masson Trichrome Stain of Lamprey Mid-Body - II

An example of the Masson Trichrome dye specificity is demonstrated in this micrograph where nuclei of erythrocytes in the lumen of the dorsal aorta are distinctly stained black.

Composition of Hagfish, Lamprey, and Trout Plasma

Following the initial unsuccessful attempts at isolating vascular smooth muscle cells from lamprey aortas, species-specific physiological saline solutions were developed for use in subsequent experiments. An analysis was performed on plasma collected from hagfish, lamprey, and trout to determine their chemical composition. Major plasma electrolytes (i.e., Na^+, Ca^{2+}, K^+, Mg^{2+}, and Cl^-) were measured by ion selective electrode and bichromatic spectrophotometry and osmolality was measured via freezing point depression osmometry.

Analysis of hagfish, lamprey and rainbow trout plasma revealed: 1) approximately 90% of the total cation concentration was attributable to the Na^+ concentration; 2) Na^+ and Cl^- were the most abundant extracellular ions; 3) K^+ was the least abundant extracellular ion; and 4) Mg^{+2} concentrations were highest in marine fish (Table 6). Use of saline solutions that matched the animal's unique plasma chemistry (particularly with isolated cells) was designed to prevent differences in osmotic pressure across the two sides of the membrane.

Table 6. Composition of Hagfish, Lamprey, and Trout Plasma

Animal/Fluid	Na^+ mmol l^{-1}	K^+ mmol l^{-1}	Ca^{2+} mmol l^{-1}	Mg^{2+} mmol l^{-1}	Cl^- mmol l^{-1}	Osmolality mOsm/Kg	Ref
Seawater	480	10	10	55	560	1033	1
Myxine glutinosa /plasma	487	8	4	9	510	1059	2
Myxine glutinosa /plasma	523	7.8	5.0	11.6	541	1095	3
Eptatretus burgeri /plasma	531.8	12.4	6.5	10.1	397	1009.7	4
Eptatretus stoutii /plasma	518 ± 41.4 n = 15	7.04 ± 1.07 n = 15	4.28 ± 0.37 n = 15	10.6 ± 1.31 n = 15	509 ± 45.4 n = 15	1000 ± 42.5 n = 5	This study
Freshwater	1.5	0.2	3.0	0.6	1.4	-	5
Onchorhyncus mykiss /serum	152	-	-	-	127	289	5
Onchorhyncus mykiss /plasma	151.8 ± 0.4 n = 5	1.2 ± 0.14 n = 5	2.27 ± 0.12 n = 5	1.02 ± 0.062 n = 5	127.4 ± 1.3 n = 5	294.4 ± 0.89 n = 5	This study
Lampetra/ extracellular fluid	120	3.2	1.9	2.1	96	248	6
Petromyzon marinus /plasma	125.12 ± 7.3 n = 25	2.9 ± 0.7 n = 25	2.12 ± 0.2 n = 25	1.60 ± 0.206 n = 16	106.24 ± 8.1 n = 25	247 ± 12.9 n = 18	This study

1. Barnes, H. *J. Exp. Biol.* 31:582-588, 1994
2. Robertson, J.D. *J. Zool.* 178:261-277, 1976
3. Robertson, J.D. *Comp. Biochem. Physiol.* 84A:751-757, 1986
4. Inoue et al. *J. Exp. Biol.* 205:3535-3541, 2002
5. Vedel, N.E, Korsgaard, B, Jensen, B.F. *Aqua. Tox.* 41:325-342, 1998
6. Schmidt-Nielsen, 1972; Prosser, 1973

Vascular Smooth Muscle Cell Isolation

The disaggregation and isolation of viable individual smooth muscle cells from vascular tissue is at best challenging. There is no single best method to disaggregate solid tissue into single cells. The two techniques commonly used to disaggregate solid tissue into single cells are enzymatic (28, 83, 106, 138) and mechanical (10, 73, 141). Wide selections of enzymes are available for enzymatic procedures and include trypsin, nonspecific proteases, and various types of collagenase, hyaluronidase, and papain. Mechanical disruption techniques may be as simple as triturating minced tissue through pipettes or as elaborate as using a "tissue press" (141).

Regardless of the technique utilized, the ideal goal of any single-cell isolation protocol is to achieve high yield and high viability of the target cell type. An optimized isolation technique should produce the greatest number of single cells that present the characteristic relaxed spindle-shaped morphology. However, a low yield of cells with high viability may be adequate to conduct experiments.

Despite the inherent challenges, several researchers have successfully devised single-cell isolation techniques to investigate morphological and physiological characteristics in vascular smooth muscle (32, 62, 71, 76, 110, 160, 171).

Isolation of Lamprey Dorsal Aorta Smooth Muscle Cells

Single spindle-shaped vascular smooth muscle cells were isolated from lamprey dorsal aorta. Isolated smooth muscle cells were maintained for a maximum of four hours at 2-6° C. Some enzymes (e.g., elastin, papain) did not produce a recognizable amount of isolated smooth muscle cells and were for the present study deemed ineffective. Given the numerous procedural variants such as, the isolation temperature, length of enzyme incubation, the stated enzyme digestion activity versus the actual enzyme digestion activity, it is possible that the ideal combination of conditions where not satisfied for each enzyme. Thus, the "ineffective" enzymes may in fact be acceptable under optimized conditions.

The yield of viable spindle-shaped vascular smooth muscle cells using various isolation techniques were broad (5 - 60%). The highest yield of viable cells (60%) was obtained when collagenase Type XI (Sigma) and trypsin were combined and used in the disaggregation process. Dispersion of cells in a 2mM Ca^{2+} solution also enhanced the cell isolation efficiency. The extent of digestion appeared to be dependent on the specific enzyme, the concentration of the enzyme and the time of the incubation.

When collagenase Type XI was the only enzyme used in the disaggregation step, deleterious effects (e.g., ruptured cell membranes, hyper-contracted cells, and non-responsive cells) were seen in approximately 70% of the isolated cells. When trypsin was the sole enzyme used, approximately 90% of the isolated cells were damaged or non-responsive cells (Table 7). When lamprey dorsal aorta segments were

incubated for a short enzymatic period (< 30 minutes) then processed using one of the disruption techniques, dispersed cells appeared to rapidly degrade (hyper-contracted or rupture within ± 5 minutes), thus limiting the opportunity for conducting isolated vascular smooth muscle cell experiments. Both mechanical disruption techniques evaluated in this study proved to be extremely damaging to cells. Application of mechanical disruption techniques may not be possible for all tissue types and may be best used for more robust tissue types such as cardiac and skeletal muscle.

The enzymatic isolation technique eventually developed resulted in 50-75 relaxed cells per 0.02 ml aliquot. The technique was effective in isolating relaxed, spindle-shaped smooth muscle cells from the dorsal aorta of sea lamprey, *Petromyzon marinus*. Isolated single lamprey dorsal aorta vascular smooth muscle cells were viewed by light microscopy (200x magnification). Cells isolated by this technique were treated with a vital stain (Trypan Blue) to assess the integrity of the cell membrane. About 50% of the cells did not take up the stain suggesting these cells had intact membranes (n=4). Application of norepinephrine in the immediate field of isolated smooth muscle cells caused cells to tightly contract, resulting in a rounded appearance. No pre-contraction measurements of the isolated cells were taken, thus, quantitative values could not be assigned to the post-norepinephrine contraction.

The primary purpose for developing the enzymatic isolation technique described above was to characterize the electrophysiological properties of vascular smooth muscle cells isolated from fish. Intracellular recording of membrane potential in isolated cells was attempted but discontinued due to instrumentation limitations.

These limitations prompted modifications to be made which resulted in a different approach being taken to meet the original study proposal. A protocol involving whole tissue (i.e., cannulated perfused arteries) rather than isolated cells was developed to measure membrane potential in the arteries of fish included in the present study.

Although the primary purpose for developing the enzymatic isolation technique (i.e., characterization of membrane potential in piscine vascular smooth muscle cells) was not met in the present study, the technique was successfully used by M.J. Russell to visualize intracellular calcium in single isolated cells from the dorsal aorta of sea lamprey (PhD Dissertation: University of Notre Dame, Biological Sciences, December 2002).

Table 7. Enzymatic Isolation Protocols

Enzyme/ Reagents	n	Incubation Time	Temp ° C	Dispersion Solution	Relaxed or Contracted	Viable	Notes
Trypsin (0.2%)	2	16 hours	4	4mM Ca^{2+}	95%Contracted	Not Tested	No Change in Tissue
Trypsin (0.2%)	2	8 hours	10	4mM Ca^{2+}	No cells	Not Tested	Tissue Clumps
Trypsin (0.2%)	2	4 hours	25	4mM Ca^{2+}	No cells	Not Tested	Tissue Debris
Trypsin (0.2%)	2	1 hour	37	4mM Ca^{2+}	No cells	Not Tested	No cells
Trypsin 0.2% / VP2000	2	3.0/1.5 hours	15	Ø Ca^{2+}	No cells	Not Tested	Decrease time/ No change
VP2000:LPSS (2:1)	1	1.5 hours	25	Ø Ca^{2+}	No cells	Not Tested	Lethal
VP2000:LPSS (2:1)	1	1.5 hours	37	Ø Ca^{2+}	No cells	Not Tested	Lethal
Dipase	2	2 hours	37	4mM Ca^{2+}	No cells	Not Tested	Activity 0.6-2.4 UI/ml
Collagenase C-2139	3	12 hours	12	4mM Ca^{2+}	Contracted	Not Tested	Cells ~ 30/0.2 ml
Dipase + Collagenase	2	8 hours	12	4mM Ca^{2+}	No cells	Not Tested	No Cells C-2139
Trypsin 0.2% + Collagenase	2	8 hours	12	4mM Ca^{2+}	No cells	Not Tested	C-2139 Cell Debris
Trypsin 0.1% + Collagenase	2	8 hours	12	4mM Ca^{2+}	Contracted	Not Tested	C-2139
Collagenase C-0130 Type I	3	4 hours	12	2mM Ca^{2+}	95%Contracted	No	289 units/mg FALGPA 0.49 units/mg
Collagenase Type XI	3	4 hours	12	2mM Ca^{2+}	Relaxed ~ 30%	Yes	1,630 units/mg FALGPA 3.4 units/mg
Coll. Type XI + Trypsin	4	2-3 hours	14	2mM Ca^{2+}	Relaxed ~ 60%	Yes	1,630 units/mg FALGPA 3.4 units/mg

LPSS = Lamprey Physiological Saline Solution

Membrane Potential Measurement in Perfused Arteries

Whole tissue studies were developed to characterize membrane potential in systemic arteries from hagfish, lamprey, and rainbow trout. Arteries were isolated, perfused and placed on cannula in a temperature-controlled perfusion bath. Multimeter data acquisition software (MeterView®) was used to log data over an extended period of time while displaying measurements and waveforms as a virtual oscilloscope on a personal computer monitor. Data were sampled and plotted at 1second intervals. Hardcopies of records were made either on a chart recorder or from printable computer files.

Initial experiments (n = 4) resulted in less successful impalements in the dorsal aorta of hagfish and lamprey than in the efferent branchial artery rainbow trout. An increase in microelectrode resistance and distortion to waveforms on the oscilloscope was seen when microelectrodes approached the adventitial side of some vessels. Not surprisingly, the sub-micron microelectrode tip openings were occasionally plugged by extraneous tissue adhering to arteries. An increase in baseline noise was an indicator of a plugged microelectrode tip. To overcome this problem, lamprey and trout arteries were carefully cleaned of extra-adventitial tissue to minimize plugging of microelectrode tip openings.

Membrane potential measurements, in vascular smooth muscle cells was made via direct contact with the cell interior by advancing micromanipulator held glass microelectrodes filled with 3M KCl through the adventitial side of constantly perfused arteries. A successful impalement was considered when an immediate

negative deflection was displayed upon impaling the cell with time allowed for the membrane potential to reach a stable value and an immediate return to baseline (within ± 5%) after withdrawing the microelectrode (Fig. 8). Additionally, the microelectrode resistance for pre and post impalements was required to be within ± 10%.

Resting membrane potential measurements in unstimulated perfused vessels were similar, - 52.7 ±2.9 mV, n=15, - 54.3 ±5.2 mV, n=32 and – 48.3 ±1.6 mV, n=27 for hagfish, lamprey, and trout respectively (Fig. 9). The graphical display for a typical at rest membrane potential was generally similar between hagfish, lamprey, and trout (Fig. 10, 11, and 12).

The effects of changes in extracellular K^+ concentration were examined by varying the K^+ concentration in the physiological saline perfusate during membrane potential measurements. 100mM KCl depolarized hagfish vascular smooth muscle cells 42 .6 ± 6.6 mV, n=5. Changing the perfusate KCl concentration from 100mM to 4 mM (normal), re-polarized K^+ depolarized hagfish vascular smooth muscle cells to near resting potential values (Fig. 13).

In an experiment utilizing lamprey dorsal aorta (n=7), the resting membrane potential (-48.2 ± 4.7) was depolarized 30.3 ± 1.3 mV when the KCl concentration was approximately 40 mM. When the perfusate concentration was 80 mM KCL, vascular smooth muscle cells completely depolarized to 40.2 ± 1.8 mV (Fig. 14).

During membrane potential measurement of rainbow trout efferent branchial arteries, two consecutive 20 mM KCl perfusate increases resulted in an initial 25 mV

depolarization followed by an abrupt positive change in voltage. This abrupt change was suggestive of a compromise in the integrity of the cell impalement (microelectrode dislodged from the cell) and termination of membrane potential recording (Fig 15).

The effects of hypoxia on resting membrane potential in lamprey vascular smooth muscle cells were evaluated by perfusing cannulated lamprey dorsal aorta with nitrogen-saturated physiological saline to create a hypoxic environment. Lamprey vascular smooth muscle cells depolarized 42.5 ±3.7 mV, n=7 from a resting membrane potential of –49.7 ± 5.2 in a manner similar to what was demonstrated for studies involving increases in extracellular K^+ (Fig 16). Thus, qualitatively comparable responses were received with both depolarizing stimuli (i.e., extracellular K^+ and N_2).

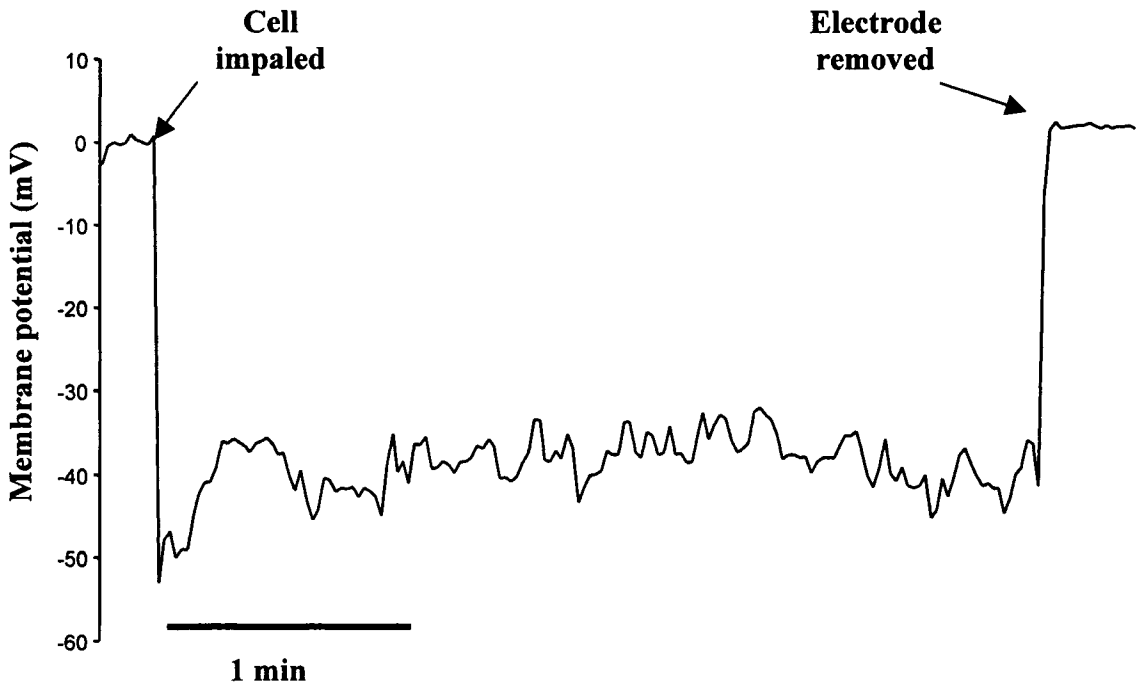

Figure 8. Criteria for Successful Vascular Smooth Muscle Cell Impalement

(1) An immediate negative deflection with time allowed reaching a stable voltage

(2) An immediate return to baseline (within ± 5%) upon microelectrode withdrawal

(3) A matching (within ± 10%) pre and post microelectrode resistance

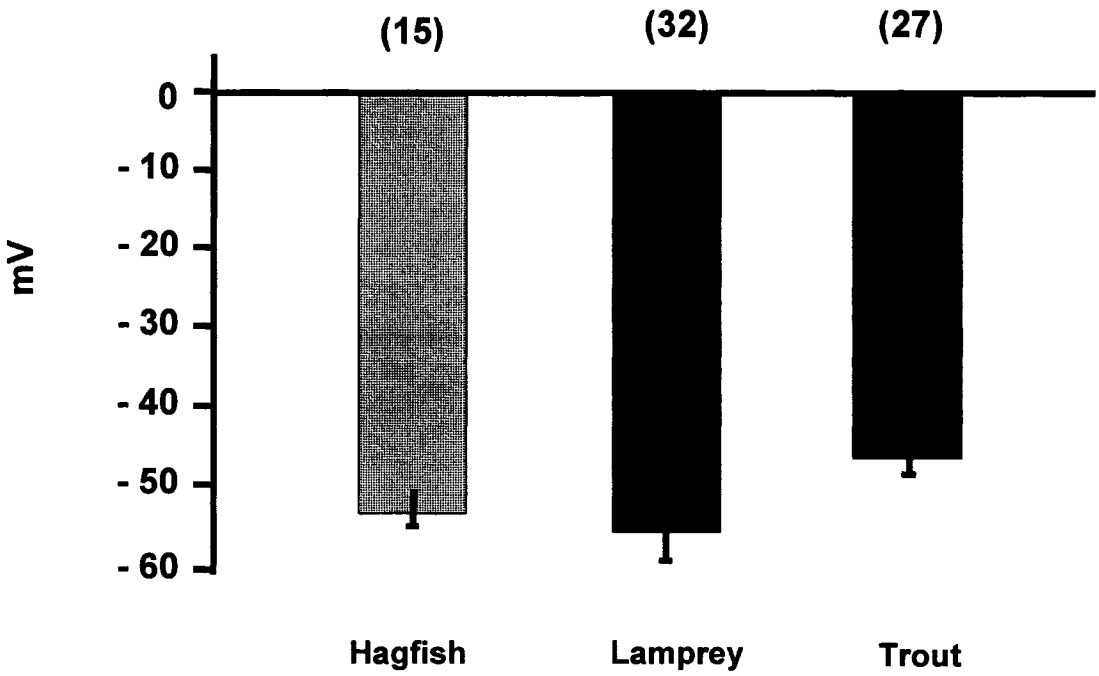

Figure 9. Resting Membrane Potential – Hagfish, Lamprey and Trout

Resting membrane potential for unstimulated vessels showed similarities in response, - 52.7 ±2.9 mV (n=15), - 54.3 ±5.2 mV (n=32) and – 48.3 ±1.6 mV (n=27) for Pacific hagfish, Sea lamprey and Rainbow trout respectively

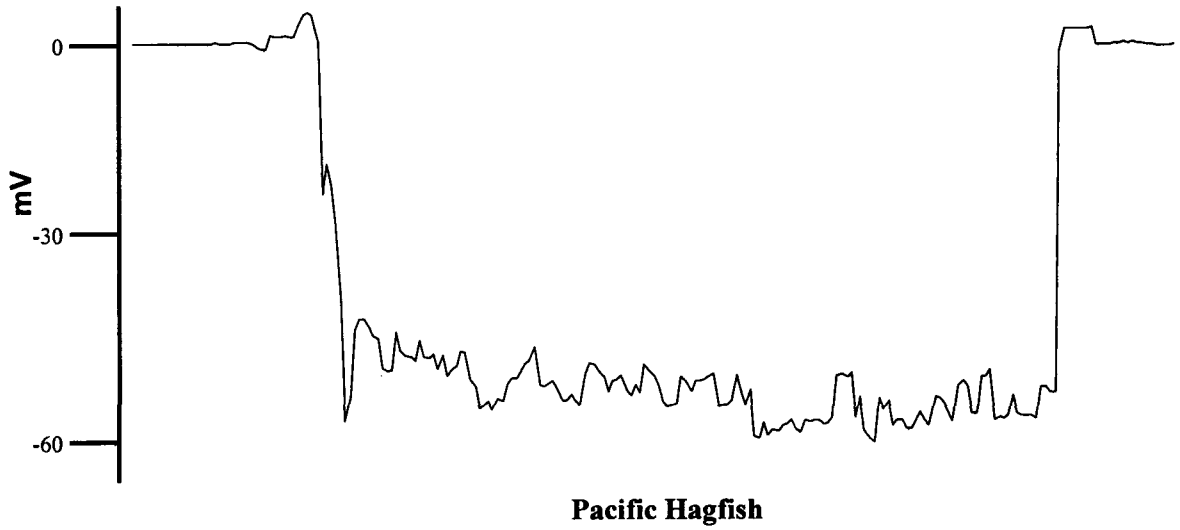

Figure 10. Typical Tracing of Resting Membrane Potential – Pacific Hagfish

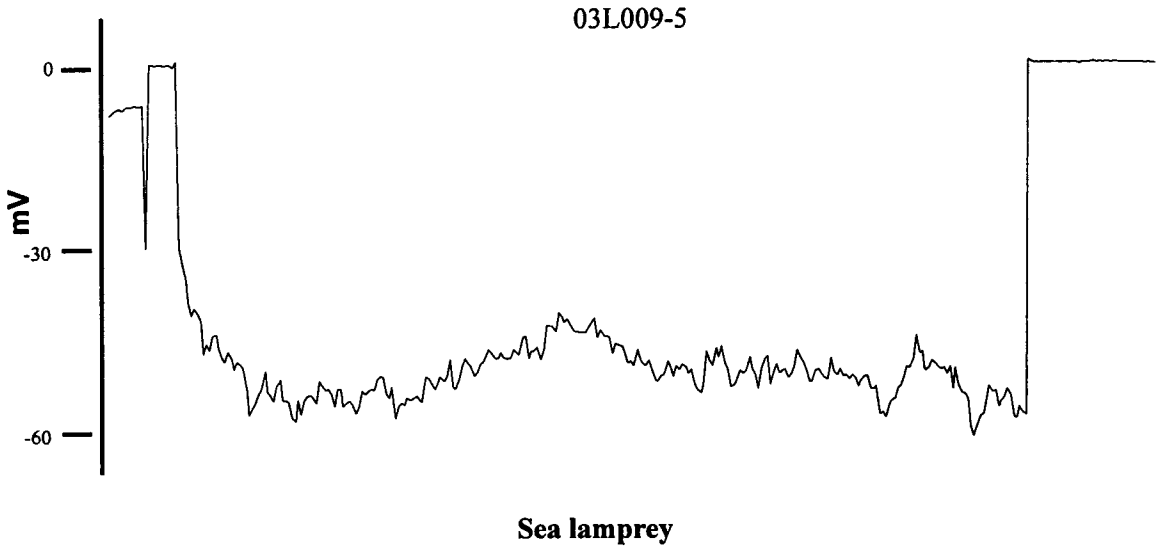

Figure 11. Typical Tracing of Resting Membrane Potential – Sea Lamprey

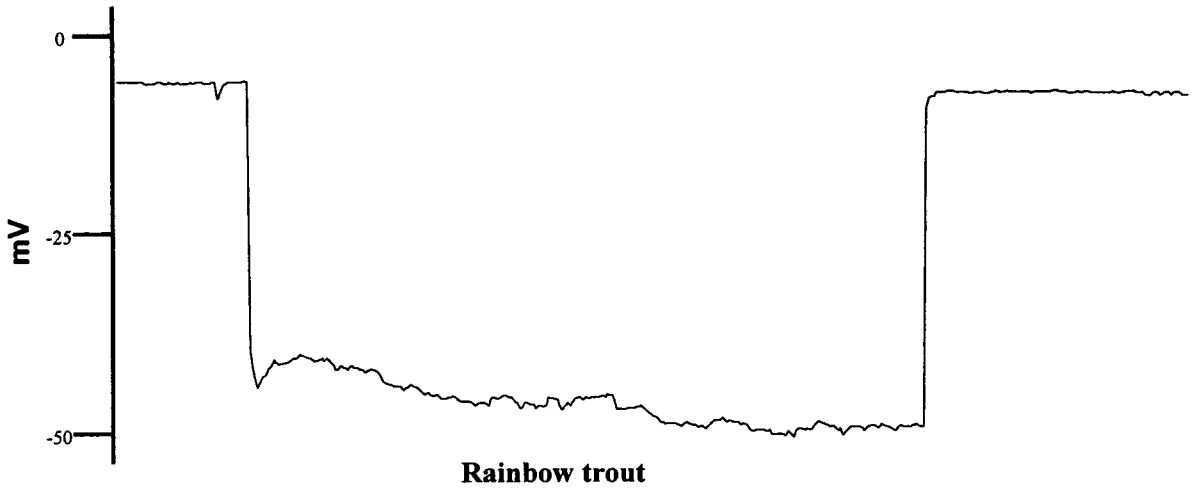

Figure 12. Typical Tracing of Resting Membrane Potential – Rainbow Trout

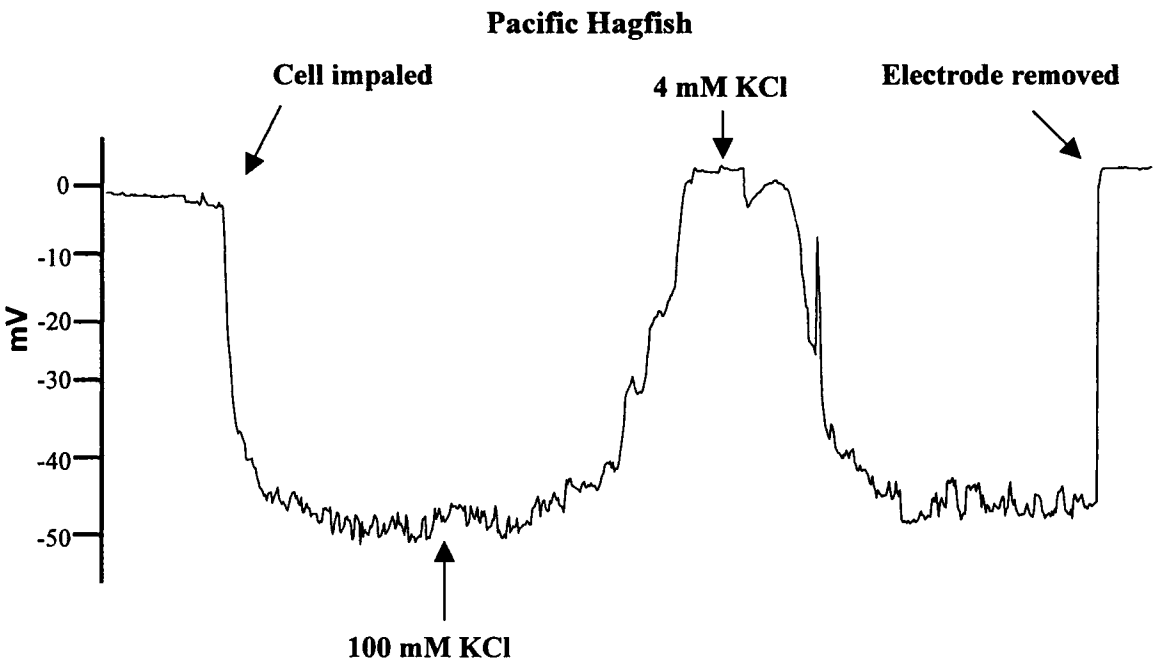

Figure 13. Altered Perfusate KCl Concentrations in Hagfish Dorsal Aorta

Changing from 100 mM hagfish physiological saline to normal (4 mM) re-polarized potassium depolarized hagfish vascular smooth muscle cells to near resting potential values

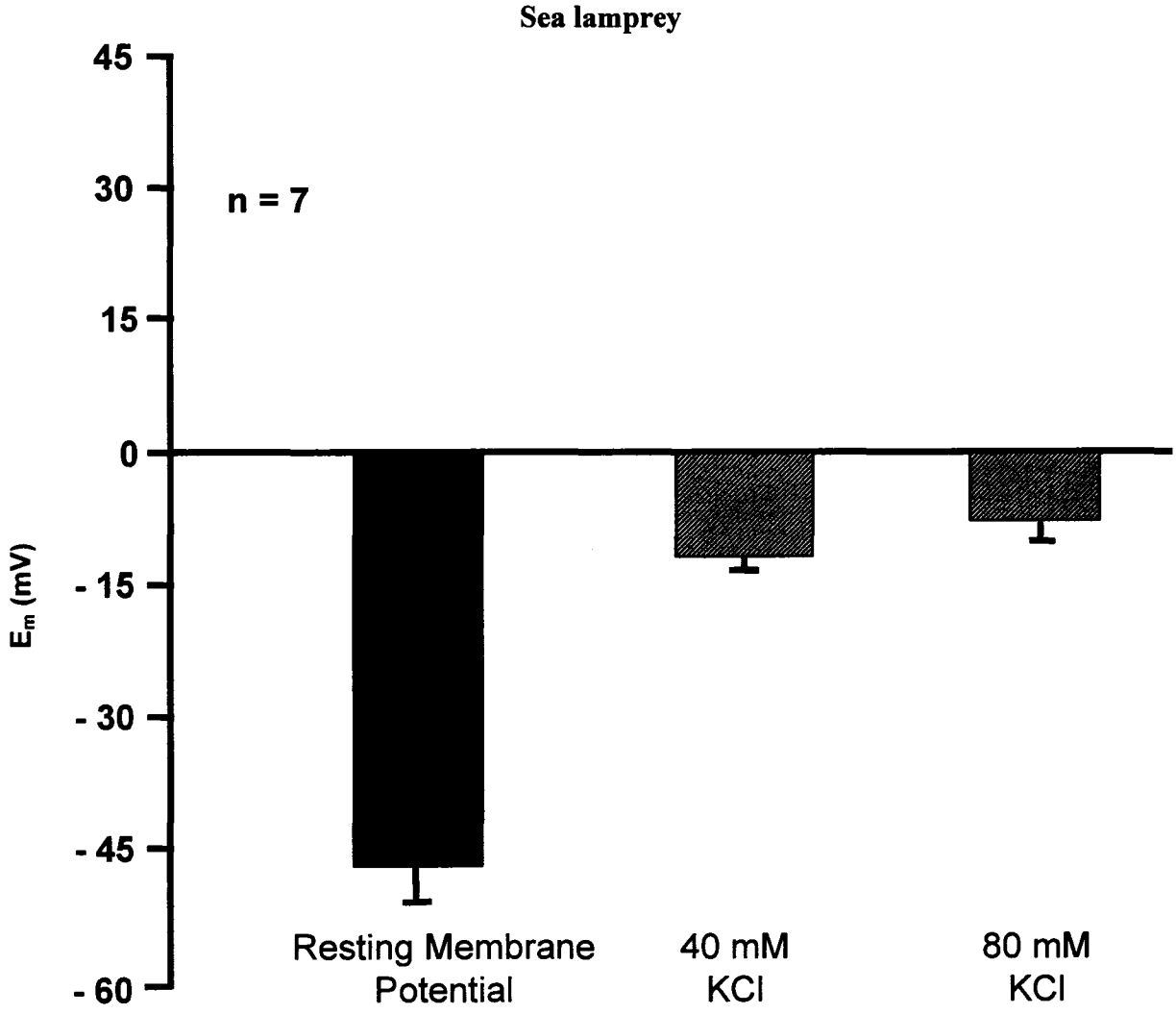

Figure 14. KCl Effects on Membrane Potential – Lamprey Dorsal Aorta

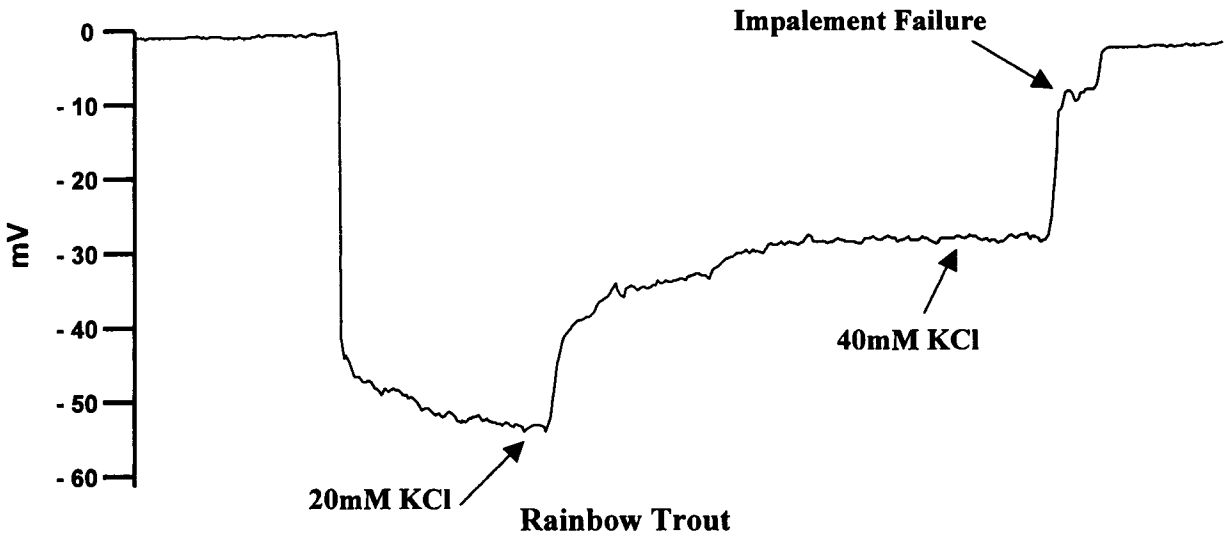

Figure 15. Effects of Consecutive KCl on Membrane Potential – Rainbow Trout

An increase in KCl perfusate concentration (total 40 mM) depolarized rainbow trout smooth muscle cells.

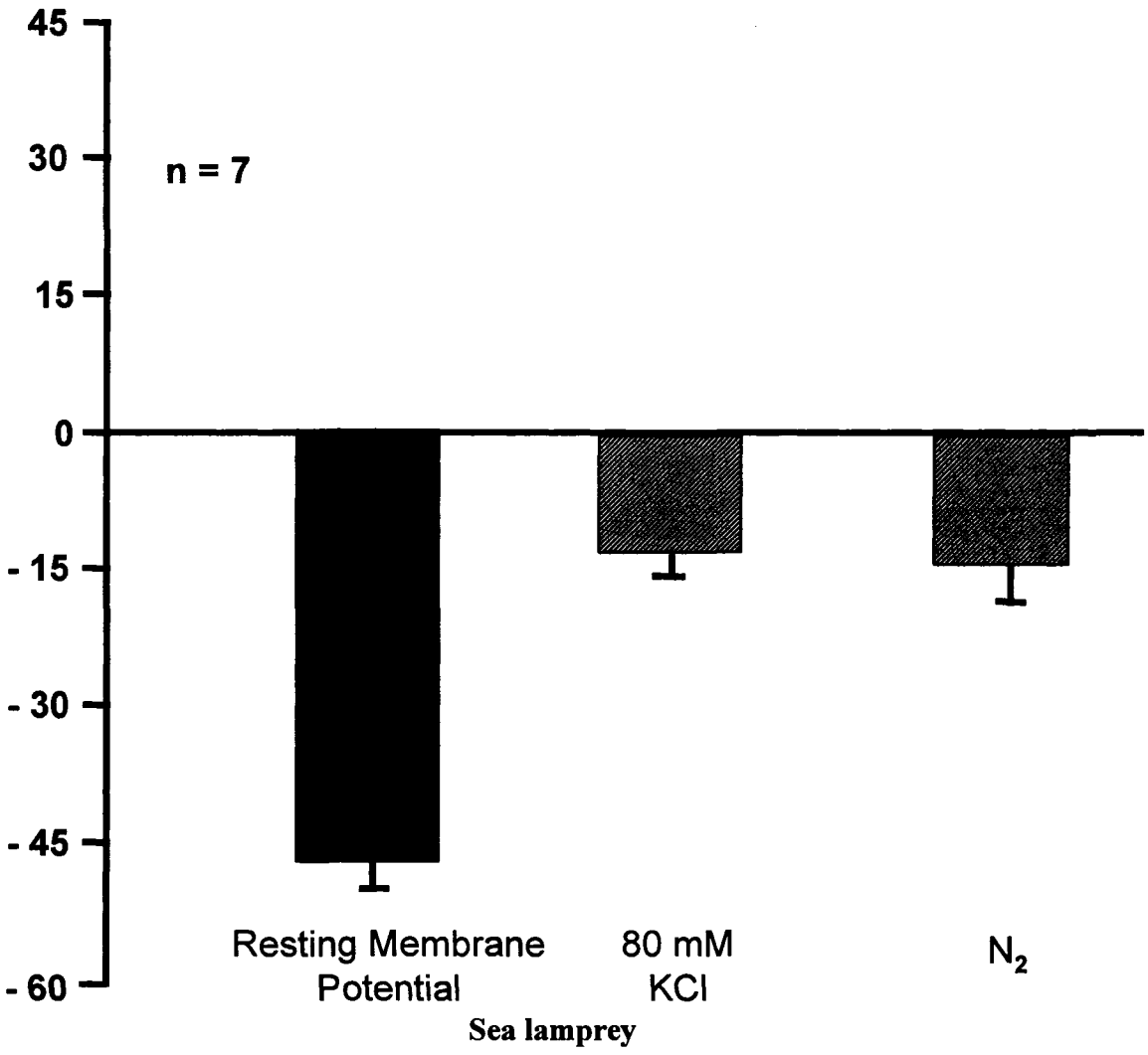

Figure 16. Effects of Hypoxia on Membrane Potential – Sea Lamprey

Hypoxia induced membrane depolarization in a manner similar to that demonstrated for studies involving increases in extracellular potassium.

Effect of Benzocaine on Post-Gill Systemic Arteries

An increase in tension (vasoconstriction) was the response generated for Rainbow trout, steelhead trout and sea lamprey post-gill systemic arteries when 80mm KCl was added to smooth muscle chambers. Average tension measurements following 80mm KCl treatments were 222 ± 8 mg, n = 24 for lamprey, 1125 ± 75 mg, n = 8 for rainbow trout, and 2800 ± 240 mg, n = 12 for steelhead trout. The average tension generated for an 80 mM KCl treatment was designated as the control response for a given artery.

A decrease in vessel tension was observed when a 10^{-3} M concentration of benzocaine was added to KCl constricted rainbow trout and steelhead trout efferent branchial artery rings (Fig. 17). Application of 10^{-3} M benzocaine to KCl contracted rainbow trout and steelhead trout efferent branchial artery rings attenuated the typical 80 mM KCl response to 506 ± 34 mg, n = 8 and 1280 ± 240 mg, n = 12 for rainbow trout and steelhead trout, respectively (Fig 18). Vessel relaxation was initiated within 10-15 minutes post benzocaine application and was sustained until the experiment was terminated (30-40 minutes). Application of a higher concentration (10^{-2} M) resulted in a shorter onset to relaxation (5-10 minutes) and plateau but the overall relaxation response was unchanged. A lower concentration (10^{-4} M) resulted in a longer onset to relaxation and to maximal relaxation (~25 minutes).

Twenty-four lamprey dorsal aorta rings were studied to determine the effects of benzocaine on tension. Lamprey dorsal aorta rings did not relax in response to benzocaine applications; surprisingly contraction was the generated response. The

lowest concentration of benzocaine to cause a measurable increase in tension was 10^{-5} M. Vasoconstriction for 10^{-5} M benzocaine was 50 ± 10 mg. At the lowest vasoactive concentration, benzocaine induced a contraction after a short latency period (3-6 min post-application). At 10^{-3} M benzocaine, maximum tension achieved was 600 ± 45 mg approximately 10 minutes after application and was sustained at that level until vessels were washed (20-25 min). The contractions in response to benzocaine were found to be concentration-dependant, reaching maximal contraction at 2 x 10^{-3} M (Fig. 19). Application of a higher concentration (10^{-2}M) did not result in any noticeable change in the magnitude of contraction but resulted in a shorter onset to contraction (about 3 minutes) and to maximal contraction.

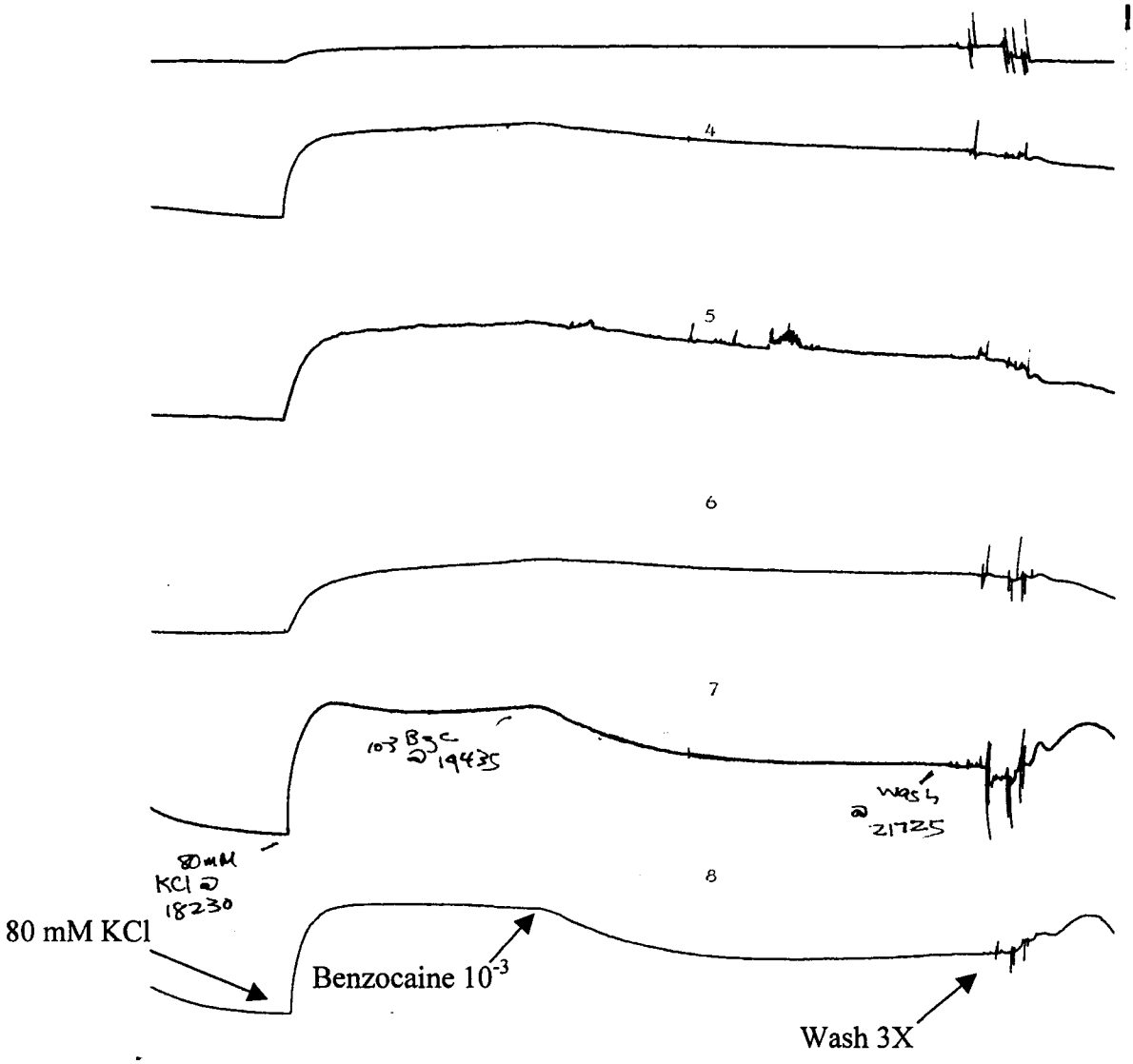

Figure 17. Tracings of Myography Response for Steelhead Trout EBA

Steelhead trout efferent branchial arteries (EBA) rings dilated upon addition of Benzocaine (10^{-3} M). Dilation was sustained until the experiment was terminated.

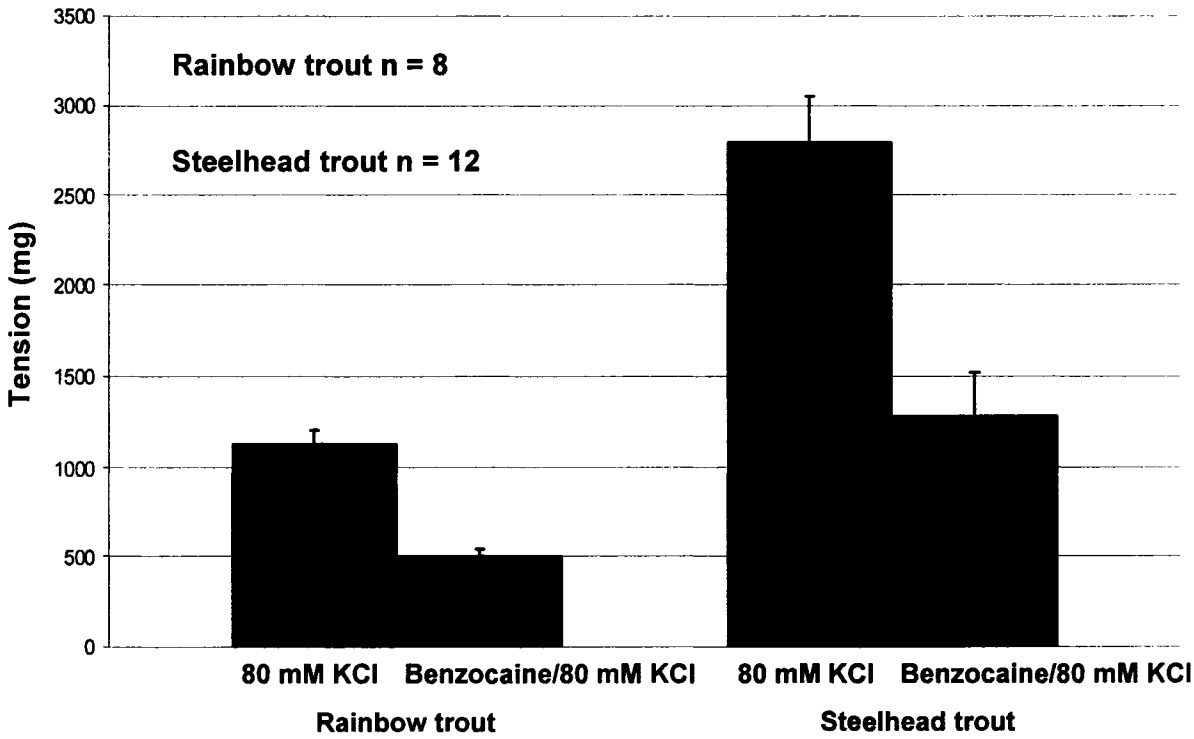

Figure 18. Effect of Benzocaine on KCl Contracted Trout EBA Rings

Benzocaine (10^{-3} M) attenuated the typical KCl response.

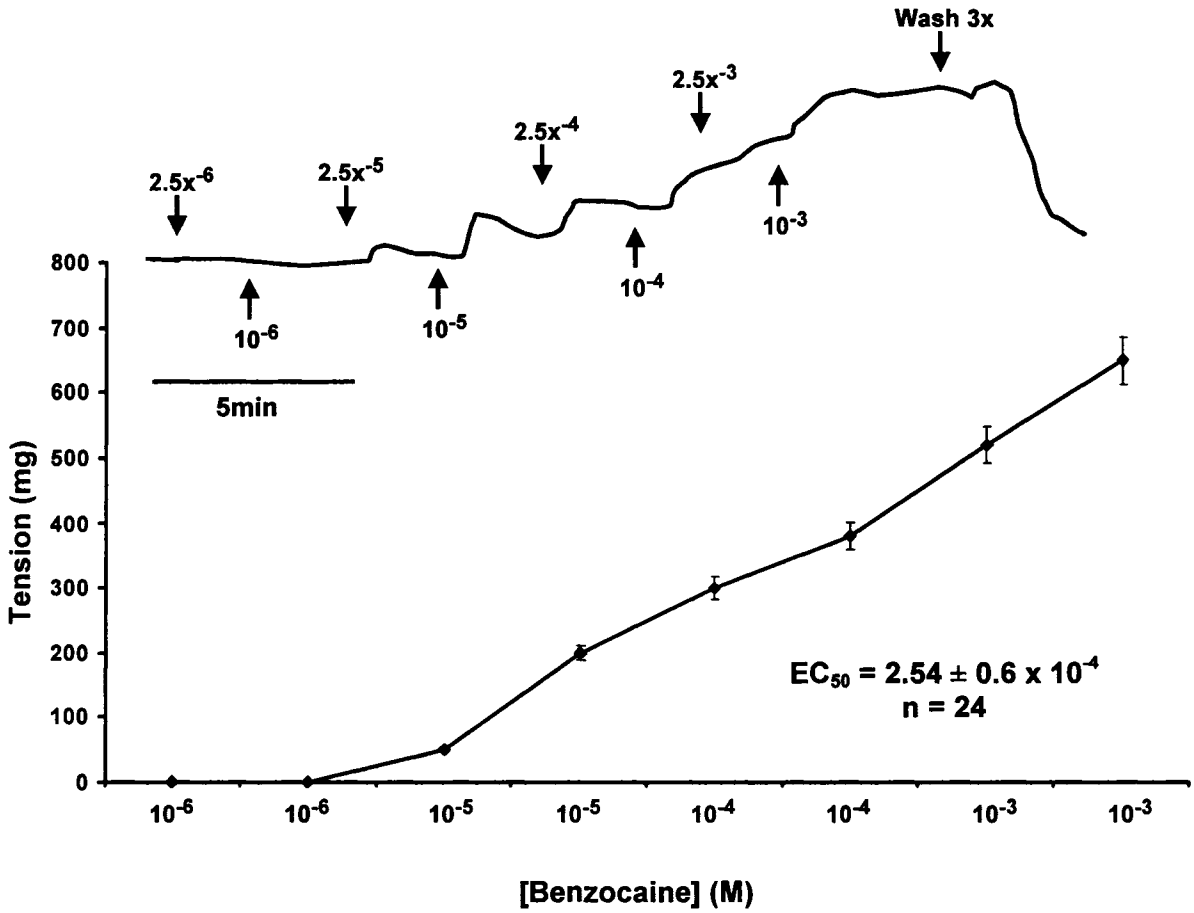

Figure 19. Benzocaine Dose Response Curve for Sea Lamprey Dorsal Aorta

Tension for 10^{-5} M benzocaine was 50 ± 10 mg. At 10^{-3} M benzocaine, maximum tension achieved was 600 ± 45 and was sustained until arteries were washed (20-25 min). Contractions were found to be dose-dependant.

Benzocaine Gas Chromatography/Mass Spectrometry Method Development

Four sets of benzocaine standards were prepared in drug-free plasma at the following concentrations: 2, 5, 10, 25, 50, 100 and 200 ng/ml. The extraction efficiency as determined by the mean recovery was within ± 15% (n = 24) of the assigned concentration for each standard. The maximum deviation for a mean recovery was at the defined concentration of 50.0 μg/ml (Table 8). A plot of the measured results versus defined concentration indicates that the assay is linear over a concentration range of 2 - 200 ng/ml, slope (Y) = 0.943 and intercept = 3.30 (Fig. 20).

Acceptable chromatography, proper ion ratios, peak retention times within ±2% of the calibrating standard and the appropriate fragmentation pattern made the identification of benzocaine unequivocal. Samples were prepared at 1 ng/ml but failed ion ratio and quantitation requirements (n = 6). The chromatography for samples from 2.0 ng/ml to 200 ng/ml exhibited Gaussian peak symmetry and met ion ratio requirements. The Limit of Detection (LOD) was defined as the lowest concentration tested that had acceptable chromatography and met ion ratio requirements; 2.0 ng/ml samples consistently met these criteria. The Limit of Quantitation (LOQ) was defined as the lowest concentration that met the LOD requirements and also quantitated within +/- 20 % of target concentration; 2.0 ng/ml samples consistently met these criteria.

Carryover was not seen at the upper limit of linearity, which was set at 200 ng/ml. Chemically similar compounds were extracted by this method to assess the

method's specificity. No evidence of analytical interference was seen for the compounds included in this assessment. A difference of 0.4 ± 0.1 minutes was achieved between the chromatographic peaks for benzocaine and the internal standard. Thus, the peaks were well resolved with no extraneous interfering peaks.

Table 8. Benzocaine Linearity Analysis

The linearity of benzocaine was analyzed by gas chromatography/ mass spectrometry over a range of 1.88 to 187.00 μg/ml. The maximum deviation recovery from 100% was 15.50% at a defined concentration of 50.0 μg/ml.

Defined		Measured	Values		Mean	% Recovery
2.0	1.9	2.4	1.5	1.7	1.88	93.8
5.0	4.5	5.6	5.0	4.8	4.97	99.5
10.0	10.0	10.0	10.0	10.0	10.0	100.0
50.0	51.6	64.0	54.8	60.6	57.75	115.5
100.0	111.3	97.6	97.8	110.8	104.38	104.4
200.0	178.1	180.1	191.7	198.1	187.00	93.5

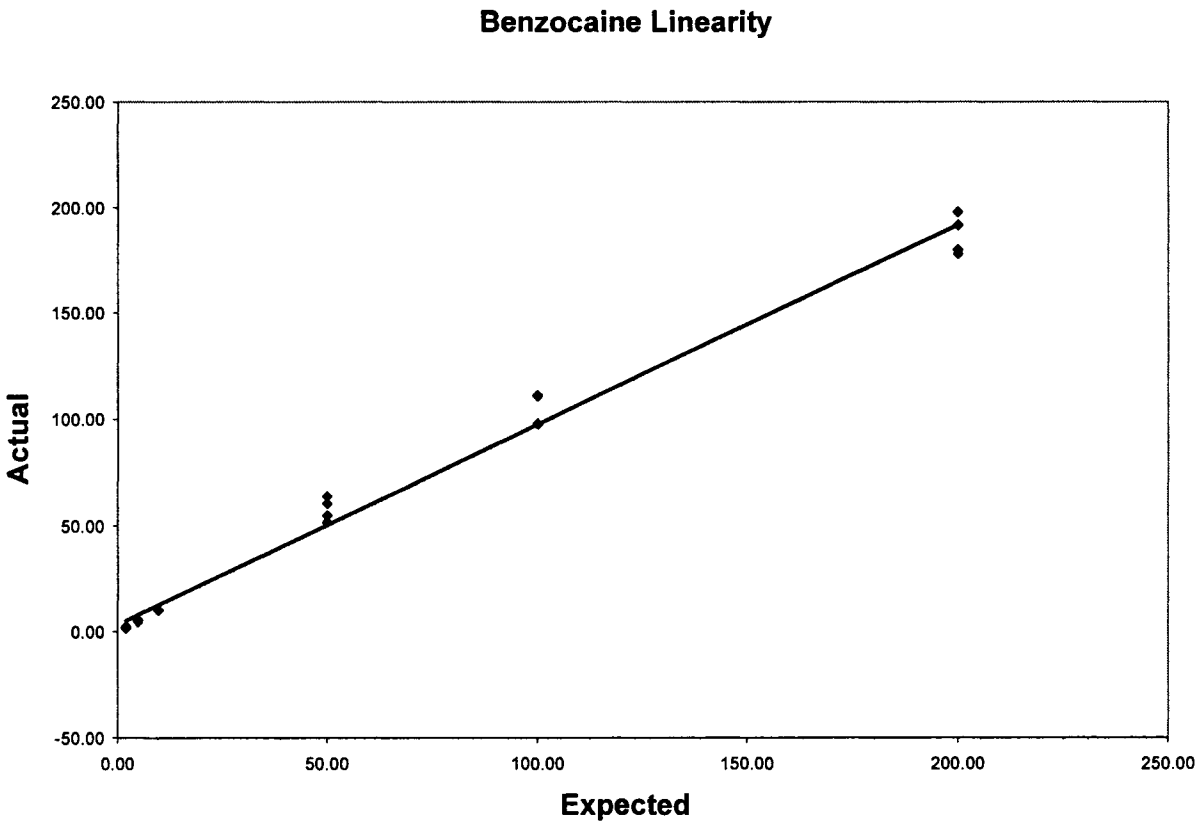

Figure 20. Benzocaine Linearity via Gas Chromatography Mass Spectrometry

Acquisition and Interpretation of Benzocaine Mass Spectral Data

Gas chromatography/mass spectrometry was used to acquire mass spectral information for benzocaine. The molecular weight of benzocaine is 165.19 and the molecular ion is mass 165. Figure 21 represents the major fragments produced by electron impact of benzocaine. Given the tightly controlled conditions possible with Gas Chromatography/Mass Spectrometry, the electron impact fragments produced and the relative amounts of the various fragments were used to identify the presence of benzocaine and aprobarbital in samples.

The total ion current chromatogram displaying the retention times for a typical extract is shown in Figure 22, the most abundant peak represents benzocaine (7.61), which has the shortest retention time followed by the peak for aprobarbital (7.95). The EI mass spectra generated for benzocaine via the gas chromatography/mass spectrometry method (Fig. 23) was consistent with published spectral data (i.e., prominent peaks at 92, 120, 137, and 165 daltons). The extraction technique and selected ion monitoring gas chromatography/mass spectrometry program employed in the method provided correct identification of certified drug-free plasma samples as negative and samples expected to contain benzocaine as positive (n = 116). No differences in chromatographic characteristics (e.g., peak shape, resolution) were seen across different sample matrices (e.g., bile, blood, myography solutions, water).

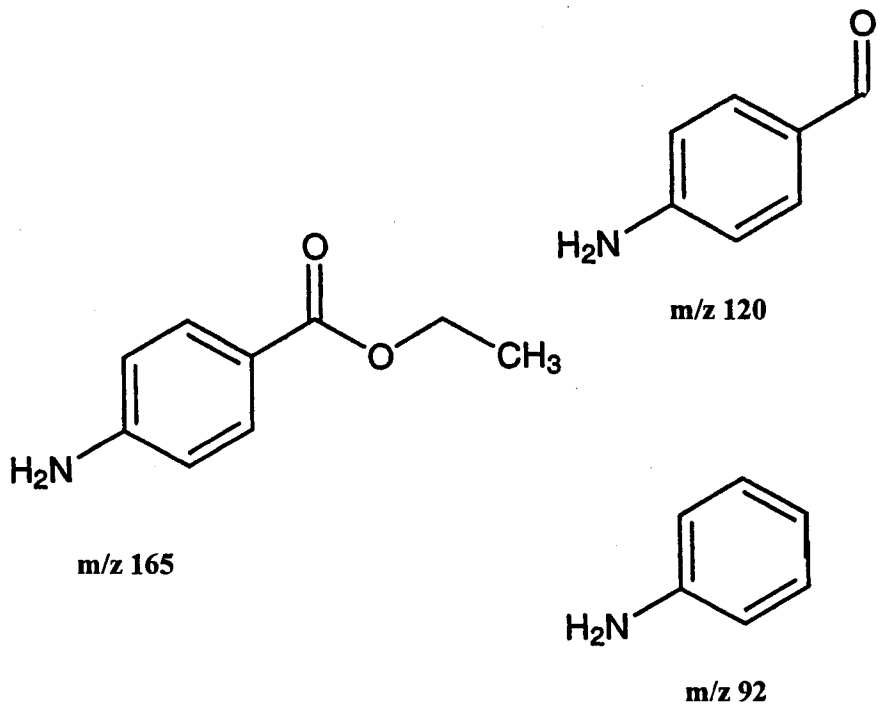

Figure 21. Major Benzocaine Fragments Produced by Electron Impact

Under electron ionization, the fragmentation of benzocaine includes the molecular ion of mass 165, as represented by a peak in its mass spectrum at a mass-to-charge value (m/z) of 165 and peaks at m/z 92 and m/z 120.

Area Percent Report

Data File : C:\HPCHEM\1\DATA\066\BZC41.D
Acq On : 7 Mar 2005 21:28
Sample : 04L011
Misc :

Vial: 41
Operator:
Inst : GC/MS Ins
Multiplr: 1.00
Sample Amount: 0.00

MS Integration Params: rteint.p
Method : C:\HPCHEM\1\METHODS\BZCNSIM.M (RTE Integrator)
Title : Benzocaine

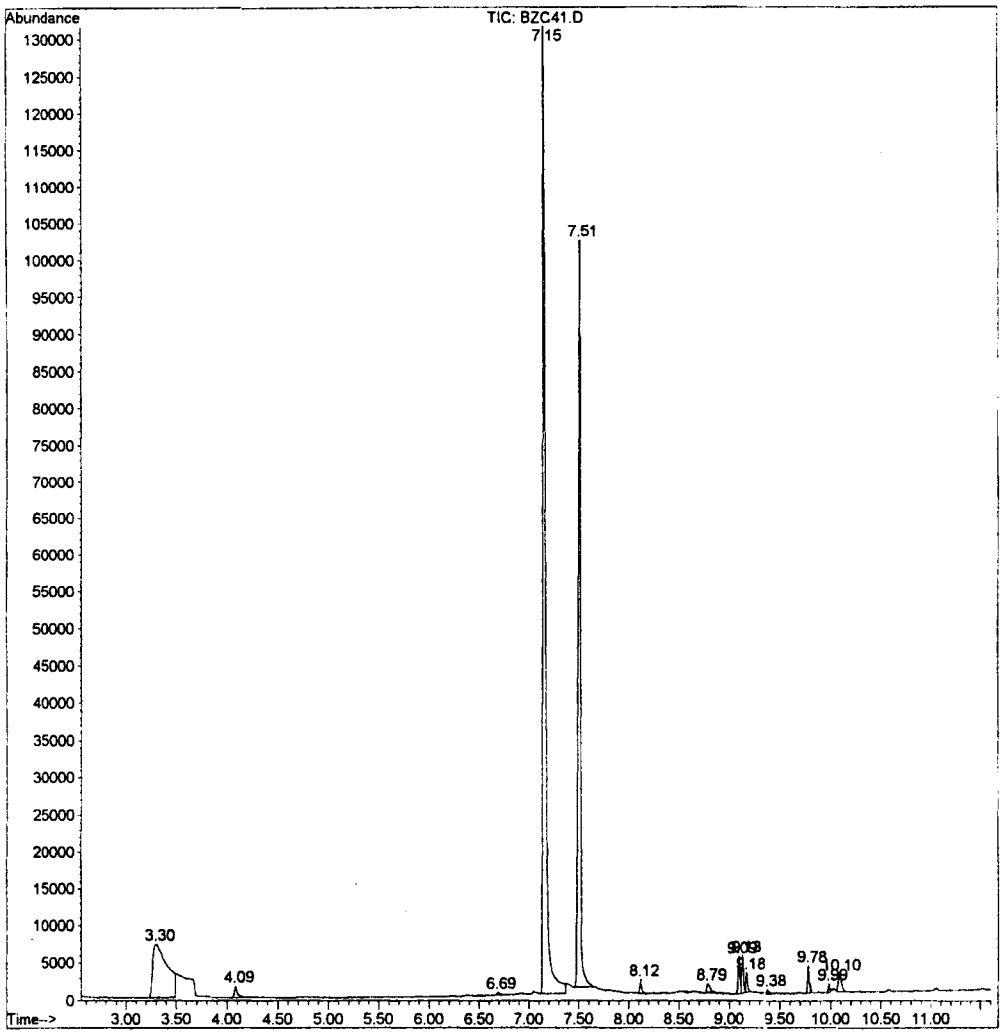

BZC41.D BZCNSIM.M Tue Mar 08 11:32:41 2005

Figure 22. Total Ion Current Chromatogram

The retention times for benzocaine and aprobarbital in this chromatogram are 7.15 and 7.51, respectively.

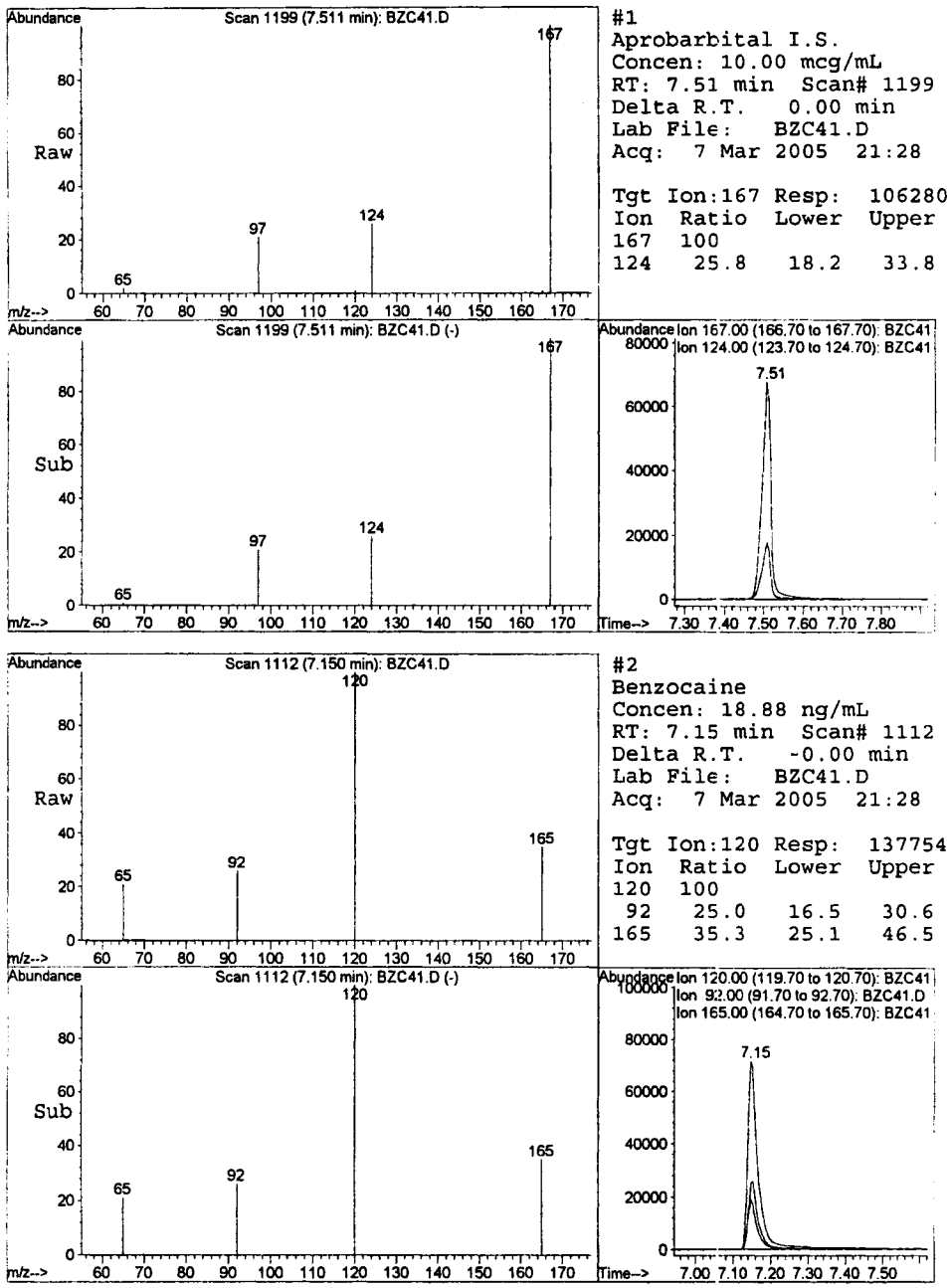

Figure 23. Mass Spectra for Aprobarbital and Benzocaine

Quantitative Analysis of Benzocaine in Sea Lamprey Sera

To determine if benzocaine concentrations used in myography studies were compatible with the benzocaine concentrations measured in the blood of anesthetized lamprey, plasma benzocaine concentrations from ten benzocaine anesthetized lampreys were measured and compared to the physiological saline solutions used in their smooth muscle chambers. In each case, the dorsal aorta, plasma, and physiological saline solutions were matched to correspond to the same lamprey.

The average concentration of benzocaine in the holding tank was 186 ±13 μg/ml, n = 16. Mean plasma benzocaine concentrations from lamprey anesthetized in these tanks was 28.9 ±4.0 μg/ml, n = 10. The median plasma concentration was 27.7 μg/ml with values from 23.6 to 36.1 μg/ml. The distribution of plasma results was within a small range, with 7 out of 10 (70%) within 23.5 and 29.8 μg/ml and 30% of the results measuring in the range 30.7 to 36.1 μg/ml. Plasma results were within the assay's proposed linear range (2.0 to 200 μg/ml) and in close proximity to the concentrations measured in myography solutions. Benzocaine concentrations measured in myography solutions used to treat dorsal aorta were distributed more or less evenly around the mean (36.304 ± 5.026 μg/ml, n = 16).

In the present study, lamprey dorsal aorta rings treated with benzocaine concentrations slightly less than or equal to mean plasma benzocaine concentrations generated tension responses (i.e., contraction) that were equivalent to that produced for 80 mM KCl.

Quantitative Analysis of Benzocaine in Rainbow Trout Sera

There was little difference in the benzocaine concentrations measured in the plasma collected from four rainbow trout (mean 66.5 ±8.0 μg/ml). The average concentration of benzocaine in the anesthetizing solution was 195 ±6 μg/ml, n = 4. The median plasma concentration was 67.7 μg/ml, with a range from 57.2 to 73.3 μg/ml. Mean benzocaine concentrations were substantially higher in rainbow trout sera than in lamprey sera (66.5 ±8.0 μg/ml, n = 4 and 28.9 μg/ml ±4.0, n = 10, respectively). A decrease in tension was observed when rainbow trout efferent branchial artery rings were treated with benzocaine concentrations slightly less than or equal to the mean benzocaine concentration measured in their plasma.

These findings suggest that benzocaine concentrations that provide adequate levels of anesthesia (i.e., therapeutic levels) are capable of inducing vasoactive responses in post-gill systemic vessels. Benzocaine induced dose-dependent contraction in lamprey dorsal aorta and relaxation in rainbow trout and steelhead trout efferent branchial arteries.

Comparison of Ethanol via Gas Chromatography and Enzymatic Method

A comparison of the ethanol concentration measured by flame ionization detection and by nicotinamide dinucleotide reduction was performed by comparing twenty specimens analyzed via headspace gas chromatography and an enzymatic (alcohol dehydrogenase) method (Table 9). The headspace gas chromatography analysis yielded baseline separation between similar volatile compounds (e.g.,

acetone, methanol, and isopropanol) with no interference from the samples, tissue or other sources (Fig. 24).

The correlation between the headspace gas chromatography and enzymatic methods for positive and negative samples was very good to excellent. An adequate number of results (n= 20) were spread across a broad range (16 to 860 mg/dl). The differences between pairs of results was minimal (paired t test = 2.31), the dispersion of data points of the two methods around the regression line was essentially equal, and the correlation coefficient was high, R= 0.9996 (Fig. 25). The headspace gas chromatography and enzymatic methods were statistically similar; however, the headspace gas chromatography was a more definitive method because of its ability to differentiate between the volatile of interest (ethanol) and similar volatile compounds such as acetone and the reducing alcohols methanol and isopropanol.

Two observations of interest and possible importance: (1) When lamprey with body weights 206 ± 15 g, n = 6 were exposed to identical ethanol concentrations as lamprey with body weights 264 ± 21.3 g, n = 6 (> 20% difference in weights without overlap between groups), plasma ethanol concentrations in lower weight lamprey (64.2 ± 20.8 mg/dl, n = 6) was higher than the plasma ethanol concentrations in higher weight lamprey 35.7 ± 16.3 mg/dl, n = 6) (Table 10) and (2) Blood samples collected from fish exposed to benzocaine prepared in water did not show the presence of ethanol, although the chemical structure of benzocaine favors hydrolysis to ethanol by plasma and liver esterases (Fig. 26). Ethanol has been proposed as a

possible metabolite of benzocaine in man, although this metabolic profile has not been demonstrated (6).

Table 9. Headspace Gas Chromatography/Alcohol Dehydrogenase Comparison

A comparison of the headspace gas chromatography (HSGC) ethanol method and alcohol dehydrogenase (ADH) ethanol method was conducted to assess the correlation between these two analytically discreet methodologies. The correlation between these methods was very high (i.e., $R > 0.99$, $n = 20$).

Lamprey ID #	HSGC Ethanol mg/dl	ADH Ethanol mg/dl
99L01	46	44
99L18	18	16
99L20	20	29
99L21	24	26
99L23	16	17
00L010	860	855
04L004	95	99
04L005	61	61
04L006	76	77
04L007	95	90
04L008	160	154
04L009	61	62
04L012	142	136
04L013	242	234
04L016	25	22
04L018	29	22
04L023	44	33
04L024	46	38
04L025	33	22
04L027	34	36

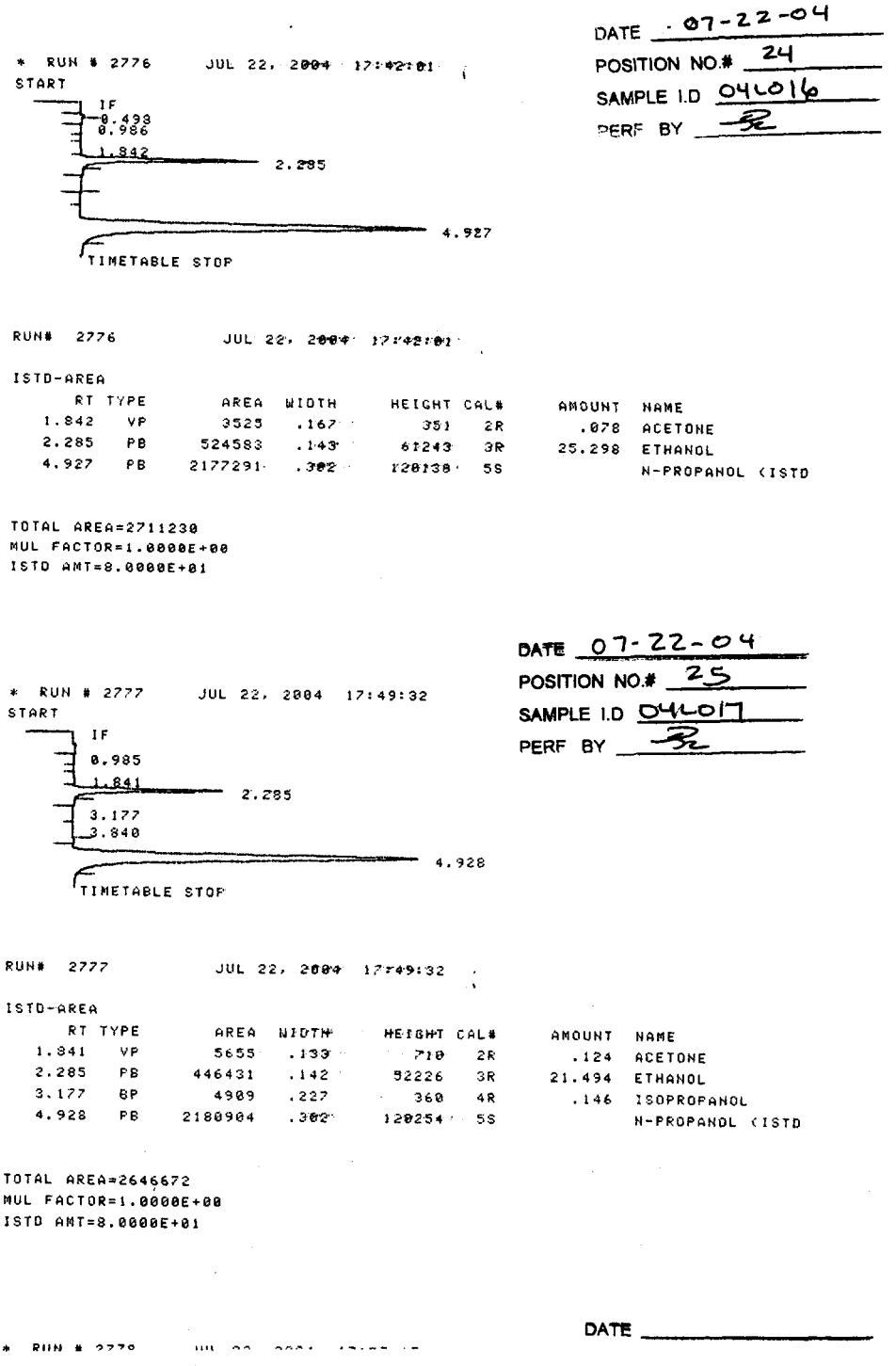

Figure 24. Typical Chromatogram for Headspace Analysis of Ethanol

Peaks at retention time 2.285 represent ethanol in these chromatograms. Peaks at retention time 4.927 and 4.928 represent the internal standard isopropanol.

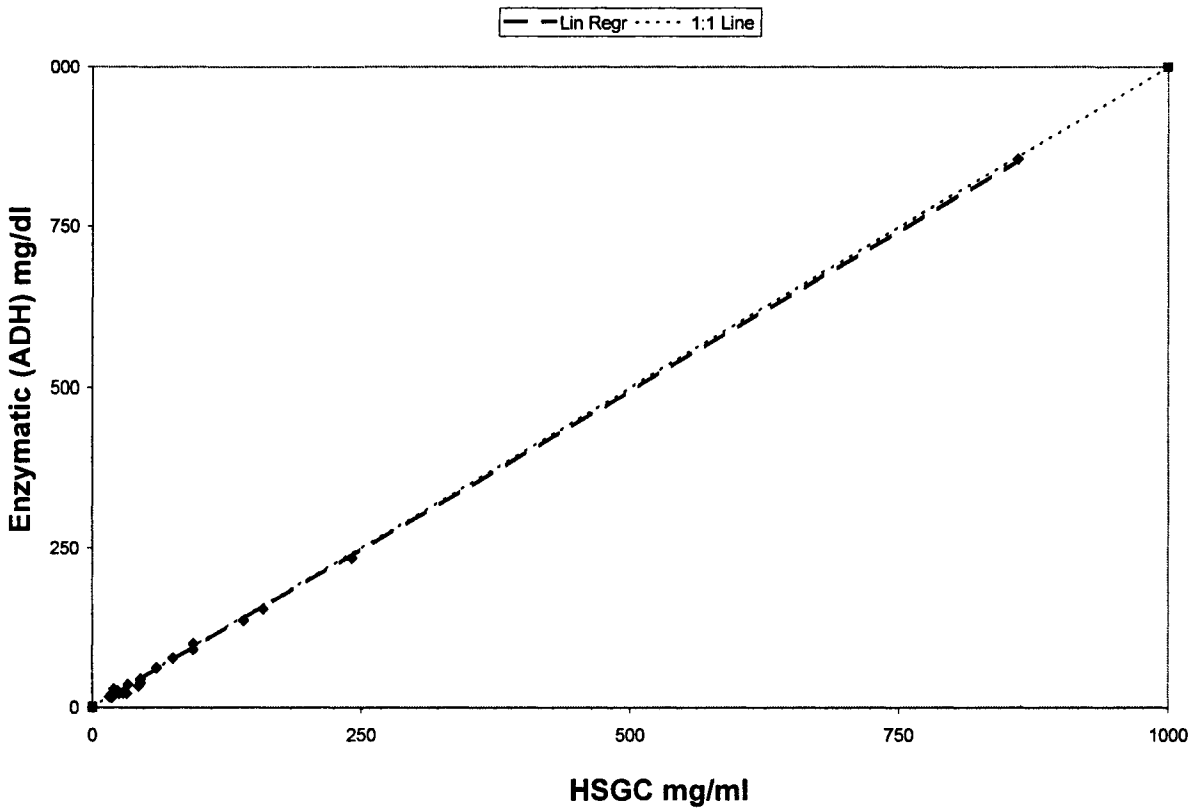

Figure 25. Method Comparison (Headspace versus Enzymatic)

The correlation between the headspace gas chromatograph method and the enzymatic method was high, R= 0.9996 (n= 20; range 16 to 860 mg/dl.

Table 10. Sea Lamprey: Weight versus Ethanol Distribution

When mixed weight lamprey pairs were exposed to similar ethanol concentrations, a higher plasma ethanol concentration was achieved in lamprey with the lowest body weight.

ID #	Gender	Weight (g)	Ethanol mg/dl	Ethanol/Weight	Tank Ethanol mg/dl	Ethanol/Tank
02L013	F	200	59	0.3	147	40.10%
03L007	F	244	49	0.2	145	33.70%
04L014	F	210	88	0.42	130	67.60%
03L003	F	250	20	0.08	131	15.20%
04L006	F	230	76	0.33	223	34.00%
04L005	F	292	61	0.21	223	27.30%
04L026	F	204	37	0.18	206	17.96%
04L027	F	250	34	0.13	207	16.42%
04L023	M	184	44	0.23	131	33.58%
04L018	M	260	29	0.11	137	21.10%
04L015	F	208	81	0.39	132	61.30%
04L017	F	290	21	0.07	134	15.60%

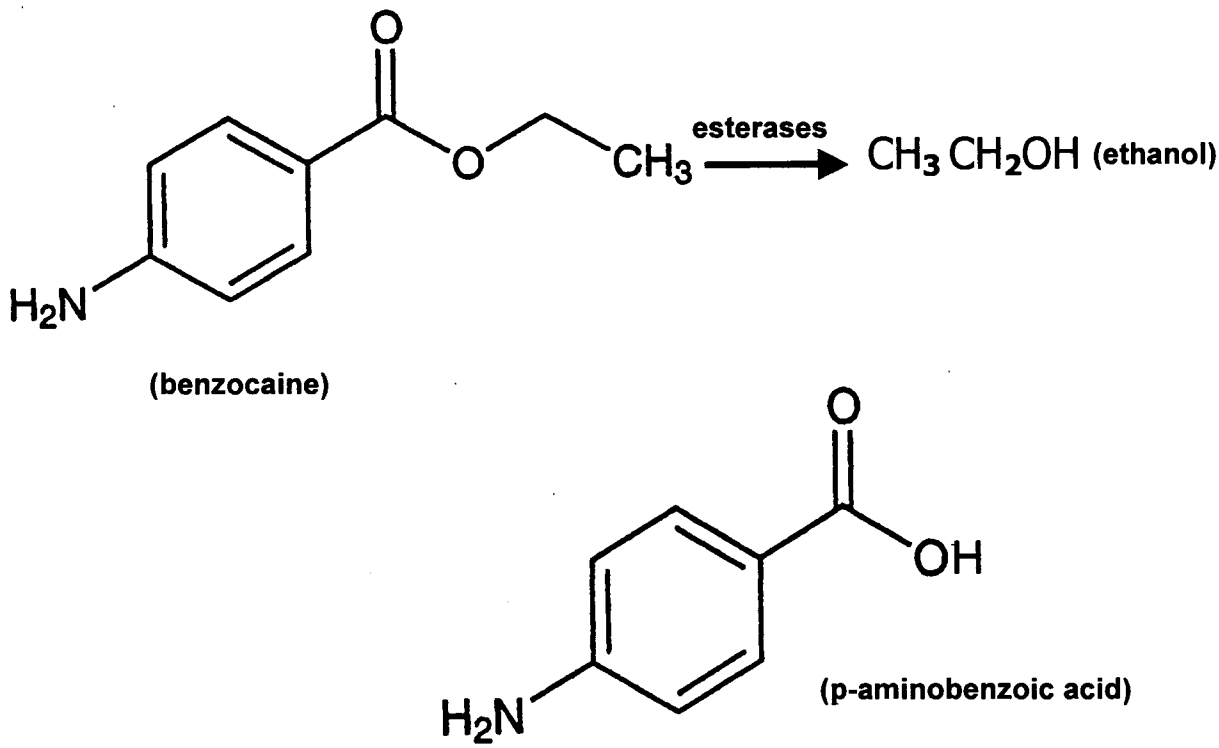

Figure 26. Proposed Metabolism of Benzocaine

The chemical structure of benzocaine favors hydrolysis by esterases. Plausible sources of esterases include the plasma and liver.

Osmolality and Osmolal Gap in Sea Lamprey

Osmolality was measured in lamprey plasma using a freezing point depression osmometer and also calculated using the following formula which was derived by Dorwart (30): $1.86(Na^+)$ + (Glucose/18) + (Blood Urea Nitrogen/2.8) + 9. This empirical formula accounts for the contribution of other osmotically active substances in the plasma, such as K^+, Ca^+ and proteins but not for low molecular weight substances such as methanol, ethanol and ethylene glycol.

Using the measured and calculated values for osmolality, the osmolal gap was determined. When the osmolal gap was less than or equal to 10 mOsm/kg H_2O, the results were considered normal and abnormal when the osmolal gap was greater than 10 mOsm/kg H_2O (34).

In the present study, the measured osmolality (275.8 ±11.7 mOsm/Kg H_2O, n=6) was greater than the calculated osmolality (252.3 ±9.1 mOsm/Kg H_2O, n=6) and the osmolal gap (23.5 ±5.7, n=6) was abnormal for lamprey anesthetized in benzocaine/ethanol. The measured osmolality (250.8 ±21 mOsm/Kg H_2O, n=5) and calculated osmolality (246 ±18.4 mOsm/Kg H_2O, n=5) were essentially equal and the osmolal gap (6.5 ±5.1, n=5) was normal for lamprey anesthetized in benzocaine/water.

CHAPTER 4

DISCUSSION

The objective of the present study was to evaluate the electrophysiology of vascular smooth muscle in fish. This objective was met by characterizing resting membrane potential and membrane potentials generated in response to factors such as changes in extracellular potassium and oxygen tension acting on the vascular smooth muscle of hagfish, lamprey, and trout post-gill systemic arteries. The present study indicates that despite differences in vascular architecture, differences in intracellular and extracellular ionic compositions, and differences in the response to some stimuli, vascular smooth muscle membrane potential in lower vertebrate fish and higher vertebrate fish are similar.

It has been reported by several researchers that membrane potential is a fundamentally important component in the regulation of tone in vascular smooth muscle of various animals (20, 51, 78, 87). However, membrane potential in fish vascular smooth muscle cells has not been well characterized but is of interest, particularly in hagfish and lamprey because they are the only surviving members of one of the most primitive class of vertebrates (Agnatha) and given the recent discovery that post-gill systemic arteries in cyclostomes respond to hypoxia in a manner similar to small resistance arteries in the pulmonary circulation in man (117).

In pulmonary vasculature, hypoxia has been shown to alter membrane potential and initiate depolarization, causing vasoconstriction.

Membrane potential exists due to the concentration of several ions, chiefly Na^+, K^+, and Ca^+ distributed on either side of the membrane, the permeability of the membrane to each ion, impermeable intracellular anions, and the activity of ion channels, transporters and exchangers (e.g., K^+ channels, Na^+/K^+-ATPase, Na^+/H^+ exchanger) (20, 75, 87, 108).

For each permeable ion, there is a theoretical equilibrium potential at which there is no net driving force for the ion to move across the membrane. That is, the chemical gradient on one side of the membrane is balanced by the electrical gradient across the membrane (and vice versa).

The theoretical equilibrium potential (E_X) for a single ion can be calculated using the Nernst equation:

$$E_X = RT/zF \ln[X^+]_{Out}/[X^+]_{In}$$

simplified the equation becomes:

$$E_X = -61 \log([X]_{In}/[X]_{Out}) \text{ at } 25°C$$

Where $[X]_{Out}$ is the extracellular concentration of the ion and $[X]_{In}$ is the intracellular concentration (55, 126). As an example, if the extracellular concentration of K^+ equals 5mM and the intracellular concentration of K^+ equals 125mM, the calculated equilibrium potential equals -84 mV. At this membrane potential there would be no net force driving K^+ into or out of the cell. Thus, -84 mV is the membrane potential necessary to oppose the outward movement of K^+ down its concentration gradient.

Similarly, if the extracellular concentration of Na^+ equals 145mM and the intracellular concentration of Na^+ equals 20mM, the calculated equilibrium potential equals +50 mV. Thus, a membrane potential of +50 mV would be necessary to oppose the inward movement of Na^+ down its concentration gradient.

The Nernst equation does not account for all the processes (e.g., activity of pumps, transporters) and other ions involved in the establishment of membrane potential. The Nernst equation can be modified to reflect a more realistic representation of the resting membrane potential (55, 126). This revised Nernst equation is referred to as the "Goldman equation". The Goldman equation accounts for the contributions of multiple ions and the differences in their membrane permeability (126). In terms of bioelectric relevance, K^+, Na^+, and Cl^- ions exert the greatest influence. The Goldman equation for K^+, Na^+, and Cl^- is: $(E_{K+,\,Na+,\,Cl-}) = -61mV \log (P_K[K]_{In} + P_{Na}[Na]_{In} + P_{Cl}[Cl]_{Out})/ (P_K[K]_{Out} + P_{Na}[Na]_{Out} + P_{Cl}[Cl]_{In})$, where $E_{K+,\,Na+,\,Cl-}$ is the calculated potential difference across the membrane.

The concentration terms in the Goldman equation remain relatively constant under normal physiological conditions. However, the ratios of membrane permeability for the ions undergo considerable changes, due in part to the activity of membrane channels (126).

In the present study, membrane potential was measured using sharp microelectrodes (tip resistance $\geq$ 60 mΩ) to impale smooth muscle cells. The microelectrode served to establish an electrical connection with the interior of the cell thus allowing the absolute values of the membrane voltages to be measured relative to

the outside of the cell. The resting membrane potential was similar for hagfish (-52.7 ±2.9 mV, n=15), lamprey (-54.3 ±5.2 mV, n=32), and trout (-48 ±1.6 mV, n=27) and consistent with the values reported for smooth muscle in other animals. The resting membrane potentials reported for other animals include: rat mesenteric arteries, -51.4 ±1.5 mV, n=12 (29); dog common carotid arteries, -43.3 mV, n=19 (140); fetal rabbit pulmonary arteries, -49.5 ±0.8 mV, n=27 (67); guinea pig stomach muscle, -58.2 mV, n=50 (88); rabbit common carotid arteries, -44.5 ±1.4 mV, n=30 (103); and adult mongrel cat middle cerebral arteries, -54 ±0.51 mV, n=40 (93). This study shows that resting membrane potential values in vascular smooth muscle of fish fit in the widely accepted quantitative range (–60 to –40 mV) for smooth muscle (27, 56, 1 108,109, 126, 131).

As described earlier in this work, potassium channels play a significant role in determining membrane potential. Given the abundance of these channels in the plasma membrane, changes in extracellular K^+ concentration have predictable effects on the resting membrane potential. For example, when the electrochemical gradient for K^+ ion favors movement out of the cell, K^+ ions diffuse down their concentration gradient through open K^+ channels. This outward movement of K^+ ions results in an increased intracellular negativity (hyperpolarization). Conversely, an inward flux of K^+ ions results in depolarization.

Decreasing the extracellular K^+ concentration causes a decrease in K^+ permeability and results in the membrane potential being more easily displaced from the equilibrium potential for K^+ (~ -84 mV) towards the equilibrium potential for Na^+

(~ +50 mV). Increasing the extracellular K^+ concentration causes an increase in K^+ permeability and stabilizing the resting membrane potential near the equilibrium potential. Because the resting membrane potentials for the above smooth muscle types are within the previously mentioned typical range (i.e., -60 to –40 mV), it is reasonable to assume that other ion channels are as important as K^+ channels, otherwise, resting membrane potentials near the equilibrium potential for K^+ (i.e., -90 to –80 mV) would be expected.

In the present study, increases in extracellular K^+ caused depolarization in hagfish, lamprey and rainbow trout post-gill systemic arteries. Changing the extracellular K^+ concentration back to normal (i.e. 4mM) re-polarized K^+ depolarized hagfish vascular smooth muscle cells to near resting potential values. These findings are consistent with the results reported in other studies (63, 107, 108, 109, 157).

Vascular Smooth Muscle and Benzocaine Interactions

The pharmacokinetics of benzocaine is not well documented. However, it is known that local anesthetics such as the tertiary amines: bupivacaine, mepivacaine, prilocaine, lignocaine and tetracaine; the esters: cocaine and procaine; as well as uncharged benzocaine reversibly block the propagation of action potentials of excitable membranes by binding to a common binding site. Bindings by these chemicals make the site non-conducting (65, 162, 163).

It has long been shown that a common receptor is located in the pore of voltage-gated Na^+ channels (65, 163). It has also been shown that benzocaine binding

to this receptor is strongly voltage dependent (163). The origin of this common binding site is likely ancient. In fact, several studies have shown that receptors for signaling systems in mammalian vasculature are also expressed in the vasculature of primitive and advanced fish vertebrates (16, 17, 36, 113, 114, 115, 116, 174). These studies show that receptors for endogenous chemicals (e.g., acetylcholine, angiotensin II, arginine vasotocin, atrial naturetic peptides, bradykinin, catecholamines, endothelin) extend from the earliest fish vertebrates, hagfish and lamprey to more advance fish vertebrates such as rainbow trout.

The binding capability and other unique physical and chemical characteristics of benzocaine such as: rapid absorption, distribution, metabolism and elimination in biological tissues, and its predominance in unionized form at physiological pH make it an ideal chemical for use as a local anesthetic in fish (2, 1983, 45, 46, 102, 151). In addition to targeting voltage-gated Na^+ channels, benzocaine can block other ion channels such as the numerous types of K^+ channels (Slesinger).

In the present study, benzocaine induced contraction in lamprey aortas and relaxation in trout arteries at concentrations that were equivalent to concentrations measured in the plasma of these fish when under anesthesia. Benzocaine induced contraction in lamprey aortas was paradoxical because it has been shown that local anesthetics (with the exception of cocaine) cause relaxation in systemic arteries (66). Similar to benzocaine, cocaine induces contraction. Both are ester type local anesthetics that can bind to the pores of voltage-gated Na^+ channels and block other ion channels (163, 164).

The present study demonstrates that benzocaine can effectively modulate vascular tone and that a benzocaine compatible binding site exists in both the primitive animal model and the more advanced animal model. Benzocaine concentrations that elicited vasoactivity in vascular rings were well within the range of benzocaine concentrations measured in the plasma of animals included in the present study thus suggesting that benzocaine is capable of modulating vascular tone at physiological concentrations.

Vascular Smooth Muscle and Ethanol Interactions

Ethanol is very hydrophilic and can be found in any body compartment as a function of the water content of that compartment. Physiologic factors that affect the concentration of ethanol in plasma are absorption, distribution, metabolism and excretion. In the majority of the experiments, fish were exposed to dilute solutions of ethanol (0.2%). Because the endogenous ethanol concentration was zero, a significant gradient for diffusion was established; (2) Considerable differences in the volume of distribution of ethanol may be seen in fish of the same sex and similar body weight but such differences may be attributable to adiposity, and (3) Short exposure times and rapid onset of anesthesia mitigates the loss of ethanol via metabolic conversion and excretion.

Combined Benzocaine and Ethanol Interactions

The solubility of benzocaine in water is extremely poor (1:2500) thereby requiring its preparation in other solvents (e.g., chloroform, clove oil and ethanol). Benzocaine is highly dissolved in ethanol (1:5); thus, ethanol was an ideal solvent to prepare stock solutions of benzocaine that could be rapidly and thoroughly mixed with water. In fact, benzocaine/ethanol combinations are commonplace and are available in a variety of over-the-counter and prescription medicines, topical sprays, mouthwashes, weight loss aids and ointments (6).

Benzocaine/ethanol combinations are routinely used in experimental procedures involving aquatic animals. In such procedures, benzocaine and ethanol are rapidly transported across the gills during respiration then enters the circulatory system (46, 72, 101).

In the present study, a reliable analytical technique was developed to identify and quantitate benzocaine in plasma and other biological fluids. Previous studies describing methods for the identification and quantitation of benzocaine have utilized a variety of labor-intensive analytical techniques including ultraviolet spectroscopy, gas chromatography, high-pressure liquid chromatography and gas chromatography/mass spectrometry (9, 101, 102, 151).

In this study, commonly used extraction steps were modified and different reagents were selected to create a liquid-liquid extraction technique that is simple and inexpensive. The level of sensitivity achieved with this extraction allows for a lower limit of detection and accurate measurement at both the lower limit of quantitation

and upper limit of linearity. The extraction technique coupled with the high sensitivity obtained via gas chromatography/mass spectrometry selective ion monitoring provides for an unequivocal identification of benzocaine based on its unique electron impact fragmentation pattern.

No gain or loss of benzocaine was noted during the analytical phase of testing which may be attributable to the use of a splitless mode of injection, a low initial oven temperature and the elimination of active sites in the injector liner and analytical column. The extract buffering system employed provided ideal conditions for the concentration and reconstitution of samples without sample degradation.

The electrochemical nature of benzocaine was unaltered by the extraction thus; the electron impact induced fragmentation pattern was consisted with published electron impact spectra. The extraction technique and selective ion monitoring program presented herein is rapid, accurate and reproducible and can be confidently employed to positively identify and quantitate benzocaine.

The primary use of ethanol in the present study was to serve as an organic solvent for benzocaine. However, ethanol appeared to increase the anesthetic efficacy of benzocaine. The enhanced anesthetic effect (shortened onset of anesthesia) of benzocaine in the presence of ethanol seems to suggest synergism between these two chemicals.

An increase in plasma osmolality and osmolal gap was also observed with the concomitant administration of benzocaine and ethanol. Benzocaine prepared in water did not cause an increase in plasma osmolality and was not associated with an

elevated osmolal gap. An increased osmolal gap due to the presence of low molecular weight compounds is well documented (26, 30, 35, 48, 120, 155, 156).

Measuring the osmolality of a sample that contains low molecular weight volatile compounds (e.g., ethanol, methanol, ethylene glycol and dissolved CO_2) is more accurately performed using a freezing point depression osmometer rather than a vapor pressure osmometer (39, 42). Freezing point depression osmometry accounts for the osmolal contribution of such compounds via lowering of the freezing point of the water in direct proportion to the number of particles in the solution (44). The osmolal contribution for all the compounds in solution may not be accounted for using vapor pressure osmometry (44). Low molecular weight volatile compounds can escape from the sample during vapor pressure analysis and increase the vapor pressure of the water in the sample. Thus, vapor pressure osmometers are insensitive to osmolal changes contributed by these compounds (3).

Plasma osmolality values generated in this study closely matched those reported in other studies (86, 133). The plasma osmolality of lamprey and rainbow trout was about one-third of hagfish plasma osmolality and artificial seawater. These results coincide with the fact that lampreys are osmoregulators and hagfish are osmoconformers.

The following observations were also made: (1) In the absence of low molecular weight compounds such as ethanol, a reasonable approximation of plasma osmolality may be obtained by summing the major plasma ionic constituents (e.g., Na^+, K^+, glucose blood urea nitrogen); (2) Benzocaine has a low molecular weight

(165.19) but has no influence on plasma osmolality; (3) Benzocaine causes contraction in some and relaxation in other post-gill systemic vessels; and (4) Synergism may exist between ethanol and benzocaine.

Finally, this study raises the following questions; Does benzocaine exhibit vasoactivity in mammalian vascular smooth muscle?; What are the effects of benzocaine on membrane potential? Are the combined effects of benzocaine and ethanol reductive, synergistic or simply additive? Which K^+ channels are important in the underlying resting membrane potential in the post-gill systemic arteries of the extant Agnathans?

REFERENCES

1. Alberts B, Bray D, Lewis J, Raff M, Roberts K and Watson J. (1994). The Cytoskeleton. In: *Molecular Biology of the Cell,* 3rd Edition (ed. B. Alberts, D. Bray, J. Lewis, M. Raff, K. Roberts and J. Watson), Garland Publishing: New York, NY. pp. 787-861.

2. Ali SL. (1983). Benzocaine. In: *Analytical Profiles of Drug Substances,* vol. 12 (K Flory), Academic Press. 73-104.

3. Barlow WK. (1976). Volatiles and osmometry. *Clin. Chem.* 22: 1230-1232.

4. Bartels H, Potter IC. (2004). Cellular composition and ultrastructure of the gill epithelium of larval and adult lampreys. Implications for osmoregulation in fresh and seawater. *The Journal of Experimental Biology* 207: 3447-3462.

5. Baselt RC, Danhof IE.(1993). Disposition of Alcohol in Man. In: *Medicolegal aspects of alcohol determination in biological specimens*, (JC Garriott). Lawyers & Judges Publishing. pp. 55-73.

6. Baselt RC. (2002). Benzocaine. In: *Disposition of Toxic Drugs and Chemicals in Man.* (ed. R.C. Baselt), pp. 101-102. Biomedical Publications.

7. Beaumont MW, Butler PJ, Taylor, EW. (1995). Plasma ammonia concentration in brown trout (*Salmo trutta*) exposed to sub-lethal copper concentrations and its relationship to decreased swimming performance. *The Journal of Experimental Biology* 198: 2213-2220.

8. Benet LZ. (1982). Pharmacokinetics: I. Absorption, Distribution, & Excretion. In *Basic and Clinical Pharmacology.* (ed. B.G. Katzung), pp 22-33. Los Altos, CA: Lange medical Publications.

9. Bernardy JA, Coleman KS, Stehly GR, Gingerich, WH. (1996). Determination of benzocaine in rainbow trout plasma. *Jour. Asssoc. Offc. Analy. Chem. Intl.*79: 623-627.

10. Bkaily G, Sperelakis N, Doane J. (1984). A method for preparation of isolated single adult myocytes. *Am. J. Physiol.* 247 (6 Pt 2) H: 1018-1026.

11. Black ML. (1963). Sequential blockage as a theoretical basis for drug synergism. *J. Med. Chem.* 6: 145-153.

12. Boehringer Mannheim/Hitachi 747-100 Operator's Manual, Indianapolis, 1992.

13. Brown JA, Rankin JC. (1999). Lack of glomerular intermittency in the river lamprey (lampetra fluviatilis) acclimated to seawater and following acute transfer to iso-osmotic brackish water. *The Journal of Experimental Biology* 202: 939-946.

14. Correia MA, Castagnoli N. (1982) Pharmacokinetics II. Drug Biotransformation. In *Basic and Clinical Pharmacology.* (ed. B.G. Katzung), pp 34-42. Los Altos, CA: Lange Medical Publications.

15. Claiborne JB. (1998). Acid–base regulation. In *The Physiology of Fishes* (ed. D. H. Evans), pp. 179–200. Boca Raton, FL: CRC Press.

16. Conklin DJ, Olson KR. (1994). Angiotensin II relaxation of rainbow trout vessels in vitro. *Am. J. Physiol.* 266: R1856-R1860.

17. Conklin DJ, Chavas A, Duff DW, Weaver L, Zhang YT, Olson KR. (1997). Cardiovascular effects of arginine vasotocin in the rainbow trout *Oncorhynchus mykiss. J. Exp. Biol.* 200: 2821-2832.

18. Dasmahapatra AK, Doucet HL, Bhattacharyya C, Carvan MJ, III. (2001). Developmental expression of alcohol dehydrogenase (ADH3) in zebra fish (Danio rerio). *Biochem Biophys Res Commun.* 286 (5): 1082-1086.

19. Davis MJ, Donovitz JA, Hood JD. (1992). Stretch-activated single-channel and whole cell currents in vascular smooth muscle cells. *Am. J. Physiol.* 262 (Cell Physiol. 310: C1083-C1088.

20. Davis MJ, Hill MA. (1999). Signaling Mechanisms Underlying the Vascular Myogenic Response. *Physiol. Rev.* 79: 387-423.

21. Davison G, Wright GM, DeMont ME. (1995). The structure and physical properties of invertebrate and invertebrate arteries. *Journal of Experimental Biology* 198: 2185-2196.

22. Dawson VK, Gilderhus PA. (1979). Ethyl-*p*-aminobenzoate (benzocaine): efficacy as an anesthetic for five species of freshwater fish. US Fish and Wildlife Service Investigations in Fish Control 87.

23. Degnan KJ, Karnaky KJ, Zadunaisky J. (1977). Active chloride transport in the in vitro opercular skin of a teleost (Fundulus heteroclitus), a gill-like epithelium rich in chloride cells. *J. Physiol.* 271, 155-191.

24. Delellis RA, Faller GT. (1997). Cell and Tissue Staining Techniques. In *Principles and Practices of Surgical Pathology and Cytopathology.* (ed. S.G. Silverberg, R.A. DeLellis, W.J. Frable) pp 43-62. New York, NY: Churchill Livingston Inc.

25. Delpon E, Caballero R, Valenzuela C, M. Longobardo D., J. Tamargo. (1999). Benzocaine enhances and inhibits the K+ current through a human cardiac cloned channel (Kv1.5). *Cardiovascular Research.* 42: 510-520.

26. Demedts P, Theunis L, Wauters A, Franck F, Daelemans R, Neels H. (1994). Excess serum osmolality gap after ingestion of methanol: a methodology-associated phenomenon. *Clin Chem.* 40(8): 1587-1590.

27. Devin CE, Somlyo AP. (1971). Thick filaments in vascular smooth muscle. *J. Cell Biol.* 49:636.

28. Dickman KG, and Renfro JL. (1986). "Primary Culture of Flounder Renal Tubule Cells: Transepithelial Transport." *American Journal of Physiology,* 251: F424-F432.

29. Dora KA, Garland CJ. (2001). Properties of smooth muscle hyperpolarization and relaxation to K^+ in the rat isolated mesenteric artery. *Am J Physiol Heart Circ Physiol* 260: H2424-H2429.

30. Dorwart WV, Chalmers L. (1975). Comparison of Methods for Calculating Serum Osmolality from Chemical Concentrations, and the Prognostic Vale of Such Calculations. *Clin. Chem.* 21/1, 190-194.

31. Draeger A, Amos WB, Ikebe M, Small JV. (1990). The cytoskeleton and contractile apparatus of smooth muscle. *J. Cell Biol.* 111:2463.

32. Driska SP, Porter R. (1986). Isolation of smooth muscle cells from swine carotid artery by digestion with papain. *American Journal of Physiology* 251(3Pt 1): C474-81.

33. Droogmans G, Casteels R. (1976). Membrane Potential and ion Transport in Smooth Muscle Cells. In *Physiology of Smooth Muscle.* (ed. E. Bulbring, M.F. Shuba), pp11-18. New York: Raven Press.

34. Ellenhorn MJ, Barceloux DG. (1988). Alcohols and Glycol. In *Medical Toxicology: Diagnosis and Treatment of Human Poisoning.* (ed M.J. Ellenhorn, D.G. Barceloux), pp 781-812. New York, NY: Elsevier Science Publishing Company, Inc.

35. Epstein FB. (1986). Osmolality. *Emerg Med Clin North Am.* 4(2): 253-261.

36. Farrell AP, Johansen JA. (1995). Vasoactivity of the coronary artery of rainbow trout, steelhead trout, and dogfish: Lack of support for non-prostanoid endothelium-derived relaxation factors. *Can J Zool.* 73:1899-1911.

37. Fay FS, Fujiwara K, Rees DD, Fogarty KE. (1983). Distribution of alpha actin in single isolated smooth muscle cells. *J. Cell Biol.* 96:783.

38. Ferreira JT, Schoonbee HJ, Smit GL. (1984). The anesthetic potency of benzocaine-hydrochloride in three fresh water fish species. *Afr. J. Zool.* 19: 46-50.

39. Fiske (1996). User's Guide for the Advanced Multi Sample Osmometer, Fiske, Model 2400. Norwood, MA.

40. Forey P, Janvier P. (1993). Agnathans and the origin of jawed vertebrates. *Nature* 361: 129-134.

41. Forsberg AM, Bergstrom J, Lindholm B, Hultman E. (1997). Resting membrane potential of skeletal muscle calculated from plasma and muscle electrolyte and water contents. *Clin. Sci (Lond).* 92(4):391-6.

42. Freier EF. (1994) Osmometry. In *Tietz Textbook of Clinical Chemistry* (ed. C.A. Burtis and E.R. Ashwood), pp 184-190. Philadelphia: W.B. Saunders Company.

43. Garriott JC. (1993). Pharmacology of Ethyl Alcohol. *Medicolegal Aspects of Alcohol Determination in Biological Specimens.* (JC Garriott), Lawyers & Judges Publishing Co. 36-55.

44. Gennari FJ. (1984). Current Concepts serum osmolality uses and limitations. *The New England Journal of Medicine.* Vol. 310 No. 2.

45. Gilderhus PA. (1990). Benzocaine as a Fish Anesthetic: Efficacy and Safety for Spawning-Phase Salmon. *Prog. Fish Cult.* 52: 189-191.

46. Gilderhus PA, Lemm CA, Woods LC. (1991). Benzocaine as an Anesthetic for Striped Bass. *Prog. Fish Cult.* 53: 105-107.

47. Gontijo AM, Barreto RE, Speit G, Reyes VAV, Volpato GL, Salvadori, DMF. (2003). Anesthesia of fish with benzocaine does not interfere with comet assay results. *Mutation Research* 534165-172.

48. Green, RA. (1978). Perspectives of clinical osmometry. *Vet Clin North Am.* 8(2): 287-299.

49. Greizerstein HB. (1977). Tolerance to ethanol: effect of congeners present in bourbon. *Psychopharmacology* 53:201-203.

50. Grosell M, McDonald MD, Wood CM, Walsh PJ. (2004). Effect of prolonged copper exposure in the marine gulf toad fish (*Opsanus beta*) I. Hydromineral balance and plasma nitrogenous waste products. *Aqua. Tox.* 68: 249-262.

51. Gurney AM, Osipenko ON, MacMillan D, Kempsill FEJ. (2002). Potassium channels underlying the resting potential of pulmonary artery smooth muscle cells. *Clinical and Experimental Pharmacology and Physiology.* 29, 330-333.

52. Gurney AM, Osipenko ON, MacMillan D, McFarlene KM, Tate RJ, Kempsill FEJ. (2003). Two-Pore Domain K Channel, TASK-1, in Pulmonary Artery Smooth Muscle Cells. *Circ. Res.* 93: 957-964.

53. Guyton AC. (1980). Partition of the Body Fluids: Osmotic Equilibria Between Extracellular and Intracellular Fluids. In *Textbook of Medical Physiology*, W.B. Saunders Company, PA. 391-402.

54. Guyton AC. (1980). Transport through the Cell Membrane. In *Textbook of Medical Physiology*, W.B. Saunders Company, PA. 41-54.

55. Guyton AC. (1980). Membrane Potentials, Action Potentials, Excitation, and Rhythmicity. In *Textbook of Medical Physiology*. W.B. Saunders Company, PA. 104-121.

56. Guyton AC. (1991). Membrane Potentials, Action Potentials, Excitation, and Rhythmicity. In *Textbook of Medical Physiology.* W.B. Saunders Company, PA. pp 104-121.

57. Harder DR. (1985). A cellular mechanism for myogenic regulation of cat cerebral arteries. *Annals of Biomedical Engineering.* Vol. 13, 335-339.

58. Harder DR, Gilbert R, Lombard JH. (1987). Vascular muscle cell depolarization and activation in renal arteries on elevation of transmural pressure. *Am. J. Physiol.* 253: F778-F781.

59. Hardisty MW. (1979). Biology of the cyclcostomes. London: Chapman and Hall.

60. Hardisty MW. (1982). Lampreys and hagfishes: an analysis of cyclostome relationships. *The Biology of Lampreys*, London: Academic Press. vol. 4B (ed. M. W. Hardisty and I. C. Potter), 165-259.

61. Hayton WL, Szoke A, Kemmenoe BH, Vick AM. (1996). Disposition of benzocaine in channel catfish. *Aqua. Tox.* 36: 99-113.

62. Heimli H, Kahler H, Endresen MJ, Henriksen T, Lyberg T. (1997). A new method for isolation of smooth muscle cells from human umbilical cord arteries. *Scandanavian Journal Clin Lab Invest*, 57(1): 21-9.

63. Hendrickx H, Vereecken RL, Casteels R. (1975). The influence of potassium on the electrical and mechanical activity of the guinea pig ureter. *Urol Res.* 30;3 (4): 155-158.

64. Hickman CP, Trump BF. (1969). The Kidney. In *Fish Physiology* (ed. W.S. Hoar and D.J. Randall), pp 91-227. New York and London: Academic Press.

65. Hille B. (1977). Local Anesthetics: hydrophilic and hydrophobic pathways for the drug receptor reaction. *J. Gen. Physiol.* 69: 497-515.

66. Hille B. (2001). Classical Mechanism of Block. In *Ion Channels of Excitable Membranes.* Sinauer Associates Inc., Sutherland, MA. 503-536.

67. Hong Z, Weir EK, Varghese A, Olschewski A. (2005). Effect of Normoxia and Hypoxia on K^+ Current and Reating Membrane Potential of Fetal Rabbit Pulmonary Artery Smooth Muscle. *Physiol. Res.* 54: 175-184.

68. Inaba DS, Cohen WE, Holstein ME. (1997). Downers: Alcohol. In *Uppers Downers, All Arounders: Physical and Mental Effects of Psychoactive Drugs.* (ed D.S. Inaba, W.E. Cohen, M.E. Holstein), pp177-210. Ashland, OR: CNS Publications, Inc.

69. Inoue I, Tsutsui I, Bone Q. (2002). Excitation-contraction coupling in skeletal and caudal heart muscle of the hagfish *Eptatretus Burgeri* Girard. *J. Exp. Biol.* 205: 3535-3541.

70. Iverson M, Finstad B, McKinley RS, Eliassen, RA. (2003) The efficacy of medomidate, clove oil, Aqui-S™ and Benzoak® as anesthetics in Atlantic salmon (*Salmo salar* L.) smolts, and their potential stress reducing capacity. *Aquaculture*. 221: 549-566.

71. Ives HE, Schultz GS, Galardy RE, Jamieson JD. (1978). Preparation of Functional Smooth Muscle Cells from the Rabbit Aorta. *Journal of Experimental Medicine*; 148(5): 1400-1413.

72. Iwama GK, McGeer JC, Pawluk MP. (1989). The effects of five fish anesthetics on acid-base balance, hematocrit, blood gases, cortisol, and adrenalin in rainbow trout. *Can. J. Zool.* 67: 2065-2073.

73. Jacobson SL. (1977). Culture of spontaneously contracting myocardial cells from adult rats. *Cell Struct. Funct.* 2: 1-9.

74. Jackson WF, Duling BR. (1983). Toxic effects of silver-silver chloride electrodes on vascular smooth muscle. *Circ. Res.* 53: 105-108.

75. Jackson WF. (1993). Arteriole tone is determined by activity of ATP-sensitive potassium channels. *Am. J. Physiol.* 265 (*Heart Circ. Physiol.* 34): H1797-H1803.

76. Jackson WF, Huebner JM, Rusch NJ. (1997). Enzymatic Isolation and Characterization of Single Vascular Smooth Muscle Cells from Cremasteric Arterioles. *Microcirculation* 4: 35-50.

77. Jackson W, Blair K. (1998). Characterization and function of Ca^{2+} activated K^+ channels in arteriolar muscle cells. *Am. J. Physiol.* 274: H27-34.

78. Jackson WF. (2000). Ion Channels and Vascular Tone. *Hypertension*: 35 [part 2]: 173-178.

79. Janvier P. (1981). The phylogeny of the craniata, with particular reference to the significance of fossil "agnathans". *J. Vertebr. Paleontol.* 1: 121–159.

80. Julien RM. (1981). Principles of Drug Action. In *A Primer of Drug Action.* pp 1-31, W.H. Freeman and Company: San Francisco.

81. Karnaky KJ, Degnan KJ, Zadunaisky JA. (1977). Chloride transport across isolated opercular epithelium of killifish: a membrane in chloride cells. *Science*. 195: 203-205.

82. Karnaky KJ. (1980). Ion-secreting epithelia: chloride cells in the head region of *Fundulus heteroclitus. Am. J. Physiol.* 238: R185-R198.

83. Karnaky KJ, Valenich JD, Currie MG, Oehlenschlager WF, and Kennedy MP. (1991). Atriopeptin Stimulates Chloride Secretion in Cultured Shark Rectal Gland Cells. *American Journal of Physiology*, 23: C1125-D1130.

84. Katzung BG. (1982). Introduction. In *Basic and Clinical Pharmacology.* (ed. B.G. Katzung), pp 1-7. Los Altos, CA: Lange Medical Publications.

85. Kirsch R, Meister MF. (1982). Progressive processing of ingested water in the gut of sea-water teleosts. *J. Exp. Biol.* 98: 67-81.

86. Kirschner LB. (1991). Water and Ions. In *Environmental and Metabolic Animal Physiology* (ed. C.L. Prosser), pp 13-107. New York: Wiley-Liss, Inc.

87. Knot HJ, Nelson MT. (1998). Regulation of arterial diameter and wall [Ca^{2+}] in cerebral arteries of rat by membrane potential and intravascular pressure. *Jour. Physiol.* 508.1: 199-209.

88. Kuriyama TO, Tasaki H. (1970). Electrophysiological Studies of the Antrum Muscle Fibers of the Guines Pig Stomach. *Jour. Gen. Physiol.* 55: 48-62.

89. Leguen I, Prunet P. (2001). In vitro effect of various xenobiotics on trout gill cell volume regulation after hypotonic shock. *Aquatic Toxicology.* 53, 201-214.

90. Lipkind GM, Fozzard HA. (2005). Molecular Modeling of Local Anesthetic Drug Binding by Voltage-gated Sodium Channels.

91. Lord RC. (1999). Osmosis osmometry, and osmoregulation. *The Fellowship of Postgraduate Medica.*, 75:67-73.

92. Ma C, Collodi P. (1996). Culture of cells from tissues of adult sea lamprey. *Cytotech.* 21: 195-203.

93. Madden JA, Christman JT. (1999). Integrin signaling, free radicals, and tyrosine kinase mediate flow constriction in isolated cerebral arteries. *Am. J. Physiol.* 277 (Heart Circ. Physiol. 46): H2264-H2271.

94. Madsen SS. (1990). Effect of repetitive cortisol and thyroxine injections on chloride cell number and Na+/K+-ATPase activity in gills of freshwater acclimated rainbow trout, Salmo gairdneri. *Comp. Biochem. Physiol.* 95A, 171-175.

95. Maehle AH. (2004). "Receptive Substances": John Newport Langley (1852-1925) and his Path to a Receptor Theory of Drug Action. *Med. Hist.* 48(2), 153-174.

96. Mallatt J, Sullivan J. (1998). 28S and 18S rDNA sequences support the monophyly of lampreys and hagfishes. *Mol Biol Evol.* 12: 1706-1718.

97. Mathers JS, Beamish FWH. (1974). Changes in serum osmotic and ionic concentration in landlocked Petromyzon Marinus. *Comp. Bochem. Physol.* Vol. 49A, 677-688. Pergamon Press, Printed in Great Britian.

98. Matsuki H., Shimanda K., Kaneshina S., Kamaya H., Ueda I. (1998). Difference in surface activities between uncharged and charged local anesthetics: correlation with their anesthetic potencies. *Colloids and Surfaces B: Biointerfaces* 11: 287-295.

99. McCormick SD, Bern HA. (1989). In-vitro stimulation of Na^++K^+-ATPase activity and ouabain binding by cortisol in gill tissue of coho salmon. Am. J. Physiol. 256, R707-715.

100. McFarland W, Munz FW. (1965). Regulation of body weight and serum composition by hagfish in various media. *Comp. Biochem. Physiol.* 14: 383-398.

101. Meinertz JR, Gingerich WH, Allen JL. (1991). Metabolism and elimination of benzocaine by rainbow trout, Oncorhynchus mykiss. *Xenobiotica*, vol.21, No.4, 525-533.

102. Meinertz JR, Stehly GR, Gingerich WH. (1996). Pharmacokinetics of benzocaine in rainbow trout (*Oncorhynchus mykiss*) after intraarterial dosing. *Aquaculture* 148: 39-48.

103. Mekata F. (1971). Electrophysiological Studies of the Smooth Muscle Cell Membrane of the Rabbit Common Carotid Artery. *Jour. Gen. Physiol.* 57: 738-759.

104. Misra PS, LeFevre A, Ishii H. (1971). Increase of ethanol, meprobamate and pentobarbital metabolism after chronic ethanol administration in man and in rats. *Am. J. Med.* 51: 346-351.

105. Mita M, Yanagihara H, Hishinuma S, Saito, M, Walsh MP. (2002). Membrane depolarization-induced contraction of rat caudal arterial smooth muscle involves Rho-associated kinase. *Biochem J.* 364: 431-440.

106. Mitra R and Morad M. (1985). A Uniform Enzymatic Method For Dissociation of Myocytes From Hearts And Stomachs of Vertebrates. *American Journal of Physiology*, 249: H1056-H1060.

107. Neild TO, Kotecha N. (1987). Relationship between membrane potential and contractile force in smooth muscle of the rat tail artery during stimulation by norepinephrine, 5-hydroxytryptamine, and potassium. *Circ Res.* 60(5): 791-795.

108. Nelson MT, Patlak JB, Worley JR, Standen NB. (1990). Calcium channels, potassium channels, and voltage dependence of arterial smooth muscle tone. *Amer. Physiol Soc.* 90: C3-C17.

109. Nelson MT, Quayle JM. (1995). Physiological roles and properties of potassium channels in arterial smooth muscle. *Am J Physiol.* 268(4 Pt 1): C799-822.

110. Okker-Reitsma GH, Dziadkowiec I.J, Groot CG. (1985). Isolation and culture of smooth muscle cells from human umbilical cord arteries. *In Vitro Cell Dev Biology,* 21(1): 22-25.

111. Olson KR, Squibb KS, Cousins RJ. (1978). Tissue Uptake, Subcellular Distribution, and Metabolism of $^{14}CH_3HgCl$ and $CH^{203}HgCl$ by Rainbow Trout, *Salmo, gairdneri. J. Fish. Res. Board Can.* 35: 381-390.

112. Olson KR, Meisheri KD. (1989). Effects of atrial naturetic factor on isolated arteries and perfused organs of the trout. *Am. J. Physiol.* 25: R10-R18.

113. Olson KR, Villa J. (1991). Evidence against nonprostanoid endothelium-derived relaxation factor(s) in trout vessels. *Am. J. Physiol.* 260: R925-R933.

114. Olson KR, Duff DW, Farrell AP, Keen J, Kellogg MD, Kullman D, Villa J. (1991). Cardiovascular effects of endothelin in trout. *Am. J. Physiol.* 260: H1214-H1223.

115. Olson K, Duff DW. (1993). Single-pass gill extraction and tissue distribution of atrial natriuretic peptide in trout. *Am. J. Physiol.* 265: R124-R131.

116. Olson KR, Conklin DJ, Weaver L, Duff DW, Herman CA, Wang X, Conlon JM. (1997). Cardiovascular effects of homologus bradykinin in rainbow trout. *Am. J. Physiol.* 272: R1112-R1120.

117. Olson KR, Russell MJ, Forester ME. (2001). Hypoxic vasoconstriction of cyclostome systemic vessels: the antecedent of hypoxic pulmonary vasoconstriction? *Am J Physiol Regulatory Integrative Comp Physiol* 280: R198-R206.

118. O'Neil MJ, Smith A, Heckelman PE, Obenchain JR, Gallipeau JAR, D'Arecca, MA, Budavari, S. (2001). The Merck Index: An Encyclopedia of

Chemicals, Drugs and Biologicals. Merck and Co., Inc.: Whitehouse Station, NJ.

119. Osol G, Brekke JF, McElroy-Yaggy K, Gokina NL. (2002). Myogenic tone, reactivity, and forced dilatation: a three phase model of in vitro arterial myogenic behavior. *Am. J. Physiol. Heart Circ. Physiol.* 283: H2260-2267.

120. Pappas AA, Gadsden RH Jr, Gadsen RH Sr, Groves WE. (1982). Computerized calculation with osmolality and its automatic comparison with observed serum ethanol concentration. *Am J Clin Pathol.* 77(4): 449-451.

121. Perry, SF. (1997). The chloride cell: structure and function in the gills of freshwater fishes. *Annu. Rev. Physiol.* 59: 325-347.

122. Pickering AD, Morris R. (1970). Osmoregulation of Lampetra fluviatilis L. and Petromyzon marinus (Cyclostomata) in hyperosmotic solutions. *J. Exp. Biol.* 53: 231-243.

123. Poe M. (1976). Antibacterial synergism. A proposal for chemotherapeutic potentiation between trimethoprim and sulfamethoxazole. *Science* 194: 533-535.

124. Potts WTW, Parry G. (1964). Osmotic and Ionic Regulation in Animals. Pergamon Press, Oxford.

125. Potter VR. (1951). Sequential blocking of metabolic pathways in vivo. *Proc. Soc. Exp. Biol. Med.* 76: 41-46.

126. Prosser CL. (1991). Excitable Membranes; Synaptic Transmission and Modulation. In *Neural and Integrative Animal Physiology* (ed. C.L. Prosser), pp 1-66. New York: Wiley-Liss, Inc.

127. Rall DP, Burger JW. (1969). Some aspects of hepatic and renal excretion in Myxine. *Am. J. Physiol.* 212(2): 354-356.

128. Randall DJ, Brauner C. (1998). Interactions between ion and gas transfer in freshwater teleost fish. *Comp. Biochem. Physiol.* 119A: 3-8.

129. Rankin JC. (1997). Osmotic and ionic regulation in cyclostomes. *Ionic Regulation in Animals: a Tribute to Professor W.T.W. Potts.* (eds. N. Hazon, F.B. Eddy and G. Flik), pp. 50-69. Springer, Berlin.

130. Rankin JC, Cobb CS, Frankling SC, Brown JA. (2001). Circulating angiotensins in the river lamprey, Lampetra fluviatilis, acclimated to freshwater and seawater: possible involvement in the regulation of drinking. *Comparative Biochemistry and Physiology* Part B 129: 311-318.

131. Rhodin JAG. (1962). Fine structure of vascular walls in mammals with special reference to smooth muscle component. Physiol. Rev 42:49.

132. Roberts JM, Bourne HR. (1982). Drug Receptors & Pharmacodynamics. In *Basic and Clinical Pharmacology.* (ed. B.G. Katzung), pp 8-21. Los Altos, CA: Lange medical Publications.

133. Robertson JD. (1974). Osmotic and ionic regulation in cyclostomes. In *Chemical Zoology.* (ed. M. Florikin M. and B.T. Scheer), Vol. VIII, pp 149-191. New York: Academic Press.

134. Robinson BF. (1983). Differences in blood vessels between species: Relation to the differences in blood vessels of varying type within the same species. *Gen Pharmac.* 14: 43-46.

135. Ross LG, Ross B. (1999). *Anesthetic and Sedative Techniques for Aquatic Animals*, 2nd ed. Blackwell, London, UK. 159.

136. Ryback R, Percarpio B, Vitale J. (1969). Equilibration and metabolism of ethanol in the goldfish. *Nature.* 222 (198): 1068-70.

137. Ryback RS. (1969). The use of goldfish as a model for alcohol amnesia in man. *Q J Stud Alcohol.* 30(4): 877-882.

138. Schacher S and Proshansky E. (1983). Neurite Regeneration by Alpysia Neurons in Dissociated Cell Culture: Modulation by Aplysia Hemolymph and the Presence of the Initial Axonal Segment. *Journal of Neuroscience,* 3: 2403-2413.

139. Sheehan DC, Hrapchak BB. (1980).Theory and Practice of Histotechnology, 2nd Ed.; St. Louis, MO: C.V. Mosby Co.

140. Siegel G, Roedel H, Nolte J, Hofer HW, Bertsche O. (1976). Ionic composition and ion exchange in vascular smooth muscle. In *Physiology of Smooth Muscle*. (ed. E. Bulbring and M.F. Shuba), pp 19-39. New York: Raven Press.

141. Singh NP. (1998). A Rapid Method for the Preparation of Single-Cell Suspensions From Solid Tissues. *Cytometry*. 31: 229-232.

142. Small JV. (1977). Studies on isolated smooth muscle cells: The contractile apparatus. *J. Cell Sci.* 24:317.

143. Smith HW. (1930). The absorption and excretion of water and salts by marine teleosts. *Am. J. Physiol.* 93: 485-505.

144. Smith HW. (1932). Water regulation and its evolution in fishes. *Q. Rev. Biol.* 7: 1-26.

145. Smithline N, Gardner K. (1976). Gaps anionic and osmolal. *Journal of the American Medical Association.* 236(14): 1594-97.

146. Somlyo AP and Somlyo AV. (1968). *Pharmacol. Rev.* 20: 197-272.

147. Speden RN. (1970). In *Smooth Muscle* (ed. E. Bulbring, A. F. Brading, A.W. Jones and T. Tomita), pp 558-588. London: Arnold.

148. Stock DW, Whitt GS. (1992). Evidence from 18S ribosomal RNA sequences that lampreys and hagfishes form a natural group. *Science* 257: 787–789.

149. Svendsen YS, Haug T. (1991). Effectiveness of formalin, benzocaine, and hypo and hypersaline exposures against adults and eggs of Entobdella hippoglossi (Muller) an ectoparasite on Atlantic halibut (*Hippoglossus hippoglossus* L.) Laboratory Studies. *Aquaculture*, 94: 279-289.

150. Sweeney M, Yuan J X-J. (2000). Hypoxic pulmonary vasoconstriction: role of voltage-gated potassium channels. *Respir. Res.* 1: 40-48.

151. Szoke A, Hayton WL, Schultz IR. (1997). Quantification of benzocaine and its metabolites in channel catfish tissues and fluids by HPLC. *Journal of Pharmaceutical and Biomedical Analysis* 16: 69-75.

152. Tallarida RJ. (2002). The interaction index: a measure of drug synergism. *Pain.* 98: 163-168.

153. Tennant M, McGeachie JK. (1990). Blood vessel structure and function: A brief update on recent advances. *Aust. N. Z. J. Surg.* 60: 747.

154. Turbeville JM, Schulz JR, Raff RA. (1994). Deuterostome phylogeny and the sister group of the chordates: evidence from molecules and morphology. *Mol. Biol. Evol.* 11: 648–655.

155. Tzamaloukas AH, Jackson JE, Long DA, Gallegos JC. (1982). Serum ethyl alcohol levels and osmolal gaps. *J Toxicol Clin Toxicol.* 19(10): 1045-1050.

156. Vasiliades J, Pollock J, Robinson CA. (1978). Pitfalls of the alcohol dehydrogenase procedure for the emergency assay of alcohol: a case study of isopropanol overdose. *Clin Chem* 24(2): 383-385.

157. Vassort G. (1975). Voltage-clamp analysis of transmembrane ionic currents in guinea pig myometrium: evidence for an initial potassium activation triggered by calcium influx. *J. Physiol.* 252(3): 713-734.

158. Vedel Niels E, Bodil Korsgaard, Frank B. Jensen. (1998). Isolated and combined exposure to ammonia and nitrite in rainbow trout (Oncorhynchus mykiss): effects on electrolyte status, blood respiratory properties and brain glutamine/glutamate concentrations. *Aquatic Toxicology* 41: 325-342.

159. Veinot JP, Ghadially FN, Walley VM. (2001). Light Microscopy and Ultrastructure of the Blood Vessels and Heart. In *Cardiovascular Pathology.* (ed. M.D. Silver, A.I. Gotlieb, F.J. Schoen), pp 30-53. Philadelphia, PA: Churchill Livingston.

160. Villaschi S, Nicosia RF, Smith, MR. (1994). Isolation of a morphologically and functionally distinct smooth muscle cell type from the intimal aspect of the normal rat aorta. Evidence for smooth muscle cell heterogeneity. *In Vitro Cell Dev Biol Anim,* 30A(9): 589-95.

161. Vornanen M, Ryokkynen A, Nurmi A. (2002). Temperature-dependent expression of sarcolemmal K^+ currents in rainbow trout atrial and ventricular myocytes. *Am. J. Physiol. Reg. Integ. Comp. Physiol.* 282: R1191-R1199.

162. Wang GK, Quan C, Wang S-Y. (1998). A common local anesthetic receptor for benzocaine and etidocaine in voltage-gated μ1 Na^+ channels. *Pflugers Arch – Eur J Physiol.* 435: 293-302.

163. Wang GK, Wang S-Y. (1994). Binding of benzocaine in batrachotoxin-modified Na^+ channels: state dependent interactions. *J. Gen Physiol.* 103: 501-508.

164. Wang S-Y, Mitchell J, Moczydlowski E, Wang GK, (2004). Block of Inactivation-deficient Na^+ Channels by Local Anesthetics in Stably Transfected Mammalian Cells: Evidence for Drug Binding Along the Activation Pathway. *J. Gen Physiol.* 124: 691-701.

165. Waring CP, Moore A. (2004). The effect of atrazine on Atlantic salmon (Salmo salar) smolts in fresh water and after seawater transfer. *Aquatic Toxicology* 66: 93-104.

166. Warsaw DM, Derosiers JM (1990). Smooth Muscle myosin cross-bridge interactions modulate actin filament sliding velocity in vitro. *J. Cell Biol.* 11:453.

167. Welsh DG, Jackson WF, Segal SS. (1998). Oxygen induces electromechanical coupling in arteriolar smooth muscle cells: a role for L-type Ca^{2+} channels. *Am. J. Physiol.* 274 (*Heart Circ. Physiol.* 43): H2018-H2024.

168. Wilson JM, Laurent P, Tufts BL, Benos DJ, Donowitz M, Vogl AW, Randall DJ. (2000a). NaCl uptake by the branchial epithelium in freshwater teleost fish: an immunological approach to ion-transport protein localization. *J. Exp. Biol.* 203: 2279-2296.

169. Wilson JM, Randall DJ, Donowitz M, Vogl AW, Ip YK. (2000b). Immunolocalisation of ion-transport proteins to branchial epithelium mitochondria-rich cells in mudskipper (*Perioopthalmodon schlosseri). J. Exp. Biol.* 203: 2297-2310.

170. Wolf K. (1963). Physiological salines for fresh water teleosts. *Progressive Fish Culturist* 25, 135-140.

171. Xiao X, Chen W, Cheng D. (1998). Isolation and identification of smooth muscle cells from pulmonary artery in rats. *Hua Hsi I Ko Ta Hsueh Hsuech Pao*, 29(3): 241-243.

172. Yalden DW. (1985). Feeding mechanisms as evidence for cyclostome monophyly. *Zool J.Linn.* Soc. 84: 291–300.

173. Zadunaisky JA. (1984). The chloride cell: The active transport of chloride and the paracellular pathways. In *Fish Physiology,* vol. 10B (ed W.S. Hoar and D.J. Randall), pp. 130-176. Orlando: Academic Press.

174. Zhang YT, Weaver L, Ibeawuchi A, Olson KR. (1998). Catecholaminergic regulation of venous function in the rainbow trout. *Am. J. Physiol.* 272: R1195-R1202.